Universität der Bundeswehr München
Fakultät für Elektrotechnik und Informationstechnik

Analytical and numerical analysis and simulation of heat transfer in electrical conductors and fuses

Audrius Ilgevicius

Vorsitzender des Promotionsausschusses: Prof. Dr.-Ing. K. Landes
1. Berichterstatter: Prof. Dr.-Ing. H.-D. Ließ
2. Berichterstatter: Prof. Habil. Dr. R. Ciegis
3. Berichterstatter: Prof. Dr.-Ing. H. Dalichau

Tag der Prüfung: 17.09.2004

Mit der Promotion erlangter akademischer Grad:
Doktor-Ingenieur
(Dr.-Ing.)

Neubiberg, den 1. November 20004

Die Dissertation wurde am 23.4.2004 bei der Universität der Bundeswehr München eingereicht.

Contents

List of symbols

A	surface area, m^2
A_f	cross section area of flat cable, m^2
A_{fu}	cross section area of the fuse, m^2
a,b,c,d	polynomial coefficients of polynomial function (in Eq. 1.1, 1.3)
a_n,b_n,c_n	intermediate variables in tri-diagonal matrix
b	width of flat cable, m
d	thicknes of flat cable,m
D	multi-wire bundle diameter, m
E	electric field strength, V/m
E_0	electric field strength at reference temperature, V/m
F	filling factor of multi-wire bundle
f	filling factor of electric wire conductor
G	heat conductance in multi-wire bundle, W/mK
Gr	Grashof number
g	gravitational acceleration, m/s^2
i	spatial index in numerical calculation
I	electric current, A
I_0	nominal electric current of electric wires or cables, A
J	electric current density, A/m^2
K	number of time steps in numerical calculation algorithm
K_{d1},K_{T1}, K_{T21},K_{T22}, K_{T31}	intermediate variable of heat convection equation (section 2)
L	characteristic length of the fuse element or cable, m
L	length of the wire, m
N	number of nodes in the numerical scheme
N	vector size in the numerical algorithm or number of time constants
Nu	Nusselt number
P	electric power per unit length, W/m or perimeter, m
Pr	Prandtl number
q	heat flux, W/m^2
q_c	heat flux caused by the convection, W/m^2
q_r	heat flux caused by the radiation, W/m^2
q_v	rate of energy generation per unit volume, W/m^3
R	ohmic resistance, Ω
Ra	Rayleigh number
r_0, r_1	cylinder radius, m
r,Φ,z	cylindrical coordinates
S	thickness of insulation of multi-wire bundle, m
T	temperature, °C
ΔT	temperature difference, K
T_{env}	environment temperature, °C
T_s	surface temperature of the conductor, °C
T_∞	absolute temperature, K
t	time, s
t_g	heating-up time, s
u	perimeter of fuse element, m

x,y,z	rectangular coordinates, m
W	energy rate, W
ΔW_{st}	stored energy in the solid, W
W_{out}	energy entering the solid, W
W_{int}	energy generated in the solid by the Joule losses, W
W_{out}	energy rate dissipated by the solid, W

Greek Letters

α	overall heat convection coefficient, W/m^2K
α_c	heat convection coefficient, W/m^2K
α_r	radiation coefficient
α_ρ,α_0	linear temperature coefficient of copper resistance, 1/K
ß	volumetric thermal expansion coefficient, 1/K
$ß_\rho,ß_0$	square temperature coefficient of copper resistance, $1/K^2$
χ	length constant, m
Δ	Laplace operator
ε	emissivity
?	heat conductivity coefficient, W/mK
ν	kinematic viscosity, m^2/s
ρ	density, kg/m^3
ρ_{el}	specific resistivity, Ωm
ρ_0	specific resistivity at reference temperature 20°C, Ωm
σ	Stefan-Bolzman constant
ϕ	azimuthal angle, rad
γ	specific heat capacity per volume, J/m^3K
τ	time constant, s
τ_g	heating-up time constant, s
τ_0	time constant at I=0, s

Subscripts

ave	average
c	convection
env	environment
el	electric
f	flat cable
fu	fuse
g	heating-up time notation
i	spatial nodes notation in numerical algorithm
r	radiation, round wire
v	volume
∞	free-stream conditions

Superscripts

*	absolute temperature - 273.15 K
n	time index in the numerical algorithm
4	temperature of fourth order

CHAPTER 1

INTRODUCTION

Thermo-electrical investigations of electrical conductors (wires, cables, fuses) have been described in a great variety of applications and gained increasing attention by a number of research works [1,2,3,4]. The major part of these works was devoted to the analysis of heat transfer in electrical conductors for high voltage power distribution systems. However, today, power supply in mobile systems like aircrafts, ships or cars have to be considered due to weight restrictions. The main difference between power lines and wires for mobile applications is the length, which does not exceeds 8 m i.e. in the cars. This causes higher current density that leads higher voltage drop.

Today, in the modern mobile vehicles electrical and electronic equipment is of great importance. Electronics is used for the applications like electromechanical drives (servomotors, pumps) as well as for air conditioners and safety equipment. In the future even safety – critical systems in the cars might be replaced by so-called "x-by-wire" technology [5,6], where steering, braking, shifting and throttle is performed by electronics. The electronics replaces the mechanical systems due to the following reasons:

- to increase passenger comfort,
- to reduce the weight of a vehicle while increasing the inner space,
- to increase safety,
- to reduce fuel consumption and costs

Since, the power consumers are distributed over the whole vehicle, the power must be delivered to the consumers by electrical wires. With increasing number of consumers, the amount of wires and the wire size rises also. Since the space in mobile systems is limited and weight is always being reduced, wire conductor sizes must be kept as small as possible. Therefore, it is necessary to investigate heat transfer in electrical conductors in order to be able to calculate optimal conductor cross-section for long lasting load. This information can be obtained from the current-temperature (= steady state) characteristic of each wire.

It is also important to consider current-time (= transient-state) characteristic of wires versus fuses. This information is important for the fuse design, whose current-time characteristic should match wire current-time characteristic in order to protect the wire reliable against overload and short-circuit currents.

The main development in the field of heat transfer computation in electric power cables was made by the work of Neher and McGrath [6] published in 1957. Later, there were a number of publications published as IEEE transactions. In 1997 based on IEEE transactions George J. Anders published the first book [7], which is the only devoted solely to the fundamental theory and practice of computing the maximum current a power cable

can carry without overheating. Almost all references to scientific articles and books of heat transfer analysis in electric cables are summarized in this book.

However, literature [7] is only devoted to the heat transfer computations for transmission, distribution, and industrial applications. The problem dealing with mobile systems, is not covered by the book. The main difference between the electric cables used in industrial applications and mobile systems is that the latter have generally shorter lengths and much higher operating temperature ranges.

The first attempt to develop a theory of heat transfer calculation in electric conductors for mobile applications was made by T. Schulz [8]. In his dissertation, the steady-state heat transfer equations of electric conductors have been solved analytically with some simplifications. This is sufficient to elaborate tendency. For more precise calculations, however, numerical methods should be applied.

In addition to this, there is also a need for the mathematical relationships of thermo-electrical characteristics for computer aided design program. The present available computer simulation programs for heat transfer like CableCad® or Ansys® [9,10] are too complex, use pure numerical methods requiring specific knowledge, and are not specialized for heat transfer calculation in electric cables and fuses. On the contrary, the implementation of a simple mathematical model into a computer program, would allow the development of a very time-efficient cable design tool.

All this shows, that there is a requirement to investigate the heat transfer in electrical conductors and to develop efficient algorithms for the calculation of the thermo-electrical characteristics. In this study, efficient algorithms means, that all characteristics of conductors should be described by simple mathematical functions. One of the possible ways to solve this problem is to combine analytical and numerical analysis methods.

1.1 Objectives of current study

The aim of the present research is to analyse heat transfer of one-dimensional electric conductor models and to develop a simplified calculation methodology of thermo-electrical characteristics for computer aided electric cable design algorithms. In order to achieve this goal the following problems must be solved:

- To create one-dimensional mathematical model of electric conductors for calculation of thermo-electrical characteristics of electrical cables and fuses;
- To analyze steady-state heat transfer by solving partial differential equations analytically;
- To calculate steady / transient – state characteristics using a one-dimensional numerical model;
- To verify the obtained numerical model by experimental data;
- To develop a simplified calculation methodology of electric conductor characteristics by fitting earlier obtained numerical results with polynomial functions.

1.2 Methodology of current research

This research work presents a one-dimensional (1-D) analytical and numerical model to simulate a heat transfer in flat cables, cylindrical wires and electric fuses separately.

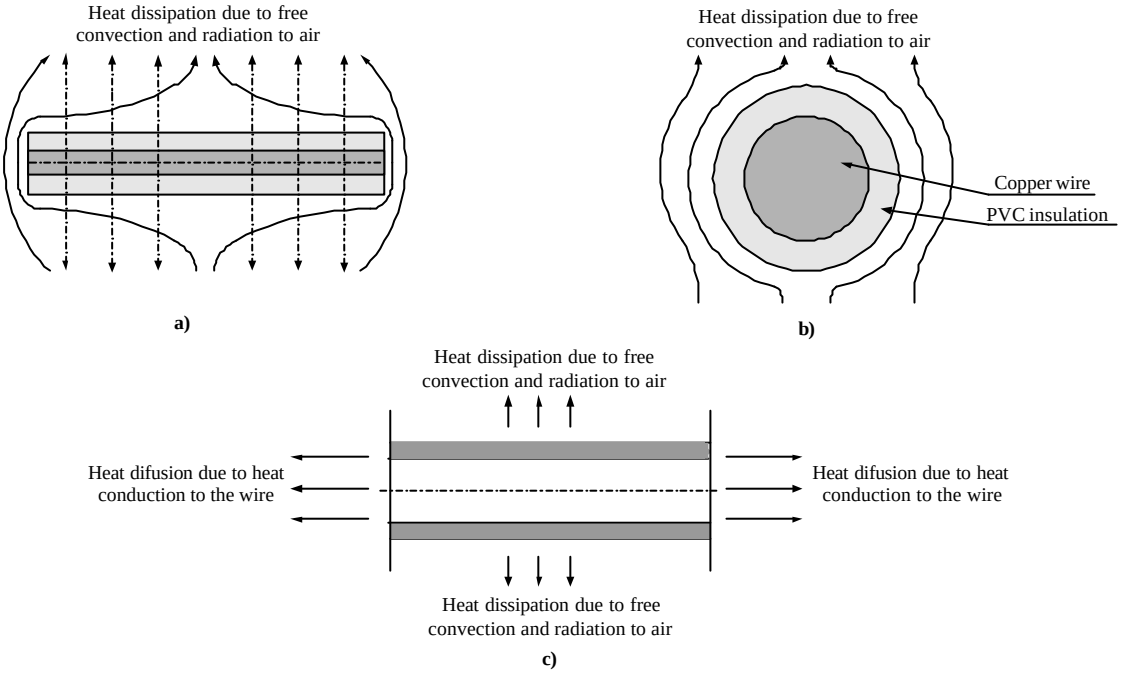

Fig. 1.1 Heat dissipation by free convection in electric conductor models: a) - flat cable, b) - round wire, c) - fuse

In this study both approaches i.e. analytical and numerical, are used for the analysis of heat transfer.

Analytical solutions were used to obtain steady-state temperatures for linearised conductor models. The linearisation was done although non-linear heat transfer models would be appreciable. The experimental data have shown that linearised model have quite a good agreement with experimental data.

Numerical model was applied for transient-state temperature calculations considering a non-linear heat transfer model.
The heat transfer in electrical systems (cables and fuses) (Figure 1.1) is obviously of two - or three -dimensional nature (2-D or 3-D). The heat transfer occurs due to the heat

diffusion from fuse to the wire or to the fuse holder; also the heat is dissipated from the surfaces of conductors to the ambient due to temperature differences. However, due to the complexity of the numerical model and large time scale of heat transfer processes in the cables it is not computationally efficient to use three-dimensional models to simulate heat transfer in electrical systems. The CPU time for simulating the same physical system using two- or three -dimensional models is significantly longer than required by a simplified 1-D model. In creating a mathematical model of flat cables (Figure 1.1a) we regard heat transfer only in y – direction (see three-dimensional drawing) while side effects are negligible. Boundary conditions are symmetrical and convective-radiative. Here, convection is assumed unforced and laminar. Flat cable has insulation/conductor/insulation layer sequence, where the insulation is PolyVinylChloride (PVC) and the conductor is copper. Insulation layer is described by heat conductivity, specific heat capacity and heat dissipation coefficient. Conductor layer is heated with uniform volumetric heat, generated by electrical current.

In the case of cylindrical wires (Figure 1.1b), the 3-D problem is reduced to 1-D regarding only radial heat transfer and as infinite length of the wire. The same material properties and boundary conditions apply as for flat cable.

The fuse model (1.1c) can also be considered as a cylindrical conductor, only with finite length and without insulation. The model is also reduced to a 1-D model neglecting radial heat transfer, because the fuse element has very high heat conductivity. Since the fuse element has finite length, axial heat transfer is modelled with prescribed temperatures on the boundaries $T(0,t)$ and $T(L,t)$. These temperatures are known from wire temperatures determined earlier.

Due to the non-linear behaviour of material properties with respect to the temperature, a numerical algorithm had to be applied. A finite volume (FV) method was used to approximate partial derivatives of heat transfer equation. The obtained system of non-linear algebraic equations was solved by iterative Newton-Raphson method in order to find nodal unknowns of temperatures in the conductors.

The final step of this work was the evaluation of numerical simulation results by the polynomial fitting procedure using the least square (LS) algorithm. A number of mathematical methods have been proposed [10,11,12,13,14] for the analysis of heat transfer in electrical conductors. Usually these methods are pure-analytical or numerical. Analytical methods are easy to handle, physically meaningful but of limited application for complicated models (non-linear, non-homogenous) and boundary conditions. A numerical approach enables us to implement more realistic boundary conditions, which can be applied to complicated geometries. In order to understand physical meaning of the results received from the numerical simulation, calculation results have to be described by simple mathematical equations with as small a number of unknown variables as possible. Therefore, thermo-electrical characteristics of electrical conductors are analysed by polynomial or logarithmical functions. The second reason of derivation of simplified equations is to implement these formulas into computer tool, where a very good time-efficiency can be achieved.

1.3 Scientific novelty

The special scientific contribution of this work is the particular way to combine analytical and numerical methods to calculate the thermal behaviour of electrical conductors. The proposed algorithm is based on the following steps:

1. Analytical derivation of the heat transfer equations.

2. Analytical solution of the obtained differential equations with mainly temperature independent or linear dependent physical constants.

3. Simplification of the obtained analytical solution to reduce the number of variables.

4. Numerical approximation of the heat transfer equations with non-linear temperature dependent physical constants.

5. Model validation of the numerical results by experimental data.

6. Interpolation (fitting) of the received numerical results with the simplified equations derived from the analytical solution of the heat transfer equations.

7. Evaluation of the results to receive a limited amount of independent constants (e.g. temperature) to describe the thermal-electrical characteristics with sufficient accuracy.

In this study, for the first time, a methodology of heat transfer analysis in electric systems for mobile applications has been formulated. It is shown that it is possible to describe main thermo-electrical characteristics by simplified quasi-analytical functions, which are valid for one particular conductor type.

Obtained thermo-electrical characteristics of electrical conductors are:

- thermo – electrical characteristic *DT(I)* :

$$\boxed{\Delta T\left(I \le I_0\right) = a\,I + b\,I^2} \tag{1.1}$$

- heating-up time characteristic $t_g(I)$:

$$\boxed{t\left(I > I_0\right) = t_0 \ln \frac{I^2}{I^2 - I_0^2}} \tag{1.2}$$

- time constant characteristic *t(I)* :

$$\boxed{t = t_I - c\,I^{0.5} + d\,I^2} \tag{1.3}$$

Having the relationship between the conductor temperature and electrical current (Eq. 1.1), voltage drop in the conductor can be calculated as following:

- voltage drop per length characteristic *E(I)* :

$$E = \frac{Ir}{A} = \frac{Ir_0(1 + a_r \Delta T + b_r(\Delta T^2))}{A} \tag{1.4}$$

here:

DT	conductor temperature difference against environment	in K
I	current	in A
I_0	nominal current	in A
a,b,c,d	constants	
t	heating up time	in s
t_0	nominal time constant	in s
t	current dependent time constant	in s
t_I	time constant at zero current	in s
E	voltage drop per length	in V/m
r	specific resistance (resistivity)	in Ωm
r_0	specific resistance at reference temperature (e.g. 20°C)	in Ωm
a_r	linear temperature coefficient of the specific resistance	in 1/K
b_r	square temperature coefficient of the specific resistance	in $1/K^2$
A	conductor cross sectional area	in m^2

In this work an algorithm is proposed to describe thermo-electrical characteristics with the simplified equations (see above 1.1-1.4), which were obtained from analytical and numerical models. This algorithm is suited for implementation in the computer aided cable design program.

Based on the proposed algorithm to calculate thermo-electrical characteristics a computer program to design electrical systems in cars has been written [15].

1.4 Research approval and publications

Created methodology and algorithms, which have been developed to calculate thermo-electrical characteristics of electrical cables for car applications were implemented by cable harness manufacturer Leoni Bordnetzsysteme GmbH and DaimlerChrysler AG. The basic achievements of present research have been presented at the following international conferences:

- The 7th International Conference “Electronics’2003” in Kaunas, Lithuania, 2003;
- The 8th International Conference “Mathematical Modelling and Analysis” in Trakai, Lithuania, 2003

The content of the dissertation includes three scientific publications: the two papers are published in the journal “Mathematical Modelling and Analysis” and one publication in “Electronics and Electrical Engineering”. Both journals are edited in Lithuania by an international editorial board.

CHAPTER 2

PHYSICAL MODELS OF CONDUCTORS AND THEIR HEAT TRANSFER EQUATIONS

2.1 Overview

Before the discussion of the theoretical model, a short “guide” will be presented at first. This “guidance” is intended to show concisely in what steps the heat transfer equations are going to be developed. It will also be discussed how these equations are solved for cable rating problems.

After a short introduction to the model geometry, heat transfer equations of different model geometries will be derived. These equations describe the temperature behaviour in electrical conductors and fuses.

As a next step, the heat convection and radiation coefficients will be determined. The heat convective coefficient is presented for cylindrical and horizontal surfaces. Because of its nonlinearity, this coefficient will have to be linearized for the later analytical analysis of the heat equation.

Following this, the main physical material parameters of the heat equation will be considered. Because of its non-linearity (e.g. heat conductivity and electrical resistance) in reality, certain simplifications have to be introduced. It will be shown that these simplifications can be tolerated for the thermal analysis of the electrical conductor and do not restrict the validity of the simplified thermal conductor model in the temperature range of interest.

Finally, required boundary conditions will be introduced. They have to be linearized in order to implement them into an analytical solution of the heat equation.

With these preparations, it will be possible to investigate the thermo-electrical characteristics of conductors and calculate their ratings.

2.2 Geometry of physical models

On the basis of electrical conductors, three different models will be considered:
flat insulated cable,
round insulated wire, and
electrical fuse.

These three different types of conductors cover the main part of power supply system in many applications. In the flat cable model, the term "cable" is used because it has more than one wire. All models are one – dimensional systems, because the other dimensions in all cases vanish due to large difference between cross-sections (for a round wire or fuse) or thickness (for flat cable) and length of the conductors.

A. The flat cable model (Fig. 2.1,a) is reduced to one-dimensional heat conduction, whereby spatial derivatives with respect to x and z are neglected:

$$(\partial_x(...) = \partial_z(...) \equiv 0).$$

The reduction of the model is possible because of infinite length of the cable L and much bigger width b compared to the thickness d. Due to lateral symmetry of this model, it is sufficient to analyse the upper part of the flat cable only. The model consists of three layers and can be extended depending on the flat cable structure. From "bottom" to "top" in the figure (2.1,a) we have:

- Polyvinylchloride (PVC) insulation
- Metallic conductors (pure copper)
- Polyvinylchloride (PVC) insulation

For the sake of simplicity, the conductors (the middle layer) are considered as a homogeneous conductor layer.

B. In round wire model (Fig. 2.1, b) all spatial derivatives of the heat equation vanish with respect to x and j :

$$(\partial_x(...) = \partial_j(...) \equiv 0).$$

The heat conduction in the axial direction is neglected, because normally the length of the wire is much larger than its area, therefore, the boundary effects can be neglected. The angular dimension j is also neglected due to rotational symmetry of the conductor and insulation layer. The whole model consists of two layers and can be extended to more layers, depending on the wire construction.

In this model, we have:

- Metallic conductor (98% copper)

- Polyvinylchloride (PVC) insulation

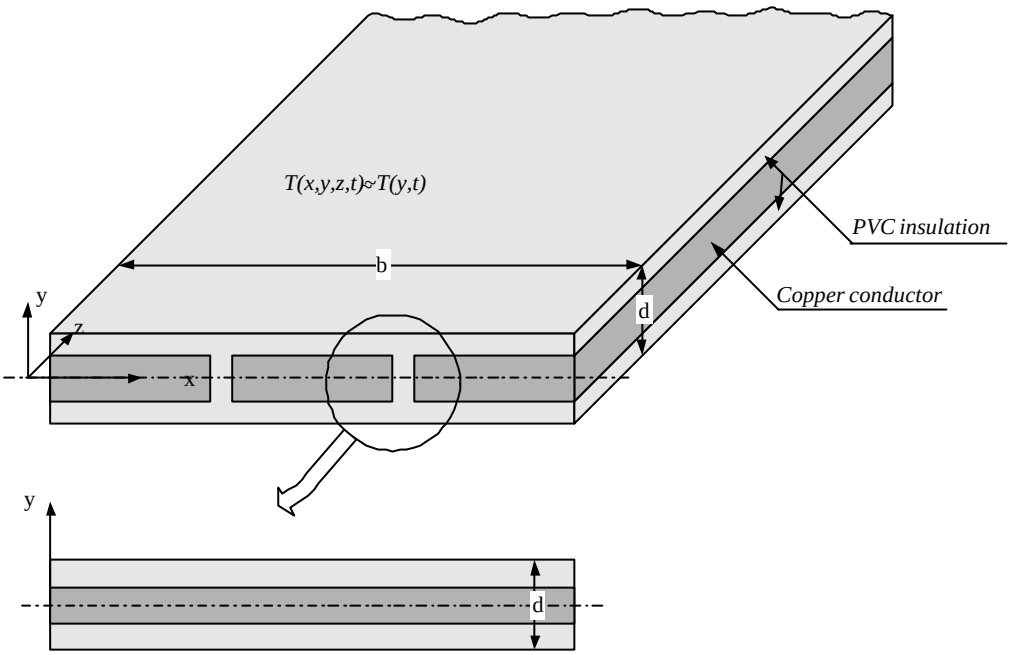

a)

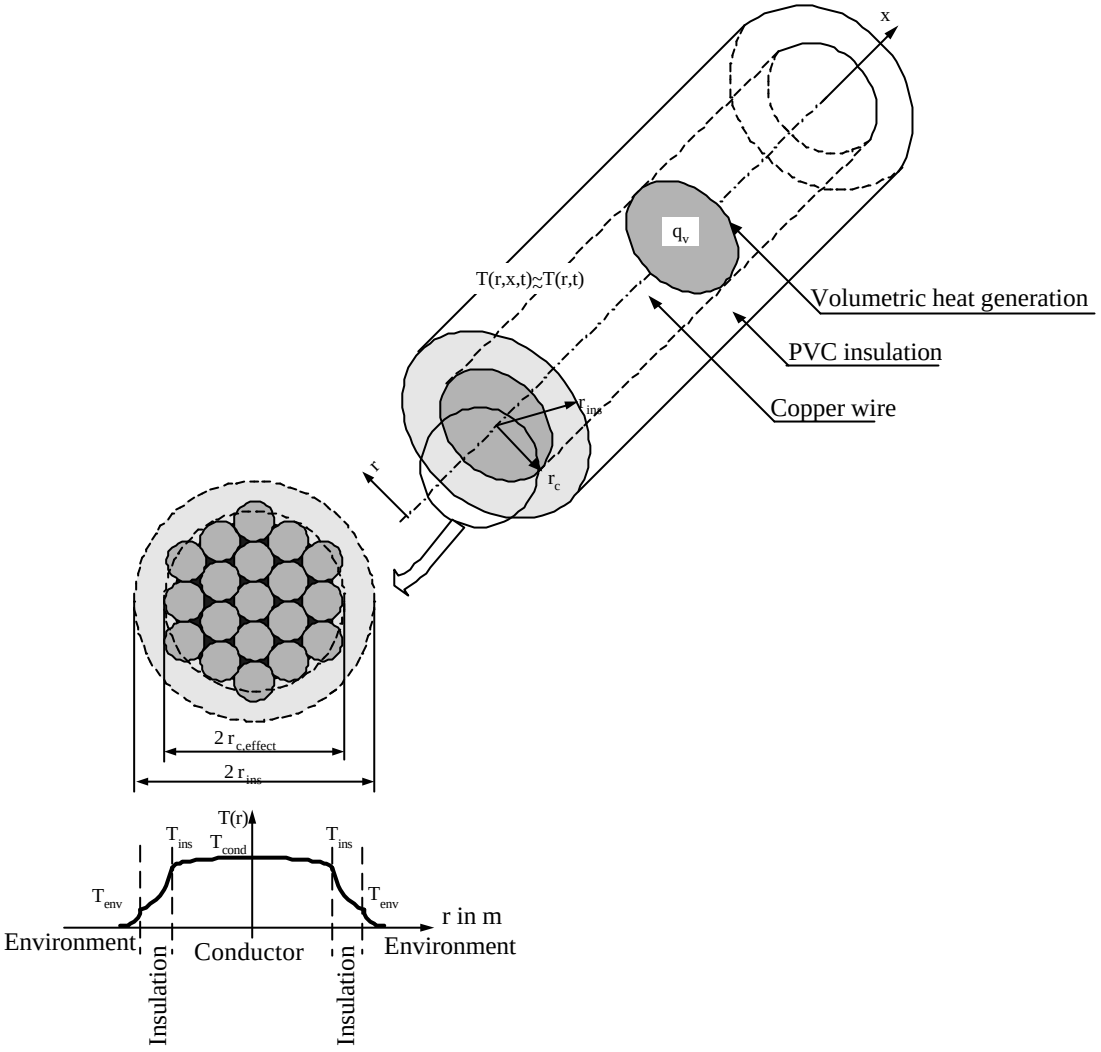
x
q_v
T(r,x,t)≈T(r,t)
Volumetric heat generation
PVC insulation
Copper wire
r_{ins}
r_c
r
$2\,r_{c,effect}$
$2\,r_{ins}$
T(r)
T_{ins}
T_{cond}
T_{ins}
T_{env}
T_{env}
r in m
Environment
Conductor
Environment
Insulation
Insulation

b)

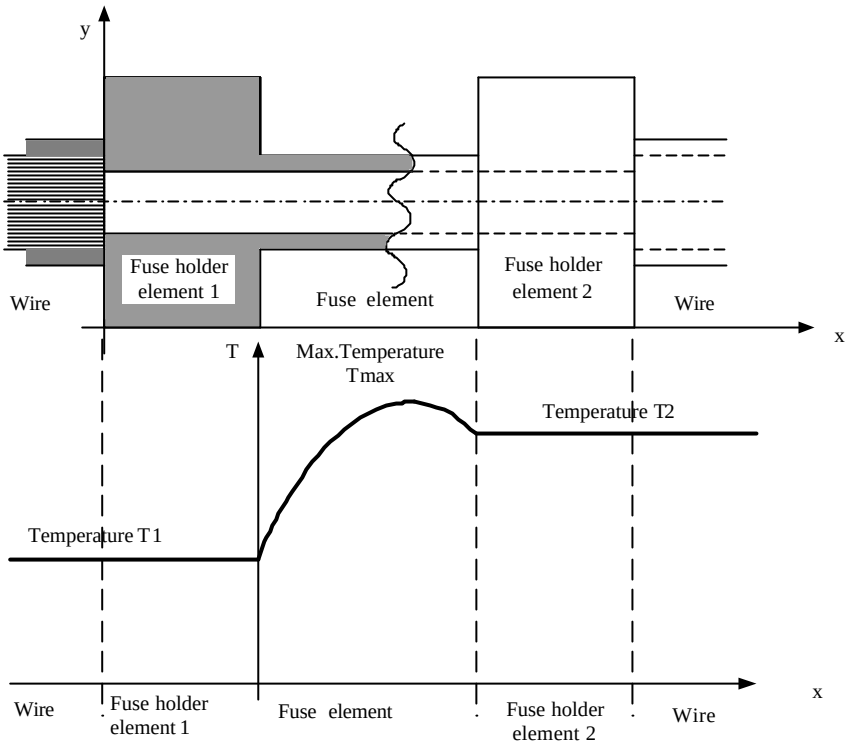

c)

Fig. 2.1 Model geometries and heat conduction parameters: a – flat cable, b – round wire, c – electric fuse

The metallic conductor is assumed homogeneous and a perfect cylinder. In reality, the core of wire is made of a number of single conductors with small air gaps in between. If single conductors are arranged symmetrically, then the wire has a hexagonal shape.

C. The electrical fuse model is one – dimensional (Fig. 2.1, c) with the heat conduction only along the x – axis. The heat conduction in y – direction is not considered because of very high heat conductivity of copper compared to the heat convection from the surface. The shape of the fuse model in x – direction is non-homogeneous. The whole model consists of one layer – copper, bras or any other alloy.

2.3 Conservative form of the heat transfer equations

In order to calculate heat dissipation (heat conduction, convection and radiation), the relevant heat transfer equations have to be solved. These equations define the relationship between the heat generated by electrical current in metallic conductor, and the temperature distribution within the wire or cable (conductor and insulation) and in its surroundings.

The analysis of heat transfer is governed by the *law of conservation of energy*. We will formulate this law on a energy *rate* basis; which means, that at any instant, there must be a balance between all power rates, as measured in Joules (= Ws). The energy conservation law can be written in following form:

$$W_{ent} + W_{\text{int}} = W_{st} + W_{out} \tag{2.1}$$

where:

W_{ent} is the rate of energy entering the electrical conductor. This energy may be generated by other cables or wires located in the vicinity of other cables or by solar energy,

W_{int} is the rate of heat generated internally by Joule losses,

W_{st} is the rate of energy stored within the cable,

W_{out} is the rate of energy which is dissipated by conduction, convection, and radiation.

The inflow and outflow terms W_{ent} and W_{out} are surface phenomena, and these rates are proportional to the surface area. The thermal energy generation rate W_{int} is associated with the rate of conversion of electrical energy to thermal energy and is proportional to the volume. The energy storage is also a volumetric phenomena, but it is simply associated with an increase ($W_{st} > 0$) or decrease ($W_{st} < 0$) in the energy of cable. Under steady-state conditions, there is, of course, no change in energy storage ($W_{st} = 0$). A detailed derivation of the heat transfer equation is given in Appendix A.

From the Equation (2.1), (see also Appendix A) general form of the heat transfer equation in *conservative form* [1]in Cartesian (2.2) and cylindrical (2.2a) coordinates is obtained as follows [11]:

$$\frac{\partial}{\partial x}\left(l \frac{\partial T}{\partial x} \right) + \frac{\partial}{\partial y}\left(l \frac{\partial T}{\partial y} \right) + \frac{\partial}{\partial z}\left(l \frac{\partial T}{\partial z} \right) + q_v = g r \frac{\partial T}{\partial t} \tag{2.2}$$

$$\frac{\partial}{\partial x}\left(l \frac{\partial T}{\partial x} \right) + \frac{1}{r}\frac{\partial}{\partial r}\left(l r \frac{\partial T}{\partial r} \right) + \frac{1}{r^2}\frac{\partial}{\partial f}\left(l \frac{\partial T}{\partial f} \right) + q_V = g r \frac{\partial T}{\partial t} \tag{2.2a}$$

here: $?$ heat conductivity in W/mK

q_V volumetric heat generation in W/m^3

[1] *The conservative form* is a form of heat conduction equation where space dependant thermal conductivity or other coefficients remains conserved within different media of materials. The conservative form is given as

$g \frac{\partial T}{\partial T} = \frac{\partial}{\partial x}\left(l \frac{\partial T}{\partial x} \right)$ and the nonconservative form as $g \frac{\partial T}{\partial t} = l \frac{\partial^2 T}{\partial x^2} + \frac{\partial l}{\partial x}\frac{\partial T}{\partial x}$

g	specific heat capacity	in W/kgK
r	density	in kg/m^3

The heat equations (2.2, 2.2a) are the basis for future heat transfer analysis in electrical conductors.

2.3.1 Flat cables

The heat transfer equation (2.2) for flat cable (Fig. 2.1, a), which is derived (in Appendix A.1) is simplified for one-dimension as follows:

$$-\frac{\partial}{\partial y}\left(l(y,T)\frac{\partial T(y,t)}{\partial y} \right)+g(y,T)\,r\,\frac{\partial T(y,t)}{\partial t}=q_V(y,T) \qquad (2.3)$$

As mentioned in the Chapter 2.3, in this model it is considered middle symmetry (Fig.2.2). This assumption is allowed because heat convection and radiation from "top" side of the cable surface has almost the same heat dissipation rate as from the "bottom" side of the cable. It is important to emphasize, that the free convection in air situation is considered. The cable is placed horizontal in the air.

In order to simplify the model, the metallic conductor is treated as a homogeneous body across the cable width d (see Fig. 2.1,a). Here, the heat conductivity coefficient l is space dependant, due to different material layers in the wire. The specific heat capacity term g is a non-linear function of temperature for copper and PVC insulation. The heat generation by electrical current is expressed as q_v term and is called volumetric specific heat flux. It is a linear function of temperature in metallic conductor and vanishes in PVC insulation.

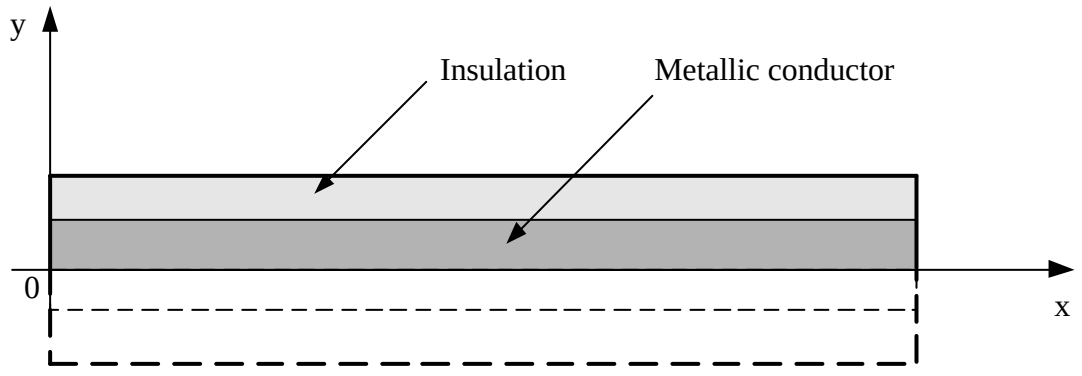

Fig. 2.2 Flat cable model with homogeneous metallic conductor

Here, in the equation (2.3), volumetric heat flux is expressed as:

$$q_V = \frac{dQ}{dV} = \frac{dR \cdot I^2}{A \cdot dl} = \frac{r_{el}\, dl \cdot I^2}{A^2 \cdot dl} = rJ^2 = \frac{I^2 r_{20}}{A^2}\left[1 + a_{20}(T - 20)\right] \tag{2.4}$$

here

r_{el}	specific resistance of the metallic conductor given by	
	$r_{el} = r_{20}\left[1 + a_{20}(T - 20)\right]$	in Om,
r_{20}	specific resistance of the conductor at 20°C temperature	
α_{20}	copper temperature coefficient at 20°C ($\alpha_{20} = 3.83 \cdot 10^{-3}$ 1/K)	in 1/K
l	length of the cable	in m
J	current density	in A/m^2
I	denotes current through the wire	in A
A	area of metallic conductor	in m^2.

2.3.2 Round wires

Heat transfer in round wires is determined, in principle, by the same equation as (2.3), heat transfer in radial direction must also be considered. The general form of heat equation in cylindrical coordinates is:

$$-\left[\frac{1}{r}\frac{\partial}{\partial r}\left(l(r,T)r\frac{\partial T}{\partial r}\right) + \frac{1}{r^2}\frac{\partial}{\partial f}\left(l(r,T)\frac{\partial T}{\partial f}\right) + \frac{\partial}{\partial x}\left(l(r,T)\frac{\partial T}{\partial x}\right)\right] + g(r,T)r\frac{\partial T}{\partial t} = q_V(r,T) \tag{2.5}$$

Taking into account the model simplifications given earlier (see Fig. 1,b), the heat equation is reduced to the one-dimensional form (see also Appendix A.2):

$$-\frac{1}{r}\frac{\partial}{\partial r}\left(l(r,T)r\frac{\partial T(r,t)}{\partial r}\right) + g(r,T)r\frac{\partial T(r,t)}{\partial t} = q_V(r,T) \tag{2.6}$$

The temperature profile in flat cables and round wires shown in Figure (2.1,a,b) under assumption, that the temperature gradient in a metallic conductor is very small due to its very high heat conductivity. In the insulation the temperature gradient is much larger. The main temperature drop, however, is between the wire surface and environment. This temperature drop is caused by convection and described by heat convection coeffi-

cient α. Therefore, here it is very important to determine this coefficient correctly. This problem will be discussed in the section 2.5.

2.3.3 Electric fuses

The following differential equation for the heat transfer in the fuse element is given (Appendix, A.3):

$$-\frac{\partial}{\partial x}\left(A(x)\,l\,\frac{\partial T(x,t)}{\partial x}\right)+\left[a_c(T)\Delta T+a_r(T^4(x,t)-T_{env}^4)\right]\cdot u + g(T)\,rA(x)\frac{\partial T(x,t)}{\partial t}=A(x)q_V(T) \tag{2.7}$$

here:

A	cross section area of the fuse element	in m^2
a_c, a_r	convection and radiation coefficients respectively	
u	circumference	in m
	$\Delta T = T(x,t) - T_{env}$	in K

According to the model (Fig. 2.1,c), the heat transfer should be analysed only in the x direction, because of the short lengths of the fuse melting element. The mathematical model of fuse element should calculate melting temperature of the fuse. Here, radial heat conduction can be neglected due to high heat conductivity of the fuse material.

In equation (2.8) the heat flux q_V is derived in the same way as in equation (2.5). In addition to this, the equation is valid also for a variable cross sectional area.

2.4 Physical material constants

Heat transfer equation given in section 2.3 depends on the specific resistance, heat conductivity and the heat capacity of the conductor material. All three values are temperature dependent, however their values are only known for certain temperatures. In order to interpolate between these given values, a linear or square function has to be used to describe the relationship. This estimation is very important in order to model the heat transfer qualitatively.

Different calculation precision criteria are defined for the analytical approach and for the numerical approach. For the analytical approach it is necessary to have temperature independent or linear dependent constants. The numerical approach of the heat transfer model allows more precise temperature calculation in the conductors. Here, non-linear functions can be implemented for the description of the material constants.

The following diagrams show the exact graphical and numerical coefficients of the specific resistance, *r*, of copper, of the heat conductivity, *?*, of pure copper and PVC, and of the specific heat capacity, *g*, of pure copper and PVC [16]. The temperature range in the diagrams is very wide, although in this work only temperature up to 200°C has been considered. The reason of this high temperature range in the charts is to show the overview how the coefficients behave within wide temperature range. Linear and non-linear approximation has been made using the available data.

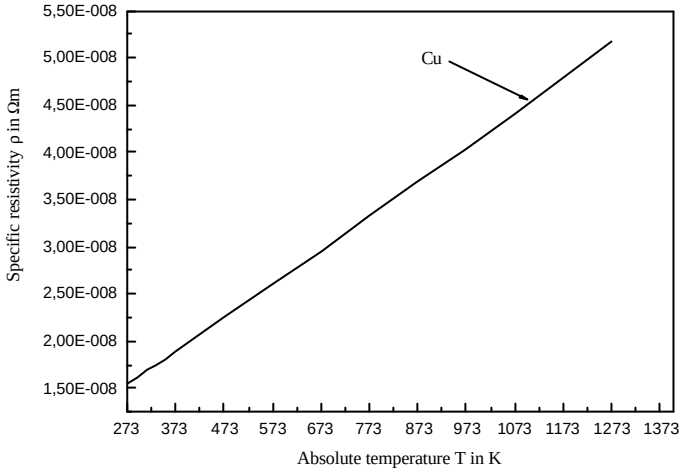

a)

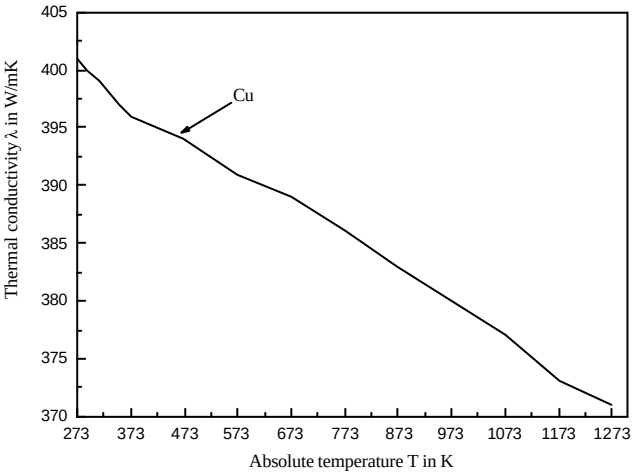

b)

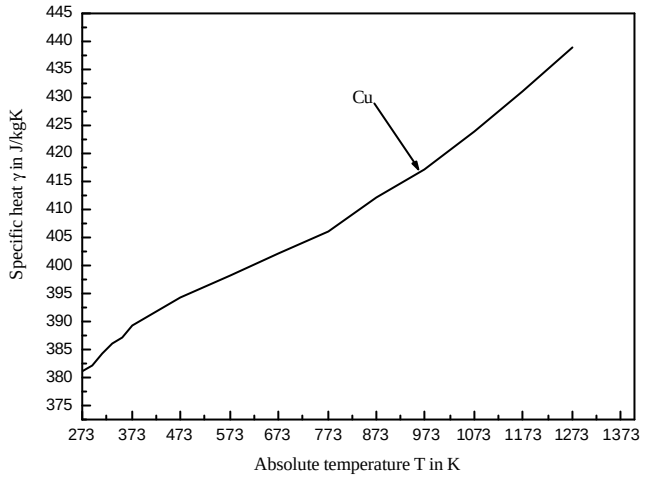

c)

Fig. 2.3 Values of: (a) specific resistance, (b) thermal conductivity and (c) specific heat capacity of pure copper

Heat conductivity and specific heat capacity values of PVC:

Name of material	**DIN code**	**Temperature in °C**		
		20	**50**	**100**
		Thermal heat conductivity ? in W/Km		
Polyvinylchloride	PVC	0.17	0.17	0.17
		Specific heat capacity γ in J/kgK		
Polyvinylchloride	PVC	960	1040	1530

Tab 2.1. Values of thermal conductivity and heat capacity of PVC

Approximation of the temperature dependent copper and PVC material coefficients:

a) Specific resistance of copper r:

$$r = r_0\left[1 + a_r\left(T - T_0\right) + b_r\left(T - T_0\right)^2\right]$$

here:	ρ_0	specific resistance at 20°C,	$\rho_0 = 1.75 \cdot 10^{-8}$	in Om
	α_ρ	linear temperature coefficient,	$\alpha_\rho = 4.00 \cdot 10^{-3}$	in 1/K
	ß$_\rho$	square temperature coefficient.	ß$_\rho = 6.00 \cdot 10^{-7}$	in 1/K^2
	T	temperature of the conductor		in °C

T_0 – reference temperature. In this study reference temperature coincides with environment temperature T_{env} .

b) specific heat capacity of copper g**:**

$g = g_0 + a_g T$, $0 \le T \le 200°C$

here: γ_0 heat capacity at 20°C reference temperature, γ_0 = 381 in J/kgK
α_γ approximated linear temperature coefficient of heat capacity in 1/K
α_γ = 0.17 1/K

c) specific heat capacity of PVC g**:**

$g = g_0 - a_g T + b_g T^2$ $0 \le T \le 100°C$

here: γ_0 heat capacity at 20°C reference temperature, γ_0 = 920 in J/kgK
α_γ approximated linear temperature coefficient of heat capacity in 1/K
α_γ = 1.3 1/K
ß$_\gamma$ approximated square temperature coefficient of heat capacity in 1/K^2
ß$_\gamma$ =0.074 1/K^2

2.5 Determination of heat transfer coefficients

The heat transfer from the surface is governed by convection and radiation. This effect can be described by the corresponding *convection* and *radiation heat transfer coefficients.* Both depend on the surface and environment temperatures.

Convection takes place between the boundary surface and a heat transport by a fluid (e.g. air) in motion at a different temperature. Radiation occurs by electromagnetic wave heat exchange between the surface and its surrounding environment separated by air.

In this work the convective heat transfer coefficient of laminar flow has to be examined for the following two different model geometries:

- horizontal cylinder surfaces
- horizontal plate surfaces

The result of this examination leads to two different heat transfer coefficients valid for round and for plate surfaces. The convection and radiation coefficient appears in the boundary conditions of the heat transfer equations for the electrical conductor models. At the lower temperatures, which are typical for electric cable applications, convection is the basic heat dissipation component (ca. 90%).

In this work, the heat transfer in electrical conductors is computed by an analytical calculation (of the heat conduction equations) in the steady state regime and by a numerical algorithm in a transient state regime. Therefore, the convection and radiation coefficients for the analytical solution has to be linearized and to be presented in an approximated form in order to obtain simple but sufficiently accurate equations of the convection and radiation coefficients. For the numerical algorithm the coefficients will be derived in a non-linear form since both are non-linear (temperature dependent).

2.5.1 Convection coefficient for the long horizontal cylinders

The mainly applied round geometry has been studied extensively. Many correlations exist between the different calculation methods. The literature [11] presents simple algorithms for the calculation of convective coefficients of the cylinders. This work follows the procedure proposed by [17], where many approaches of the various procedures are summarised. The equations of this procedure were validated by the experimental data in the diploma work [18]. All notations of physical constants and material properties will be used from the works [17, 18].

In general, the heat dissipation by convection is defined as:

$$q_c = \alpha_c (T_s - T_\infty) \tag{2.8}$$

here: T_s surface temperature of the solid in °C,
$T_¥ = T_{env} + 273.15$ the absolute temperature of the fluid in K.

The convection coefficient α_c can be calculated as follows:

$$\alpha_c = \frac{l}{d} Nu \tag{2.9}$$

here: l heat conduction of air in W/m²K,
Nu Nusselt number
d diameter of cylinder in m.

The Nusselt number for a horizontal cylinder according to Wärmeatlas (Heat Transfer Atlas) [17] is expressed by:

$$Nu = \left\{ 0.752 + \frac{0.387\, Ra^{1/6}}{\left[1 + \left(\frac{0.559}{\mathrm{Pr}} \right)^{9/16} \right]^{8/27}} \right\}^2 \tag{2.10}$$

In this equation the Rayleigh number *Ra* is calculated as:

$$Ra = Gr\,Pr \tag{2.11}$$

Here: Pr Prandtl number (see Tab. 2.2) and
Gr Grashof number defined by the following equation:

$$Gr = \frac{g d^3 b (T - T_\infty)}{\nu^2}, \tag{2.12}$$

here: g gravitational acceleration in m/s^2,
$ß$ volumetric thermal expansion coefficient in 1/K,
n kinematic viscosity in (m^2/s).

The $ß$ coefficient for ideal gas with justifiable error can be considered as:

$$b = \frac{1}{T_\infty} \tag{2.13}$$

where $T_¥ = T_{env} + 273.15$ - the absolute temperature of the fluid (in K)

The material constants l, n and Pr of air are taken from Heat Transfer Atlas [17]. These constants are dependent on the average temperature T_{ave}:

$$T_{ave} = \frac{1}{2}(T_s + T_{env}) \tag{2.14}$$

here T_s is temperature of the surface of cylinder (in °C) and T_{env} – environment temperature (in °C).

With the equations (2.9) and (2.10), the convection coefficient α_c is written as follows:

$$a_c = \frac{l}{d}\left\{0.752 + \frac{0.387 Ra^{1/6}}{\left[1 + \left(\frac{0.559}{\mathrm{Pr}}\right)^{9/16}\right]^{8/27}}\right\}^2 \tag{2.15}$$

Replacing in the equation (2.15) the Rayleigh number Ra, the Prandl number Pr and heat conductivity l leads to the following form, which is only diameter d and temperature difference ΔT dependant:

$$\boxed{a_c = \left[K_{d1}\left(\frac{1}{d}\right)^{1/2} + K_{T1}(\Delta T)^{1/6}\right]^2} \tag{2.16}$$

where: $K_{d1} = 0.752\, l^{1/2}$, (2.17)

and

$$K_{T1} = \frac{0.387\, l^{1/2}}{\left[1+\left(\frac{0.559}{\mathrm{Pr}}\right)^{9/16}\right]^{8/27}}\left(\frac{\mathrm{Pr}\, gb}{v^2}\right)^{1/6} \tag{2.18}$$

The physical constants of air i.e. (heat conductivity l, kinematic viscosity n and the Prandtl number Pr) can be found in the literature [17]. For the volumetric thermal expansion coefficient ß, air is considered as an ideal gas. For reference, environment temperature is taken.

In the table 2.2 K_{d1} and K_{T1} values for a temperature range from 20 to 140°C are given.

Surface temperature *T* in °C	**Temperature T_{ave} in °C**	**Heat conductivity *l* in 10^{-3} W/mK**	**Kinematic viscosity n in 10^{-6} m^2/s**	**Prandtl number *Pr***	**K_{d1}**	**K_{T1}**
20	20	25.67	15.35	0.7147	0.1205	1.1121
40	30	26.41	16.29	0.7133	0.1222	1.1054
60	40	27.14	17.25	0.7121	0.1239	1.0990
80	50	27.87	18.23	0.7110	0.1255	1.0928
100	60	28.58	19.24	0.7100	0.1271	1.0868
120	70	29.29	20.26	0.7091	0.1287	1.0810
140	80	30.00	21.31	0.7083	0.1302	1.0754
Average:					**0.1254**	**1.0932**

Tab 2.2. Physical constants of air for temperature from 20 to 140 °C

The averaged form of the convective coefficient for temperature range from 20 to 140°C is following:

$$\boxed{a_c = \left[0.1254\left(\frac{1}{d}\right)^{1/2} + 1.0932(\Delta T)^{1/6}\right]^2} \tag{2.19}$$

2.5.2 Convection coefficient for horizontal plates

For the application for flat cables the free convection of horizontal plates has been considered as well. For this geometry, we have to distinguish between the convection from the top side of the plate surface and the bottom side.

The convection coefficient α_c is calculated similar to equation (2.9):

$$a_c = \frac{l}{l} Nu \tag{2.20}$$

here l is characteristic length, which is defined as:

$$l \equiv \frac{A}{P},$$

where A and P are the plate surface and perimeter, respectively.

A. The Nusselt number for the **upper side** of horizontal plate according to Wärmeatlas (Heat Transfer Atlas) [17] is expressed by:

a. For laminar flow:

$$Nu = 0.766 \left[Ra \left(1 + \left(\frac{0.322}{\mathrm{Pr}} \right)^{11/20} \right)^{-11/20} \right]^{1/5}, \tag{2.21}$$

here: $Ra \left[1 + \left(\frac{0.322}{\mathrm{Pr}} \right)^{11/20} \right]^{-20/11} \leq 7 \cdot 10^4$.

b. For turbulent flow:

$$Nu = 0.15 \left[Ra \left(1 + \left(\frac{0.322}{\mathrm{Pr}} \right)^{11/20} \right)^{-11/20} \right]^{1/3} \tag{2.22}$$

here: $Ra \left[1 + \left(\frac{0.322}{\mathrm{Pr}} \right)^{11/20} \right]^{-20/11} \geq 7 \cdot 10^4$.

B. The Nusselt number for the **lower side** of a horizontal plate has the following form (only laminar convection):

$$Nu = 0.6\left[Ra\left(1+\left(\frac{0.492}{\mathrm{Pr}} \right)^{9/16} \right)^{-16/9} \right]^{1/5} \tag{2.23}$$

here $10^3 < Ra\left[1+\left(\frac{0.492}{\mathrm{Pr}} \right)^{9/16} \right]^{-16/9} < 10^{10}$

All the equations (2.1, 2.13) and Nusselt numbers given in (2.21, 2.22, 2.23) are inserted into equation (2.20). This leads to the following form of the convection coefficients:

A. Upper side

a. Laminar flow:

$$\boxed{a_c = K_{T21}\left(\frac{1}{l} \right)^{8/3} (\Delta T)^{1/5}} \tag{2.24}$$

here:

$$K_{T21} = 0.766\, l\left[\frac{\mathrm{Pr}\, gb}{\nu^2}\left(1+\left(\frac{0.322}{\mathrm{Pr}} \right)^{11/20} \right)^{-11/20} \right]^{1/5} \tag{2.25}$$

b. Turbulent flow:

$$\boxed{a_c = K_{T22} l (\Delta T)^{1/3}} \tag{2.26}$$

here:

$$K_{T22} = 0.15\, l\left[\frac{\mathrm{Pr}\, gb}{\nu^2}\left(1+\left(\frac{0.322}{\mathrm{Pr}} \right)^{11/20} \right)^{-11/20} \right]^{1/3} \tag{2.27}$$

B. Lower side (laminar flow only):

$$\boxed{a_c = K_{T31}\left(\frac{1}{l} \right)^{8/3} (\Delta T)^{1/5}} \tag{2.28}$$

here:

$$K_{T31} = 0.6\,l\left[\frac{\Pr\, gb}{v^2}\left(1+\left(\frac{0.322}{\Pr}\right)^{9/16}\right)^{-16/9}\right]^{1/5} \tag{2.29}$$

2.5.3 Exact mathematical expressions of the physical constants of air

The physical constants of air depend very much on temperature. These functions are of higher polynomial order, which were obtained by fitting of the given results in the Wärmeatlas [17]. With these functions, a very high accuracy of convection coefficient can be achieved and the function can easily be implemented into the computer program. Here, the wide temperature range is used in order to expand the validity range of temperature dependent constants in the computer program.

A. Heat conductivity in air l (T_{ave}):

Temperature range for the fitting procedure: $-200\ °C \le T_{ave} \le 1000\,°C$

Obtained polynomial function by fitting:

$$l(T_{ave}) = 0.02416 + 7.61617\cdot 10^{-5} T_{ave} - 4.3282\cdot 10^{-8} T_{ave}^2 + 4.36064\cdot 10^{-11} T_{ave}^3 - 1.99059\cdot 10^{-14} T_{ave}^4 \tag{2.30}$$

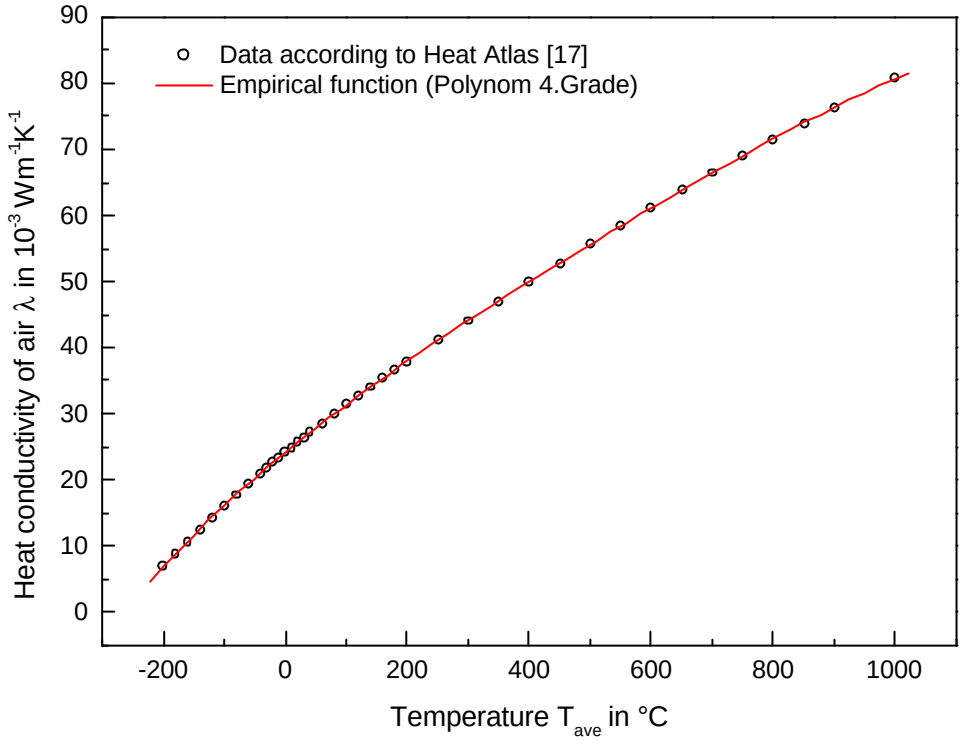

Fig. 2.4 Heat conductivity of air as a function of temperature at constant pressure P = 10^5 Pa

B. Kinematic viscosity $n(T_{ave})$:

Temperature range for the fitting procedure: $-200\,°C \le T_{ave} \le 1000\,°C$

Obtained polynomial function by fitting:

$$n(T_{ave}) = 1.35391\cdot 10^{-5} + 8.82402\cdot 10^{-8} T_{ave} + 1.14171\cdot 10^{-10} T_{ave}^{2} - 4.6463\cdot 10^{-14} T_{ave}^{3} + 1.64882\cdot 10^{-17} T_{ave}^{4} \quad (2.31)$$

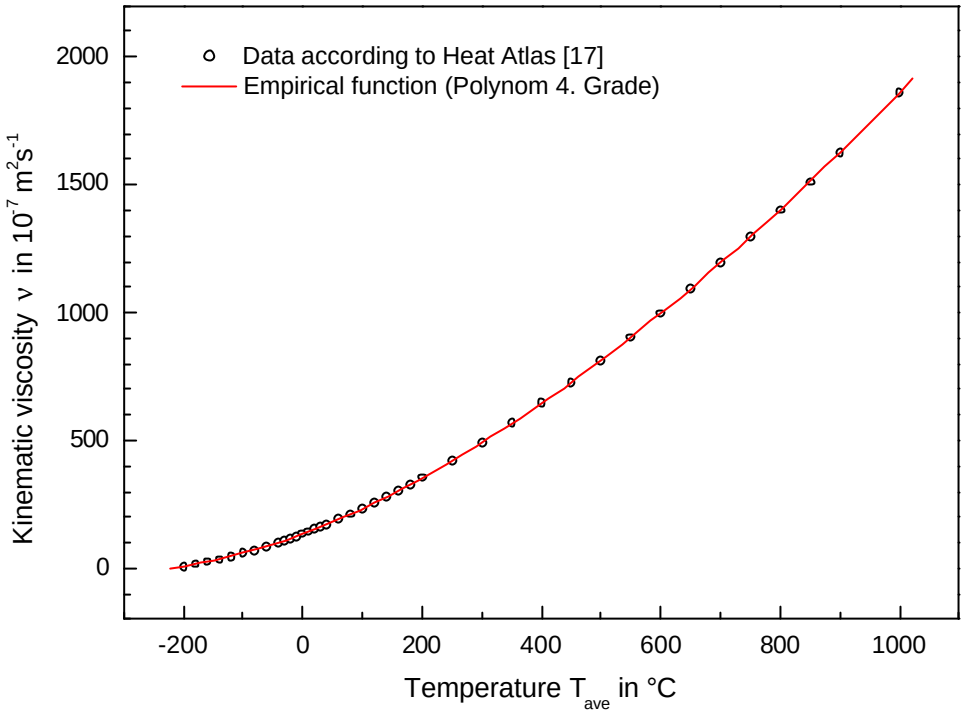

Fig. 2.5 Kinematic viscosity of air as a function of temperature at cons tant pressure P = 10^5 Pa

C. Prandtl number $Pr(T_{ave})$

Temperature range for the fitting procedure: $-125°C \le T_{ave} \le 650°C$

Obtained polynomial function by fitting:

$$\Pr(T_{ave}) = 0.71779 - 1.6855 \cdot 10^{-4} T_{ave} + 6.91108 \cdot 10^{-7} T_{ave}^2 - 9.11289 \cdot 10^{-10} T_{ave}^3 + 4.32316 \cdot 10^{-13} T_{ave}^4 \quad (2.32)$$

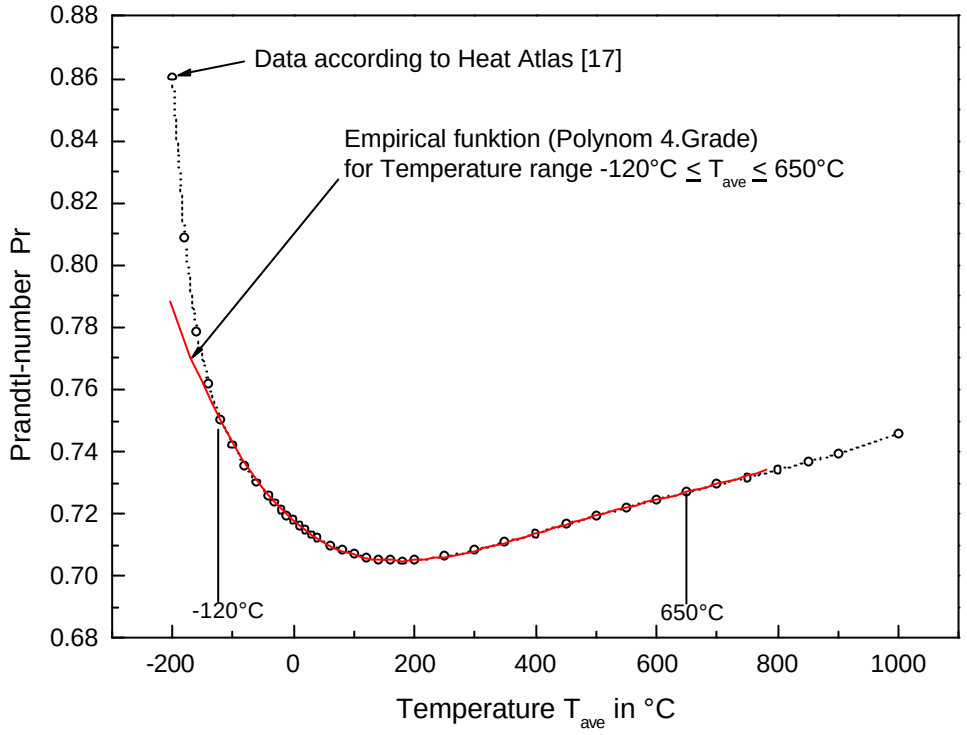

Fig. 2.6 Prandtl-number of air as a function of temperature at constant pressure $P = 10^5$ Pa

2.5.4 Radiation

In order to describe heat transfer by the thermal radiation in electrical conductors, the exchange of radiation energy between the insulated conductor surface and the infinitely large environment is considered.

It may occur not only from solid surfaces but also from liquids and gases [11]. The energy of the radiation is transported by electromagnetic waves (or alternatively, photons). While the transfer of energy by conduction or convection requires the presence of a material medium, radiation does not. In fact, radiation transfer occurs most efficiently in a vacuum. The complete electromagnetic spectrum is shown in Figure 2.7. The short wavelength gamma rays, X rays and ultraviolet (UV) radiation are primarily of interest to the high energy physicist and nuclear engineer, while the long wavelength microwaves and radio waves are of concern to the electrical engineers. It is the intermediate portion of the spectrum, which extends from approximately 0.1 to 100 µm. It includes a part of the UV and all of the visible infrared (IR), that is called *thermal radiation* and belongs to heat transfer.

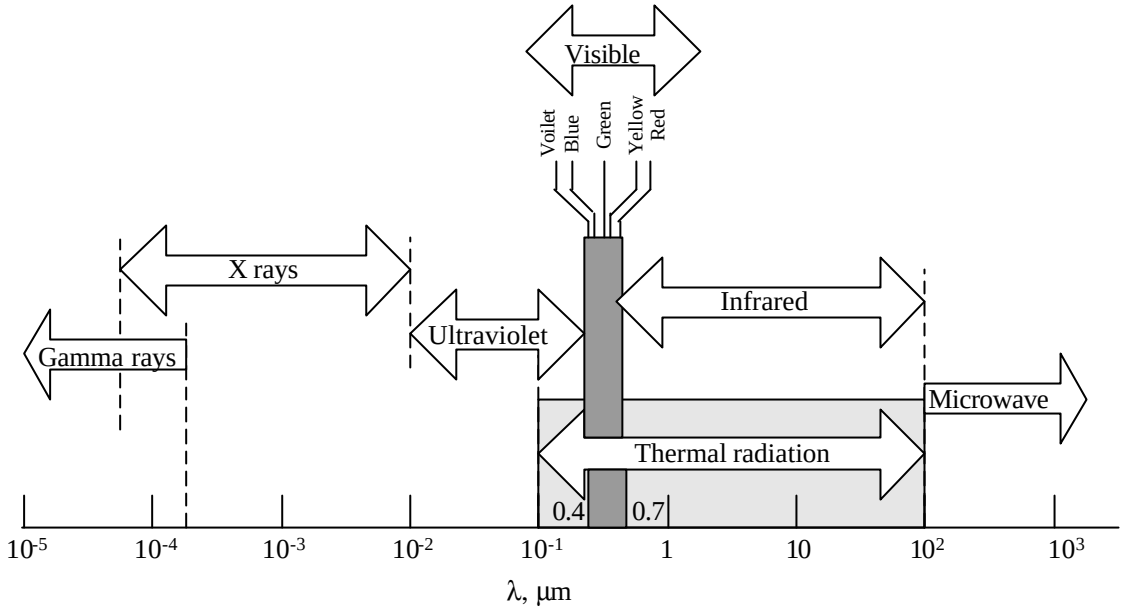

Fig. 2.7 Spectrum of electromagnetic radiation

The maximum flux (W/m^2) at which radiation may be emitted from a surface is given by the *Stefan-Boltzmann law*:

$$q_r = sT_s^4 \tag{2.33}$$

where T_S is the absolute temperature (K) of the surface and s is the *Stefan-Boltzmann constant* ($s = 5.67 \cdot 10^{-8} W/m^2 K^4$). Such a surface is called an ideal radiator or black body. The heat flux emitted by a real surface is less than that of the ideal radiator and is given by

$$q_r = e\, sT_s^4 \tag{2.34}$$

where ε is a radiative property of the surface called the *emissivity.* This property indicates how efficiently the surface emits compared to an ideal radiator.

The rate of heat exchange between the cable surface and its surroundings, expressed per unit area of the surface, is:

$$q_r = e\, s\left(T_s^4 - T_{env}^4\right) \tag{2.35}$$

In order make it compatible with heat convection, it is convenient to express the radiation heat exchange in the form:

$$q_r = a_r\left(T_s - T_{env}\right) \tag{2.36}$$

where from Equation (2.35) the *radiation heat transfer coefficient* a_r is:

$$\boxed{a_r \equiv e s (T_s + T_{env})(T_s^2 + T_{env}^2)} \tag{2.37}$$

Here we have modelled the radiation in the same way as convection. In this sense we have linearised the radiation rate equation, making the heat rate proportional to a temperature difference rather than to the difference between two temperatures to the fourth power. Note, however, that α_r depends strongly on temperature, while the temperature dependence of the convection heat transfer coefficient α_c is generally weak.

Since the free convection and radiation transfer occurs simultaneously, the convection and radiation has to be added. Then the total rate of heat transfer from the surface is as follows:

$$q = q_c + q_r = a_c (T_s - T_{env}) + e s (T_s^4 - T_{env}^4) \tag{2.38}$$

The total heat transfer by convection and radiation expressed as the *heat transfer coefficient* a is:

$$\boxed{a = a_c + a_r = a_c + e s (T_s + T_{env})(T_s^2 + T_{env}^2)} \tag{2.39}$$

2.6 Boundary conditions

In order to have a unique solution of the PDE (partial differential equation), boundary and initial conditions have to be specified as shown below. In case of differential equations for the electrical fuse, *prescribed* boundary conditions are used. PDE's of flat and round electrical cables will have *symmetry* and *non-linear convective-radiative* boundary conditions.

1. Flat electrical cable

- initial condition

$$T(y,0) = T_{env}(y) \tag{2.40}$$

- boundary conditions

$$\begin{cases} \lim\limits_{y\to 0} l\,\dfrac{\partial T(y,t)}{\partial y} = 0, \\ -\,l\,\dfrac{\partial T}{\partial y}\Big|_{y=y_N} = a\,(l,\Delta T)(T - T_{env}) + e\,s\,(T^4 - T_{env}^4). \end{cases} \tag{2.41}$$

2. Round electrical wire

- initial condition

$$T(r,0) = T_{env}(r) \tag{2.42}$$

- boundary conditions

$$\begin{cases} \lim\limits_{r\to 0} r\,l\,\dfrac{\partial T(r,t)}{\partial r} = 0, \\ -\,l\,\dfrac{\partial T}{\partial r}\Big|_{r=r_N} = a\,(d,\Delta T)(T - T_{env}) + e\,s\,(T^4 - T_{env}^4). \end{cases} \tag{2.43}$$

3. Electrical fuse

- initial condition

$$T(x,0) = T_{env}(x) \tag{2.44}$$

- boundary conditions

$$\begin{cases} T(0,t) = T_1(t) \\ T(x,t) = T_2(t) \end{cases} \tag{2.45}$$

The boundary and initial conditions in equations (2.40-2.45) are generally valid and implemented into the numerical algorithm of heat transfer calculations.

In the analytical analysis of heat transfer (Chapter 3), some additional boundary conditions will be used to solve the PDE of flat cables and round wires. Here we have to calculate with the constant heat transfer coefficient and do not take into account the nonlinear phenomena of radiation.

The following additional boundary conditions apply for a flat electrical cable:

$$\begin{cases} \left.\dfrac{dT}{dy}\right|_{y=y_0} = -\dfrac{EI}{2(d+b)\,l_{ins}}, \\ \left.\dfrac{dT}{dy}\right|_{y=y_1} = -\dfrac{a}{l_{ins}}(T - T_{env}) \end{cases} \tag{2.46}$$

In case of cylindrical wire:

$$\begin{cases} \left.\dfrac{dT}{dr}\right|_{r=r_0} = -\dfrac{EI}{2\pi r_0\, l_{ins}}, \\ \left.\dfrac{dT}{dr}\right|_{r=r_1} = -\dfrac{a}{l_{ins}}(T - T_{env}) \end{cases} \tag{2.47}$$

CHAPTER 3

ANALYTICAL ANALYSIS OF HEAT TRANSFER IN A STEADY STATE

In the preceding Chapter 2, a definition of heat transfer equations for the study of analytical and numerical heat transfer computation was given. The objective of those equations is to determine the temperature field in different kinds of electrical conductors where heat conduction, convection/radiation and energy generation takes place. Different boundary conditions were also given for the solutions of those equations.

The aim of the present chapter is to obtain exact analytical solutions in a steady-state regime. Because of the linearization of differential equations, some difference between numerical and analytical results will occur, but these mismatches can be accepted in many situations. It is always convenient to have a simple analytical solution if a steady state is required.

The following assumptions are made to simplify the partial differential equations:

a) steady-state conditions,
b) one-dimensional conduction,
c) constant or linear material properties,
d) uniform volumetric heat generation,
e) constant heat transfer coefficient.

3.1 Calculation of the thermo-electrical characteristics of flat cables

3.1.1 Vertical heat transfer with temperature-independent coefficients

For pure vertical heat transfer in flat cables equation (2.6, Chapter 2) will be used:

$$-\frac{\partial}{\partial y}\left(l(y)\frac{\partial T}{\partial y} \right)+g(T)r\frac{\partial T}{\partial t}=q_V(T,y) \tag{2.6}$$

Considering assumptions for the heat equation made before we get the following equation:

$$\frac{\partial^2 T(y,t)}{\partial y^2} + \frac{EI}{lA} - \frac{gr}{l}\frac{\partial T(y,t)}{\partial t} = 0 \tag{3.1}$$

or,

$$\frac{\partial^2 T(y,t)}{\partial y^2} + C - D\frac{\partial T(y,t)}{\partial t} = 0 \tag{3.2}$$

here: $C \equiv \frac{EI}{lA} = \frac{rI^2}{lA^2}$; $D \equiv \frac{gr}{l}$.

3.1.2 Vertical heat transfer with temperature-dependent coefficients

Considering specific resistance r and electrical field strength E dependence on temperature:

$$r(T) = r_0\left[1 + a_r\left(T(y,t) - T_{env}\right)\right] \tag{3.3}$$

$$E(T) = E_0\left[1 + a_r\left(T(y,t) - T_{env}\right)\right] \tag{3.4}$$

here:	a_r	linear temperature coefficient of resistance	in 1/K
	r_0	specific resistance at reference temperature T_0	in °C
	E_0	field strength at reference temperature T_0	in °C

Then, equation (3.2) obtains this form:

$$\frac{\partial^2 T(y,t)}{\partial y^2} + \frac{IE_0}{lA}\left[1 + a_r\Delta T(y,t)\right] - \frac{gr}{l}\frac{\partial T(y,t)}{\partial t} = 0$$

$$\frac{\partial^2 T(y,t)}{\partial y^2} + \frac{a_r IE_0}{lA}\Delta T(y,t) + \frac{IE_0}{lA} - \frac{gr}{l}\frac{\partial T(y,t)}{\partial t} = 0 \tag{3.5}$$

or,

$$\boxed{\frac{\partial^2 T(y,t)}{\partial y^2} + B\Delta T(y,t) + C - D\frac{\partial T(y,t)}{\partial t} = 0} \tag{3.6}$$

Since in equation (3.6) the term with B is temperature dependant, steady state can only be reached if additional conditions are satisfied. The necessity of such a condition arises from the fact that the specific resistance r increases with temperature.

The solution of temperature change in time can be presented in the following form:

$$T(t,y) = \sum_{j=1}^{\infty} g_j(t) \sin pj\left(\frac{y+\frac{d}{2}}{d}\right) \tag{3.6b}$$

This result is recognised as a Fourier sine-series expansion of the arbitrary function $T_j(y)$, for which the constant amplitudes g_j are given by:

$$g_j(t) = \frac{2}{d}\int_0^d T_i(y) \sin pj\left(\frac{y+\frac{d}{2}}{d}\right) y dy\,. \tag{3.6c}$$

Only, if $B < \frac{p^2}{d^2}$ the solution of steady state temperature exist.

here: $B \equiv \frac{a_r E_0 I}{lA}$; $C \equiv \frac{E_0 I}{lA}$; $D \equiv \frac{g}{l}$; $\frac{C}{B} \equiv \frac{1}{a_r} = \hat{T}$; $\Delta T = T(y,t) - T_{env}$.

3.1.3 Stationary solution of vertical heat transfer equation

The stationary solution will be obtained for rectangular cables, namely, flat cables, where the cable width b is much larger than the thickness d. This solution describes the temperature pattern in a metallic conductor of a flat cable and its insulation in vertical y direction.

Three different cases of electrical conductor are considered, for which a stationary solution of the heat equation is achieved:

A) Cable without insulation and temperature-dependent specific resistance r ($B \neq 0$), *Dirichlet boundary conditions*;
B) Cable without insulation and temperature-independent specific resistance r ($B = 0$), *symmetry and convective boundary conditions*;
C) Cable with insulation and temperature-independent specific resistance r ($B = 0$), *symmetry and convective boundary conditions*.

Case A. Cable without insulation and temperature-dependent specific resistance r ($B \neq 0$).

The heat equation (3.6) for steady-state simplifies to:

$$\frac{\partial^2 T(y)}{\partial y^2} + B\Delta T(y) + C = 0 \tag{3.7}$$

The general solution of equation (3.7) is:

$$T(y) = T_1 \sin\sqrt{B}y + T_2 \cos\sqrt{B}y - \frac{C'}{B} \tag{3.8}$$

here $T_{1,2}$ – integration constants in °C and $C' = BT_{env} - C$.

In order to get a temperature profile, boundary conditions for the equation (3.8) have to be applied. The temperatures are fixed at the boundary (Dirichlet conditions) at the bottom side of the flat cable (*y=-d/2*) and upper side - (*y=d/2*).

For *y=-d/2*:

$$T\left(-\frac{d}{2}\right) = T_{01} = -T_1 \sin\sqrt{B}\frac{d}{2} + T_2\sqrt{B}\cos\frac{d}{2} + \hat{T} \tag{3.9a}$$

For *y=d/2*:

$$T\left(\frac{d}{2}\right) = T_{02} = T_1 \sin\sqrt{B}\frac{d}{2} + T_2\sqrt{B}\cos\frac{d}{2} + \hat{T} \tag{3.9b}$$

This leads to the integration constants $T_{1,2}$:

$$T_1 = \frac{T_{01} - T_0}{2\sin\sqrt{B}\frac{d}{2}} \tag{3.10a}$$

$$T_2 = \frac{T_0 + T_{01} - 2\hat{T}}{2\cos\sqrt{B}\frac{d}{2}} \tag{3.10b}$$

The insertion of integration constants into the general solution (3.8) gives the following temperature distribution in the flat cable:

$$\boxed{T(y) = \frac{T_{02} - T_{01}}{2\sin\sqrt{B}\frac{d}{2}}\sin\sqrt{B}y + \frac{T_{01} + T_{02} - 2\hat{T}}{2\cos\sqrt{B}\frac{d}{2}}\cos\sqrt{B}y + \hat{T}} \tag{3.11}$$

here: d – thickness of the cable, T_{01}- boundary temperature at $y=-d/2$, T_{02}-boundary temperature at $y=d/2$.

For $T_{01} = T_{02}$ equation (3.11) can be simplified:

$$T(y) = \hat{T} - \frac{\hat{T} - T_{01}}{\cos\sqrt{B}\frac{d}{2}} \cos\sqrt{B}y \tag{3.12}$$

Case B. Cable without insulation and temperature-independent specific resistance r $(B = 0)$

In case the temperature dependence of the specific resistance can be neglected, the equation (3.2) simplifies to:

$$\frac{\partial^2 T(y,t)}{\partial y^2} + C = 0 \tag{3.13}$$

The general solution of this equation (3.13) is:

$$T(y) = -\frac{C}{2} y^2 + T_1 y + T_2 \tag{3.14}$$

where T_1 and T_2 are integration constants.

Symmetry and convective boundary conditions (Fig.3.1) are applied:

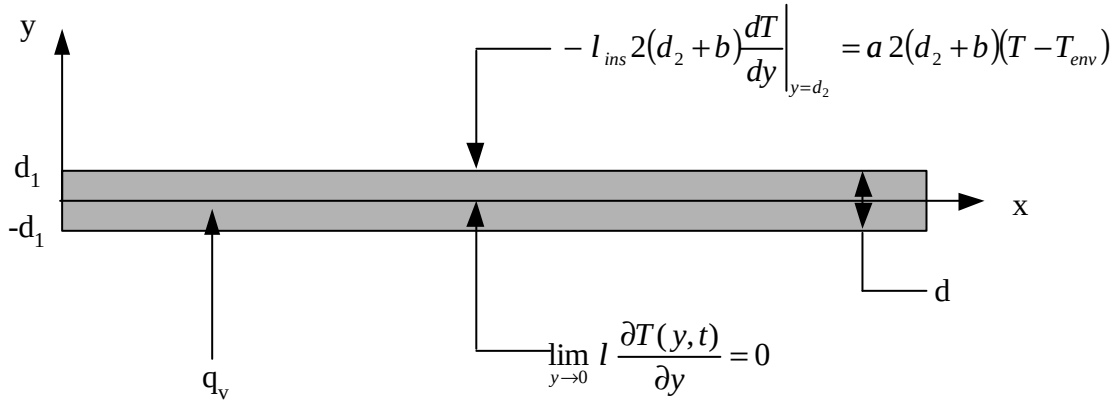

Fig. 3.1 Boundary conditions considering temperature gradient in conductor only of flat cable

at $y=0$: $$\left.\frac{\partial T}{\partial y}\right|_{y=0} = 0 \text{ ; and} \tag{3.15}$$

at $y=d_1$: $$l\,2(d_1+b)\left.\frac{\partial T}{\partial y}\right|_{y=d_1} = -a\,2(d_1+b)(T-T_{env}) \text{, or}$$

$$\left.\frac{\partial T}{\partial y}\right|_{y=d_2} = -\frac{a}{l}(T-T_{env}) . \tag{3.16}$$

The relationship (3.16) is developed by applying a surface energy balance. Here the heat transfer coefficient is considered constant.

Substituting the appropriate rate equations (3.13, 3.14, 3.15 and 3.16) temperature profile in the conductor of flat cable is obtained:

$$T(y) = \frac{C}{2}d_1^2\left(1-\frac{y^2}{d_1^2}\right)+T_{env}+\frac{EI}{a\,2(d_1+b)}d_1 \tag{3.17}$$

$$\boxed{T(y) = \frac{C}{2}d_1^2\left(1-\frac{y^2}{d_1^2}\right)+T_{env}+\frac{EI}{a\,2(d_1+b)}d_1}$$

here: C

Case C. Cable with insulation and temperature-independent specific resistance r ($B=0$)

For the calculation of the temperature distribution in an insulated flat cable (case C), the boundary conditions should be applied to the borders of the insulation (see Fig.3.2). Due to high thermal conductivity of the conductor compared to the insulation, the temperature gradient in the metallic conductor can be assumed to be zero. Applying as overall energy balance law to the flat cable model, we obtain following boundary conditions:

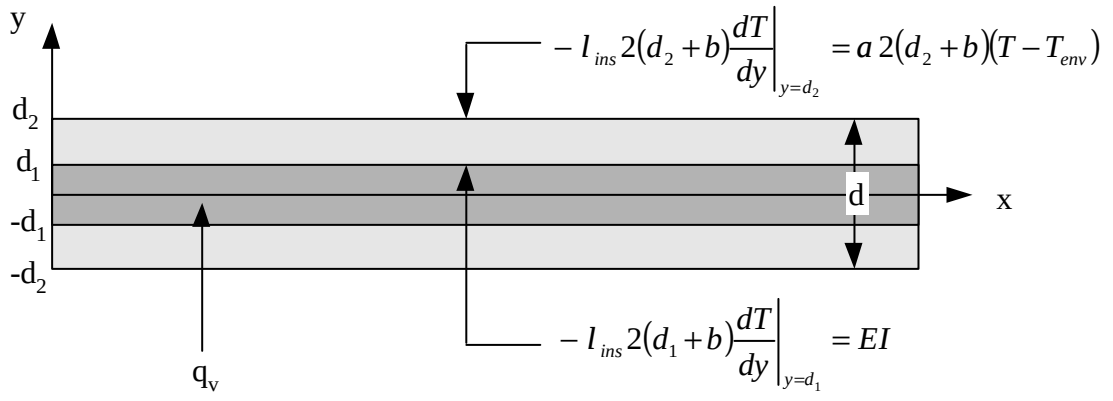

Fig. 3.2 Boundary conditions considering temperature gradient in the insulation alone of flat cable

at $y = d_1$:

$$- l_{ins} 2(d_1 + b) \left.\frac{dT}{dy}\right|_{y=d_1} = EI \text{, or} \qquad \left.\frac{dT}{dy}\right|_{y=d_1} = -\frac{EI}{2(d_1 + b) l_{ins}}; \tag{3.18}$$

at $y = d_2$:

$$- l_{ins} 2(d_2 + b) \left.\frac{dT}{dy}\right|_{y=d_2} = a\, 2(d_2 + b)(T - T_{env}) \text{, or} \qquad \left.\frac{dT}{dy}\right|_{y=d_2} = -\frac{a}{l_{ins}}(T - T_{env}) \tag{3.19}$$

The equation (3.7) can be written as follows

$$\frac{\partial^2 T(y)}{\partial y^2} = 0 \tag{3.20}$$

which by integration becomes:

$$\frac{\partial T}{\partial y} = T_1 \tag{3.21}$$

where T_1 is a integration constant.

Taking into account the limit condition (3.18) the constant T_1 is:

$$T_1 = -\frac{EI}{l_{ins} 2(d_1 + b)}$$

The temperature T_{ins} of the outer surface of the insulation, according to (3.19) is given by:

$$T_{ins} = T_{env} + \frac{EI}{2a\,(d_2 + b)} \tag{3.22}$$

The temperature profile in the insulation body can be determined by integrating the equation (3.21):

$$T(y) = T_{ins} + \frac{EI}{l_{ins} 2(d_2 + b)} y \tag{3.23}$$

Temperature at the inner side of insulation, which also means temperature of metallic conductor is given with $y=d_1$:

$$T_c = T_{ins} + \frac{EI}{l_{ins}\,2(d_1+b)}d_1 \tag{3.24}$$

or, expressed as a function of environment temperature T_{env}:

$$\boxed{T_c = T_{env} + \frac{EI}{2a(d_2+b)} + \frac{EI}{l_{ins}\,2(d_1+b)}y_1} \tag{3.25}$$

3.2 Calculation of thermo-electrical characteristics of round wires

3.2.1 Radial heat transfer with temperature-independent coefficients

For radial heat transfer we consider infinite length cylindrical wire thus neglecting end effects. This assumption is reasonable if the ratio of cylinder length L and cylinder radius r is $L/r \approx 1000$. The general heat equation for radial system is:

$$\frac{1}{r}\frac{\partial}{\partial r}\left(r\frac{\partial T(r,t)}{\partial r}\right) + \frac{EI}{lA} - \frac{g}{l}\frac{\partial T(r,t)}{\partial t} = 0 \tag{3.26}$$

or,

$$\boxed{\frac{1}{r}\frac{\partial}{\partial r}\left(r\frac{\partial T(r,t)}{\partial r}\right) + C - D\frac{\partial T(r,t)}{\partial t} = 0} \tag{3.27}$$

here: $C \equiv \frac{EI}{lA} = \frac{rI^2}{lA^2}$; $D \equiv \frac{g}{l}$

3.2.2 Heat transfer equations with temperature-dependent coefficients

Here the specific resistance dependence on temperature will be considered:

$$r(T) = r_0\left[1 + a_r\left(T(r,t) - T_0\right)\right] \tag{3.28}$$

The electrical field strength E changes with temperature as following:

$$E(T) = E_0\left[1 + a_r\left(T(r,t) - T_0\right)\right] \tag{3.29}$$

here:

α_ρ - linear temperature coefficient of resistance
ρ_0 – specific resistance at reference temperature T_0
E_0 – field strength at reference temperature T_0

Then the equation (3.27) obtains the following form:

$$\frac{1}{r}\frac{\partial}{\partial r}\left(r\frac{\partial T(r,t)}{\partial r}\right) + \frac{IE_0}{lA}\left[1 + a_r\Delta T(r,t)\right] - \frac{g}{l}\frac{\partial T(r,t)}{\partial t} = 0$$

$$\frac{1}{r}\frac{\partial}{\partial r}\left(r\frac{\partial T(r,t)}{\partial r}\right) + \frac{a_r IE_0\Delta T(r,t)}{lA} + \frac{IE_0}{lA} - \frac{g}{l}\frac{\partial T(r,t)}{\partial t} = 0 \tag{3.30}$$

or,

$$\boxed{\frac{1}{r}\frac{\partial}{\partial r}\left(r\frac{\partial T(r,t)}{\partial r}\right) + B\Delta T(r,t) + C - D\frac{\partial T(r,t)}{\partial t} = 0} \tag{3.31}$$

here: $B \equiv \dfrac{a_r E_0 I}{lA}$; $C \equiv \dfrac{E_0 I}{lA}$; $D \equiv \dfrac{g}{l}$.

3.2.3 Stationary solution of radial heat transfer equation

Before solving the equations, a short explanation of the applications shall be given where the solutions are applicable. Again, first the heat equation will be solved for the "naked" wire i.e. cylindrical wire without insulation (Fig. 3.1a). In this case, temperature distribution occurs only in the metallic conductor. Secondly, the heat equation will be applied to the round wire with insulation (Fig. 3.1b). Here the temperature distribution will be calculated whilst the insulation layer while temperature gradient of the metallic conductor is assumed to be zero.

For steady state and constant material properties, the heat transfer equation reduces to $B = 0$:

$$\frac{1}{r}\frac{\partial}{\partial r}\left(r\frac{\partial T(r)}{\partial r}\right) + C = 0 \tag{3.32}$$

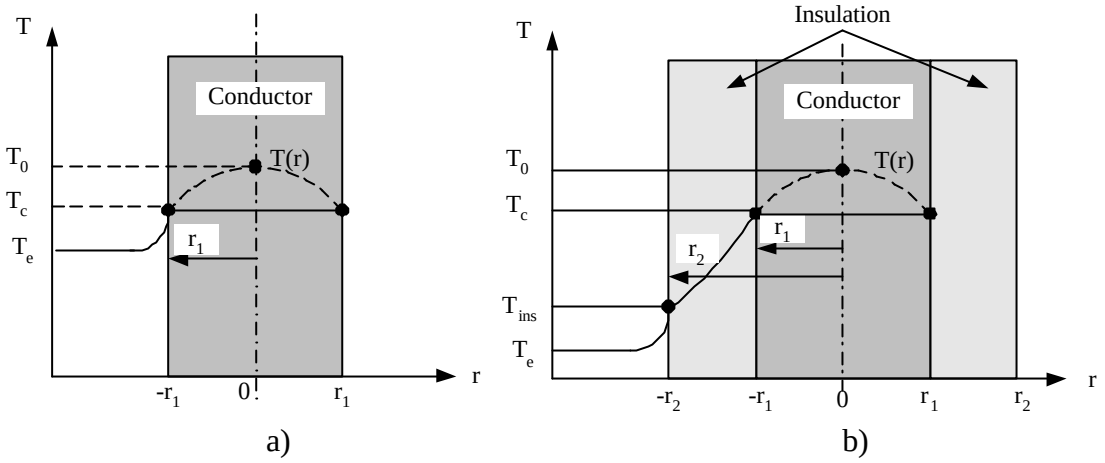

Fig. 3.1 Temperature distribution in a plane of cylindrical wire: a) – wire without insulation; b) – electrical wire with insulation

Separating variables and assuming uniform heat generation, the equation can be integrated to obtain:

$$r\frac{\partial T(r)}{\partial r} = -\frac{C}{2}r^2 + T_1 \tag{3.33}$$

Repeating the procedure, the general solution for the temperature distribution becomes:

$$T(r) = -\frac{C}{4}r^2 + T_1 \ln r + T_2 \tag{3.34}$$

To obtain integration constants T_1 and T_2 we apply the following boundary conditions:

at r = 0: $\left.\frac{\partial T(r)}{\partial r}\right|_{r=0} = 0,$ and

at r = r_1: $T(r_1) = T_{r1}$;

The first condition results from the symmetry of the cylinder. In the centre of the cylinder, the temperature gradient must be zero. Using the second boundary condition at r = r_1 with the equation (3.34) we obtain:

$$T_2 = T_{r1} + \frac{C}{4}r_1^2 \tag{3.35}$$

The temperature distribution is therefore:

$$T(r) = \frac{Cr_1^2}{4}\left(1 - \frac{r^2}{r_1^2}\right) + T_{r1} \tag{3.36}$$

To relate the surface temperature, T_{r1}, to the environment temperature T_{env}, an overall energy balance equation leads to the result:

$$\frac{EI}{\pi r_1^2} \pi r_1^2 L = \alpha 2\pi r_1 L (T_{r1} - T_{env})$$

or

$$T_{r1} = T_{env} + \frac{EI}{2\pi r_1 \alpha} \tag{3.37}$$

here: L – length of cylindrical wire in m

Then, the temperature distribution in the metallic conductor considering heat dissipation from the surface by convection:

$$\boxed{T(r) = \frac{C r_1^2}{4}\left(1 - \frac{r^2}{r_1^2}\right) + \frac{EI}{2\pi r_1 \alpha} + T_{env}} \tag{3.38}$$

In order to determine temperature in an insulated cylindrical wire (Fig.3.1b), we use the same heat equation (3.32) but different boundary conditions shall be considered:

a) from the energy balance equation for $r=r_1$ the following equation can be written:

$$-2\pi r_1 l_{ins} \left.\frac{\partial T}{\partial r}\right|_{r=r_1} = EI \ ;$$

b) neglecting radiation, for $r=r_2$ the boundary condition is as following:

$$l_{ins} 2\pi r_2 \left.\frac{\partial T}{\partial r}\right|_{r=r_2} = -\alpha 2\pi r_2 (T - T_{env}) \text{, or} \qquad \left.\frac{\partial T}{\partial r}\right|_{r=r_2} = -\frac{\alpha}{l_{ins}} (T - T_{env}) \text{ .}$$

Repeating the same procedure as in the solution of Eq. (3.7) for a non-insulated wire, we obtain the following solution for temperature profile in the insulation of cylindrical wire:

$$T(r) = \frac{EI}{2\pi\lambda_{ins}} \ln\left(\frac{r_2}{r}\right) + \frac{EI}{2\pi r_2 \alpha} + T_{env} \tag{3.39}$$

Equation (3.39) enables us to compute the temperature profile in the insulation. In the metallic conductor, the temperature gradient is considered to be zero. This assumption

is reasonable, because the heat conductivity of a metallic conductor is very high, compared with the insulation heat conductivity.

Temperature of metallic conductor at $r=r_2$ from Eq. (3.39) is therefore:

$$T_c = \frac{EI}{2\pi\lambda_{ins}} \ln\left(\frac{r_2}{r_1}\right) + \frac{EI}{2\pi r_2 \alpha} + T_{env} \tag{3.40}$$

3.3 Calculation of the thermo-electrical characteristics of electrical fuses

3.3.1 Axial heat transfer with temperature – independent coefficients

For the analytical analysis of axial heat transfer we will use similar equation to (Eq. 2.8, Chapter 2) and introduce temperature-independent coefficients. Then the equation has the form:

$$\frac{\partial^2 T(x,t)}{\partial x^2} - \frac{au}{lA} T(x,t) + \frac{EI}{lA} - \frac{g}{l}\frac{\partial T(x,t)}{\partial t} = 0 \tag{3.41}$$

here: $\frac{au}{lA} \equiv B$; $\frac{EI}{lA} \equiv C$; $\frac{g}{l} \equiv D$.

Then equation (3.41) can be rewritten following:

$$\frac{\partial^2 T(x,t)}{\partial x^2} - BT(x,t) + C - D\frac{\partial T}{\partial t} = 0 \tag{3.42}$$

Let us describe the coefficient physical meaning of equation (3.42). These coefficients do not depend on temperature. Coefficient B can be written in the following form:

$$B \equiv \frac{au}{lA} = \frac{1}{c^2} \tag{3.43}$$

here χ - is the "length constant", e.g. the inversed square root of coefficient B :

$$c \equiv \frac{1}{\sqrt{B}} = \sqrt{\frac{lA}{au}} \tag{3.44}$$

χ can be considered as a length decay in a function of temperature, which increases if the ratio A / u increases.

Coefficient C is called "Temperature field gradient" in K/m^2. The coefficient means the ratio of the volumetric generated heat EJ in the fuse and the heat conductivity coefficient *?* :

$$C \equiv \frac{EI}{lA} = \frac{rJ^2}{l} \tag{3.45}$$

We introduce the "asymptotic temperature" term $\hat{T}$. Asymptotic term can be understood as a final temperature of infinite length wire after steady state. Temperature $\hat{T}$ in the fuse will not be achieved if the fuse has a very short length. In any case $\hat{T}$ will not be reached in transient state. The formula of $\hat{T}$ is the following:

$$\hat{T} \equiv \frac{C}{B} = c^2 C = \frac{EI}{au} \tag{3.46}$$

Coefficient D can be called "reciprocal temperature conductivity" or "reciprocal heat transport velocity" and is described as the quotient of heat capacity and heat conductivity:

$$D \equiv \frac{g}{l} \tag{3.47}$$

3.3.2 Axial heat transfer with temperature-dependent coefficients

In this section we will consider temperature dependant specific electrical resistance of copper or brass. Specific resistance, r, for temperature change from 20 to 180°C can be calculated as follows:

$$r(T) = r_0 \left[1 + a_r (T(x,t) - T_{env})\right] \tag{3.48}$$

The field strength, E, changes with respect to temperature as:

$$E(T) = E_0 \left[1 + a_r (T(x,t) - T_{env})\right] \tag{3.49}$$

here: α_ρ linear temperature coefficient of resistance
ρ_0 specific resistance at reference temperature T_0
E_0 field strength at reference temperature T_0

Considering Eq. (3.49), equation (3.41) takes the following form:

$$\frac{\partial^2 T(x,t)}{\partial x^2} - \frac{au}{lA} T(x,t) + \frac{IE_0\left[1 + a_r (T(x,t) - T_{env})\right]}{lA} - \frac{g}{l}\frac{\partial T(x,t)}{\partial t} = 0$$

$$\frac{\partial^2 T(x,t)}{\partial x^2} - \left(\frac{au - a_r IE_0}{lA}\right)(T(x,t) - T_{env}) + \frac{IE_0}{lA} - \frac{g}{l}\frac{\partial T(x,t)}{\partial t} = 0 \tag{3.50}$$

or,

$$\boxed{\frac{\partial^2 T(x,t)}{\partial x^2} - B(T(x,t) - T_{env}) + C - D\frac{\partial T}{\partial t} = 0}$$

where the coefficients have the following meaning:

$$c \equiv \frac{1}{\sqrt{B}} = \sqrt{\frac{lA}{au - a_r IE_0}} \tag{3.51}$$

$$\hat{T} \equiv \frac{C}{B} = c^2 C = \frac{EI}{au - a_r IE_0} + T_{env} \tag{3.52}$$

3.3.3 Avalanche effect in metallic conductor

Any conductor with a positive temperature coefficient α_ρ shows a so-called *avalanche effect*, where due to too larger energy generation, the equilibrium, generated between energy in the fuse and dissipated heat to ambient can not be achieved. This is valid for the length constant as well as for the final temperature of a wire with infinite length. Because of this effect, temperature rises continuously and the length constant χ_A and final temperature $\hat{T}_A$ becomes infinite if the following conditions are satisfied:

$$\boxed{au = a_r IE_0 = \frac{a_r r_0 I^2}{A}} \tag{3.53}$$

Then: $c_A = \infty, \hat{T}_A = \infty$

Avalanche current can be calculated in this way:

$$\boxed{I_A = \sqrt{\frac{auA}{a_r r_0}}} \tag{3.54}$$

3.3.4 Stationary solution for axial heat transfer equation

The solution of the equation for axial heat transfer gives the temperature distribution in the x – direction. For steady-state we apply boundary conditions given in equation (2.46, Chapter):

$$\begin{cases} T(0) = T_0 \\ T(x) = T_l \end{cases} \tag{2.46}$$

Then, the equation (3.42) of axial heat transfer simplifies to:

$$\frac{\partial^2 T(x)}{\partial x^2} - B\Delta T(x) + C = 0 \tag{3.55}$$

The general solution of Eq. (3.55) is:

$$T(x) = T_1 e^{\sqrt{B}x} + T_2 e^{-\sqrt{B}x} - \frac{C'}{B} \tag{3.56}$$

here: B linear temperature dependent heat dissipation coefficient to ambient
in $1/m^2$

$C' = BT_{env} - C$
temperature dependent heat generation by electrical current
in $1/m^2$

$T_{1,2}$ integration constants, in which the boundary conditions are set
in °C

In order to find $T_{1,2}$ we introduce boundary values at $x = 0$ and $x = l$. Then, the temperature distribution in the fuse is as following:

$$T(x) = -\frac{\hat{T}\left(1-e^{-\sqrt{B}l}\right)+T_0 e^{-\sqrt{B}l}-T_l}{1-e^{-2\sqrt{B}l}}e^{\sqrt{B}(x-l)} - \frac{\hat{T}\left(1-e^{-\sqrt{B}l}\right)+T_l e^{-\sqrt{B}l}-T_0}{1-e^{-2\sqrt{B}l}}e^{-\sqrt{B}x}+\hat{T} \qquad (3.57)$$

here:	l	length of fuse	in m
	$T(x)$	temperature distribution along the fuse	in °C
	T_0	the boundary temperature of the fuse at $x = 0$	in °C
	T_l	the boundary temperature of the fuse at $x = l$	in °C

Replacing B by $\frac{1}{c^2}$, equation (3.17) can be written as:

$$T(x) = -\frac{\hat{T}\left(1-e^{-\frac{l}{c}}\right)+T_0 e^{-\frac{l}{c}}-T_l}{1-e^{-\frac{2l}{c}}}e^{\frac{x-l}{c}} - \frac{\hat{T}\left(1-e^{-\frac{l}{c}}\right)+T_l e^{-\frac{l}{c}}-T_0}{1-e^{-\frac{2l}{c}}}e^{-\frac{x}{c}}+\hat{T} \qquad (3.58)$$

Equation 3.58 gives the temperature distribution in a fuse element with the finite length and fixed boundary temperatures. From the analytical solution the “avalanche effect” (Eq. 3.52) can be observed, the length constant c is obtained (Eq.3.51), and “hypothetical temperature” $\hat{T}$ can be derived (Eq. 3.52).

CHAPTER 4

NUMERICAL CALCULATION OF TEMPERATURE BEHAVIOUR IN A TRANSIENT STATE

4.1 Overview of the numerical methods used in heat transfer computation

The heat transfer of an insulated electrical wire is described by a non-linear and non-homogeneous partial differential equation. A unique analytical solution is only feasible for idealised and simple conditions. For practical cases, it is required to implement numerical methods. Available analytical and experimental results are of considerable importance in verifying the accuracy and validity of numerical results.

The limitations of an analytical solution arise from the following properties of electrical wires:

- electrical conductivity is second order temperature dependent
- heat conductivity λ of insulation is at least linear temperature dependent
- heat convection and radiation α is at least third order temperature dependant

The numerical methods allow not only better representation of the mutual heating effects, but also permit more accurate modelling of the boundaries (e.g. a convection-radiation boundary to the environment).

A numerical solution is obtained from discretisation of the partial differential equation.

There are four distinct streams of numerical solution techniques:

- Finite Differences (FD)
- Finite Element (FE)
- Spectral Method (SM)
- Finite Volume Method (FV)

The four mentioned methods differ mainly in the approximation of the variables and in the discretisation processes.

1. *Finite difference methods (FD)*

In this method the partial derivations of equations are approximated by a truncated Taylor series. This method is particularly appropriate for an equidistant Cartesian mesh.

Taylor series expansion of a function *f(x)* about a point x_0 in the *forward* (i.e. positive x) and *backward* (i.e., negative x) directions are given, respectively, by:

$$f(x_0+\Delta x) = f(x_0) + \left.\frac{df}{dx}\right|_0 \Delta x + \left.\frac{d^2 f}{dx^2}\right|_0 \frac{(\Delta x)^2}{2!} + \left.\frac{d^3 f}{dx^3}\right|_0 \frac{(\Delta x)^3}{3!} + ...$$

$$f(x_0-\Delta x) = f(x_0) - \left.\frac{df}{dx}\right|_0 \Delta x + \left.\frac{d^2 f}{dx^2}\right|_0 \frac{(\Delta x)^2}{2!} - \left.\frac{d^3 f}{dx^3}\right|_0 \frac{(\Delta x)^3}{3!} + ...$$

These two expressions form the basis for developing difference approximations for the first order derivative *df/dx* about x_0. Rearranging the expressions, the *forward* and *backward* finite difference approximations for the first order derivative, respectively, become:

$$\left.\frac{df}{dx}\right|_0 = \frac{f(x_0+\Delta x) - f(x_0)}{\Delta x} + 0(\Delta x) \qquad \text{(forward)}$$

$$\left.\frac{df}{dx}\right|_0 = \frac{f(x_0) - f(x_0-\Delta x)}{\Delta x} + 0(\Delta x) \qquad \text{(backward)}$$

More about FD method in heat transfer can be found in the relevant literature [19].

2. *Finite element method (FE)*

This method originated from the structural analysis as a result of many years of research, mainly between 1940 and 1960. In this method the problem domain is ideally subdivided into a collection of small regions of finite dimensions, called finite elements. The elements in a 2-D case have either a triangular or quadrilateral form (Figure 4.1,a) and can be rectilinear or curved. After subdivision of the domain, the solution of the discrete problem is assumed to have prescribed form. This representation of the solution is strongly linked to the geometric division of sub domains and characterised by the prescribed nodal values of the mesh.

For heat transfer in the electrical wires, the discrete solution with FE can be constructed as follows:

1. A finite number of points in the solution region is identified. These points are called *nodal points* or *nodes*.
2. The value of temperature at each node is denoted as a variable which has to be determined.

3. The solution region is divided into a finite number of subregions called *ele ments*. These elements connect common nodes, and collectively approximate the shape of the region.
4. Temperature is approximated over each element by a polynomial expression that is defined using nodal values of the temperature (see Fig. 4.1, b):

$$T_P = Aw_i + Bw_j + Cw_m$$

where ω_i, ω_j, ω_m are the area coordinates defined as in Fig. 4.1, b. These area coordinates uniquely define the position of any point *P* inside the triangle *ijm*.

A different polynomial is defined for each element, but the element polynomials are selected in such a way that continuity is maintained along the element boundaries. The nodal values are computed so that they provide the "best" approximation possible to the true temperature distribution. This selection is ac complished by minimising some quantity associated with the physical prob lem or by using Galerkin's method [29], which deal with the differential equa tions directly. The solution vector of the algebraic equations gives the required nodal temperatures. The answer is then known throughout the solution region. More about FE method can be found in literature [20].

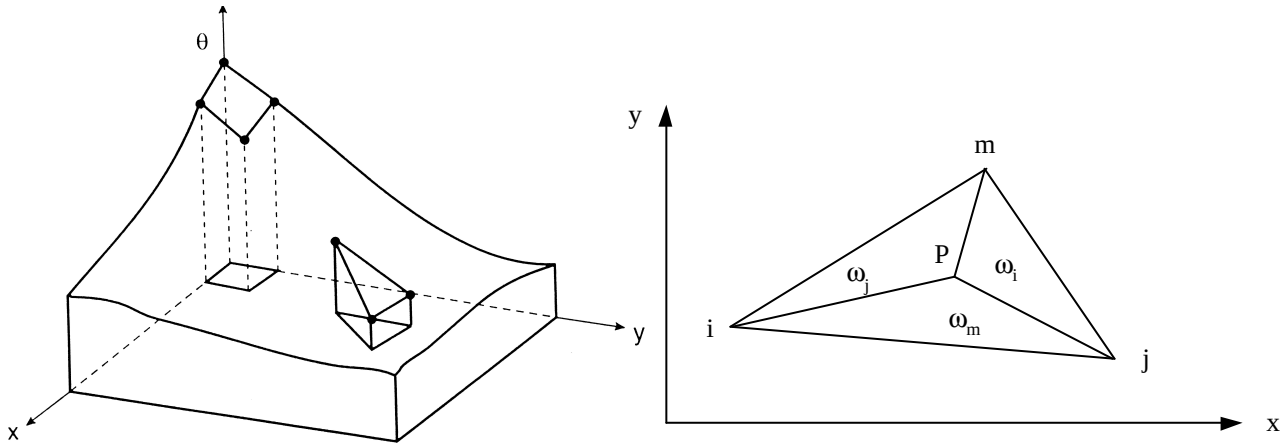

a) **b)**

Fig. 4.1 Triangular or quadrilateral finite elements of a two-dimensional domain (a) and area coordinates (b)

3. *Spectral method*

Spectral methods approximate the unknowns by means of truncated Fourier series or series of Chebyshev polynomials. Unlike the finite difference or finite element approach the approximations are not local but valid throughout the entire computational domain. The unknowns in the governing equation are replaced by the truncated series. The constrain that leads to the algebraic equations for the coefficients of the Fourier or Chebyshev series is provided by a weighted residuals concept similar to the finite element method or by making the approximate function coincide with the exact solution at a

number of grid points. Further information on this specialised method can be found in [21]

4. *The finite volume method*

The finite volume method was originally developed as a special finite difference formulation [22, 23]. In FV method, the partial derivation of equations is not directly approximated like in FD approach. Instead, the equations are integrated over a control volume *V*, which is defined by nodes of grids on the mesh:

$$\int_V div(\lambda\ grad\ T)dV + \int_V q_v dV = \int_V g\ \frac{\partial T}{\partial t} dV$$

The volume integral terms will be replaced by surface integrals using the Gauss formula. For a vector **a** this theorem states:

$$\int_V div\ a\, dV = \int_A n.a\ dA$$

These surface integrals define the convective and diffusive fluxes through the surfaces. Due to the integration over the volume, the method is fully conservative. This is an important property of FV method.

This clear relationship between the numerical algorithm and the underlying physical conservation principle forms one of the main attractions of the finite volume method and makes its concept much simpler to understand by engineers than finite element and spectral methods. In fact, 40 years ago Lax and Wendroff proved mathematically that conservative numerical methods, if convergent, do converge to correct solution of the equation. This study shall be solely concerned with this most well – established and thoroughly validated general-purpose computational fluid dynamic (CFD) and heat transfer technique. Therefore the method is discussed in more detailed.

4.2 Fundamentals of the finite volume method

The basic laws of heat transfer are the conservation equations, which are statements that express the conservation of:

- mass,
- momentum, and
- energy

in a volume closed by its surface.

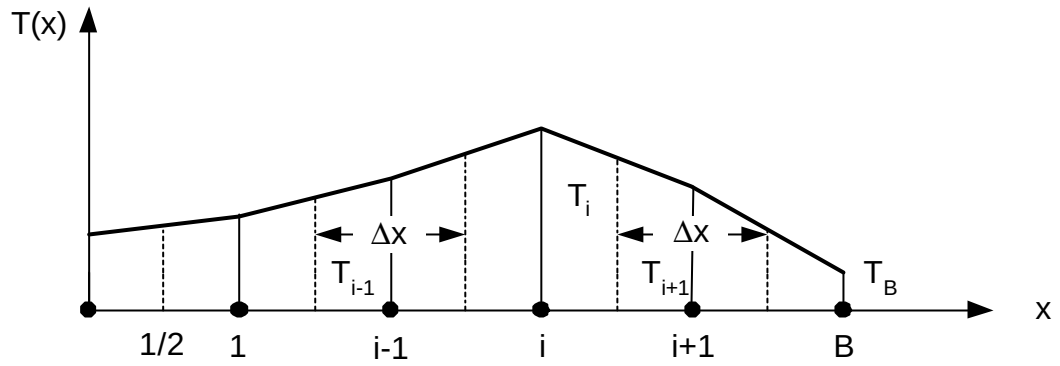

Figure 4.2 One-dimensional Finite Volume Mesh

Certain requirements are necessary to convert these laws into partial differential equations. These requirements cannot always be guaranteed. In a case where a discontinuity occurs, an accurate representation of the conservation laws is important. In other words, it is of big importance that these conservation equations are accurately represented in their integral form. The most natural method to accomplish this is obviously to discritise the integral form of the equations but not the differential form. This is the basis of finite volume (FV) method.

In two dimensional cases the field or domain is subdivided in the same way as in the finite element method, namely, into a set of non-overlapping cells that cover the whole domain on which the equations are applied. On each cell the conservation laws are applied to determine the flow variables in some discrete points of the cells, called nodes, which are typical locations of the cells such cell-centre (cell centered mesh) or cell-vertices (cell vertex mesh) (Figure 4.3).

Obviously, there is considerable freedom in the choice of the cell shapes. They can be triangular, quadrilateral etc. and generate a structured or unstructured mesh. Due to this unstructured form, very complex geometries can be handled with ease. This is clearly an important advantage of the method. Additionally the solution of the equation of the cell is not strongly linked to the geometric representation of the domain. This is another important advantage of the finite volume method in contrast to the finite element method.

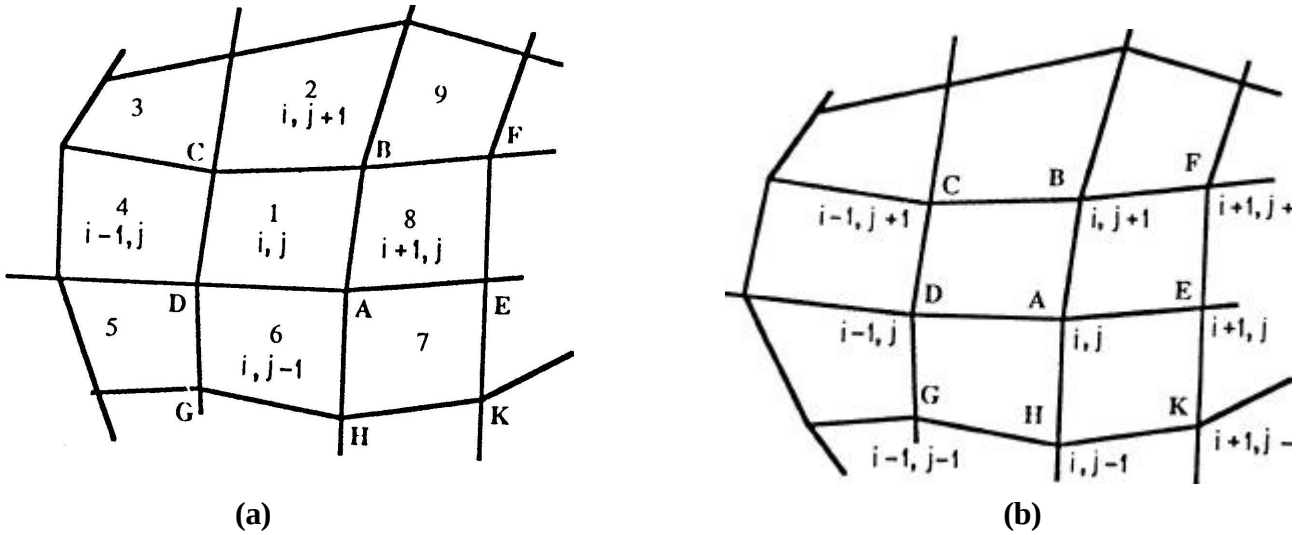

Figure 4.3 Two-dimensional structured Finite Volume Mesh system:
(a) Cell Centred mesh (b) Cell Vertex mesh

Numerical properties of discretisation schemes.

It is normally distinguished between time and spatial discretisation of continuum equation. The spatial discretisation can be applied on different forms of grids such as Cartesian, non-orthogonal, structured and unstructured. Time discretisation is usually done by FD scheme, which can be explicit or implicit. Normally, the explicit method is used for strong unsteady flows or when time gradient is very big.

When a direct computation of the dependent variables can be made in terms of known quantities, the computation is said to be *explicit.*

In contrast, when the dependent variables are defined by coupled sets of equations, and either a matrix or iterative technique is needed to obtain the solution, the numerical method is said to be *implicit.*

The choice of whether an implicit versus explicit method should be used depends ultimately on the goal of the computation. The consequences of using both methods have to do with numerical stability and numerical accuracy. Using explicit methods we can achieve required accuracy in time with more computational effort than implicit method. Although, explicit methods are simpler to implement mathematically, they are almost in all cases only conditionally stable. Implicit formulation is said to be always unconditionally stable. A solution for the unknowns at one time level n+1 may be obtained for any size of time step. In computational heat transfer, the governing equations are nonlinear. Under these conditions implicitly formulated equations are almost always solved using iterative techniques. Since heat transfer in electrical conductors has no strong unsteady flows as well as considering efficiency and stability of implicit method,

whenever possible implicit methods are used in this work but explicit method can be applied optionally.

Good understanding of the numerical solution algorithm is crucial. Three mathematical concepts are useful in determining the success or otherwise of such algorithms: **convergence**, **consistency** and **stability**.

Convergence is the property of a numerical method to produce a solution, which approaches the exact solution as the grid spacing, control volume size or element is reduced to zero ($\lim_{mesh \to 0} (T - T_n) = 0$, T – exact solution of partial differential equation, T_n – solution of finite difference equation).

Consistent numerical schemes produce systems of algebraic equations, which can be demonstrated to be equivalent to the original governing equations, as the grid spacing tends to zero.

Stability is associated with damping of errors as the numerical method proceeds. If a technique is not stable even round off errors in the initial data can cause erratic oscillations and divergence.

Convergence is usually very difficult to establish theoretically and in practice Lax's equivalence theorem is used [4], which states that for linear problems a necessary and sufficient condition for convergence is that the method is both consistent and stable. In heat transfer calculations this theorem is of limited use since we stated that the governing equations are non-linear. In such problems consistency and stability are necessary conditions for convergence, but not sufficient.

4.3 Non-linear heat transfer model of electrical conductors

It has already been mentioned that using the numerical methods the differential and the integral equations can be transformed into discrete algebraic equations. Based on the mentioned reasons in the previous section (4.2), the FV method has been chosen for the discretisation of PDE.

Equation (2.2, Chapter 2)

$$\frac{\partial}{\partial x}\left(l \frac{\partial T}{\partial x} \right) + \frac{\partial}{\partial y}\left(l \frac{\partial T}{\partial y} \right) + \frac{\partial}{\partial z}\left(l \frac{\partial T}{\partial z} \right) + q_v = g \frac{\partial T}{\partial t} \tag{4.1}$$

can be rewritten in the integral form. We integrate Equation (2.2) over a small fixed volume **V**:

$$\int_V div(\lambda \, grad \, T) dV + \int_V q_v dV = \int_V \gamma \frac{\partial T}{\partial t} dV \tag{4.2}$$

The volume integral over the divergence of heat flux vector is transformed to a surface integral by means of the divergence theorem. Then Equation (4.2) becomes

$$\oint_S (\lambda\, grad\, T) \times n\, dS + \oint_V q_v dV = \oint_V \gamma \frac{\partial T}{\partial t} dV \qquad (4.2a)$$

where **S** is the surface area of the finite volume. Since,

$$grad\, T \cdot n = \frac{\partial T}{\partial n} \qquad (4.2b)$$

then, the equation (4.2a) gives:

$$\int_S l \frac{\partial T}{\partial n} dS + \int_V q_v dV = \int_V g \frac{\partial T}{\partial t} dV \qquad (4.2c)$$

here: V small finite volume;
n *outward drawn* normal unit vector
$\frac{\partial}{\partial n}$ derivative along the outward drawn normal to the surface of the control volume.

Equation (4.2a) represents the principle of conservation of energy over finite volume *V*. It states that the rate of energy entering the control volume through its boundary surface *S* plus the rate of energy generated in the volume element is equal to the rate of increase of stored energy in the control volume. Furthermore, since fluxes are conserved in transport between the control volumes, the conservation principle is also satisfied for an assembly of finite volumes. That is, the numerical solution will satisfy both the local and global conservation properties, hence the formulation given by Equation (4.2) is fully conservative.

4.3.1 Approximation of heat transfer equations by FVM

4.3.1.1 Flat electric cable

We consider the transient state diffusion with convective-radiative boundary condition of a flat electrical cable in a one-dimensional domain defined in Figure 4.4.

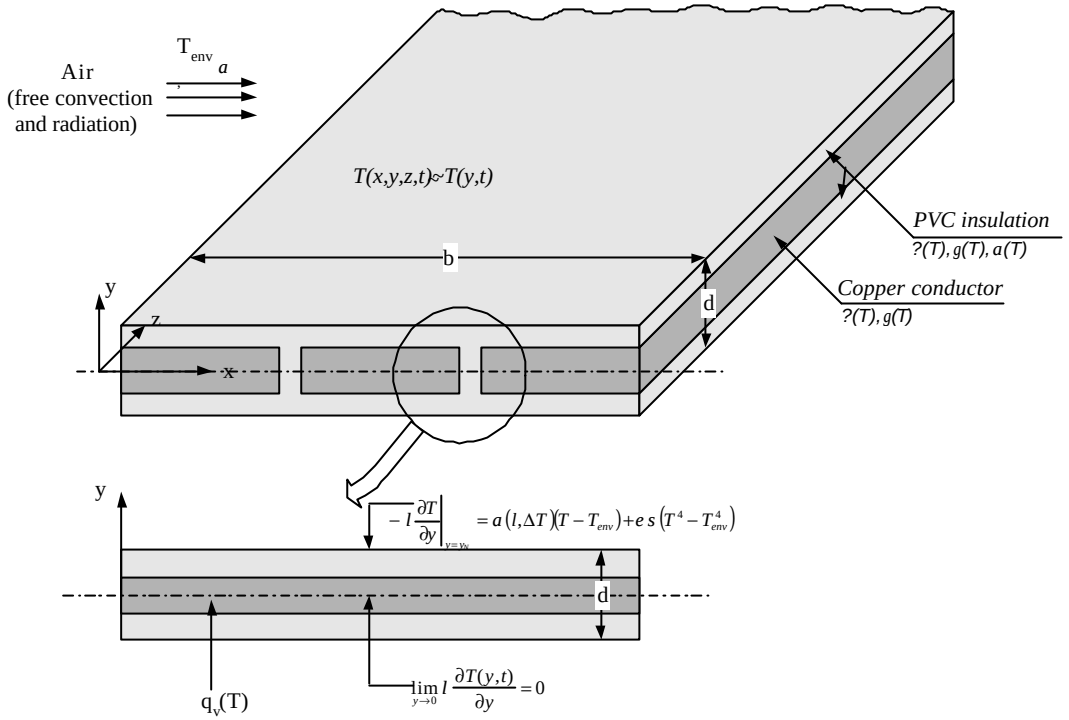

Figure 4.4 The physical model of flat electrical cable heated by electrical current

It is assumed that the dimensions in the x- and z- directions are so large that temperature gradients are significant in the y- direction only. The used grid is shown in Figure 4.5:

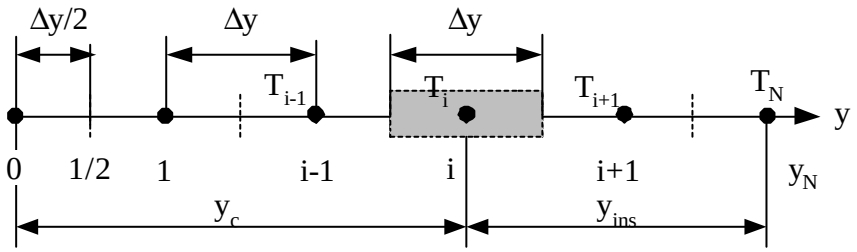

Figure 4.5 The finite volume grid of flat cable

The governing equation is:

$$-\frac{\partial}{\partial y}\left(l(y)\frac{\partial T}{\partial y} \right)+g(T,y)\frac{\partial T}{\partial t}=q_v(T,y) \tag{4.3}$$

The Equation (4.3) models the heat conduction in an electrical wire, which has different materials namely a conductor (here: copper) and an insulator (here: PVC = PolyVinyl-Chloride) with different heat conductivities l. Moreover, there is no heat generation q_v in wire (PVC) insulation. Therefore the equation has discontinuous coefficients l and q_v:

$$\begin{cases} l = l_c,\ q_v \neq 0; & 0 < y < y_c, \\ l = l_{ins}, q_v = 0; & y_c < y < y_{ins}; \end{cases} \tag{4.4}$$

The integral form of the governing equation for interior nodes of flat cable gives:

$$-\int_{\Delta V} \frac{\partial}{\partial y}\left(l(y)\frac{\partial T}{\partial y} \right) dV + \int_{\Delta V} g(T,y)\frac{\partial T}{\partial t} dV = \int_{\Delta V} q_v dV \tag{4.5}$$

Applying this integral form to the finite volume V_i= [i-0.5; i+0.5] (Figure 4.5) the Equation (4.5) can be rewritten whereby the volume element dV is replaced by the surface element dy (using Gauss theorem):

$$-\int_{i-0.5}^{i+0.5} \frac{\partial}{\partial y}\left(l(y)\frac{\partial T}{\partial y} \right) dy + \int_{i-0.5}^{i+0.5} g(T,y)\frac{\partial T}{\partial t}\Delta y dy = \int_{i-0.5}^{i+0.5} q_v(T,y)\Delta y dy \tag{4.6}$$

Integration of the Equation (4.6) over [i-0.5; i+0.5] leads to:

$$-l(y)\frac{\partial T}{\partial y}\bigg|_{i+0.5} + l(y)\frac{\partial T}{\partial y}\bigg|_{i-0.5} + g(T,y)\Delta y_i \frac{\partial T}{\partial t} = q_v(T,y)\Delta y_i \tag{4.7}$$

Replacing partial derivatives in space by central differences and derivative in time by backward difference, the Equation (4.7) takes the form:

$$\boxed{-\frac{l_{i+0.5}}{\Delta y_{i+0.5}}(T_{i+1}^n - T_i^n) + \frac{l_{i-0.5}}{\Delta y_{i-0.5}}(T_i^n - T_{i-1}^n) + \frac{g_i(T)\Delta y_i}{\Delta t}(T_i^n - T_i^{n-1}) = q_i(T,z)\Delta y_i} \tag{4.8}$$

The partial derivatives Eq. (4.8) in space are of second order accuracy and in time of first order (Δy^2,Δt).

Equation (4.8) is solved implicitly in time. In this study semi-implicit scheme is used, so the time step can not be chosen too large. The space step *Dy* and time step *Dt* can be computed by these expressions:

$$\Delta y = \frac{d_c + d_{ins}}{N - 0.5} \text{ and } \Delta t = \frac{t}{K} \tag{4.8a}$$

here: t time needed to reach steady state in some y_i node,
K number of time steps needed to reach steady state regime.

The result of this numerical solution gives temperature distribution in the metallic conductor and insulation of the flat cable.

4.3.1.2 Round electric wire

Cylindrical electrical wire of infinite length is given in (Figure 4.6)

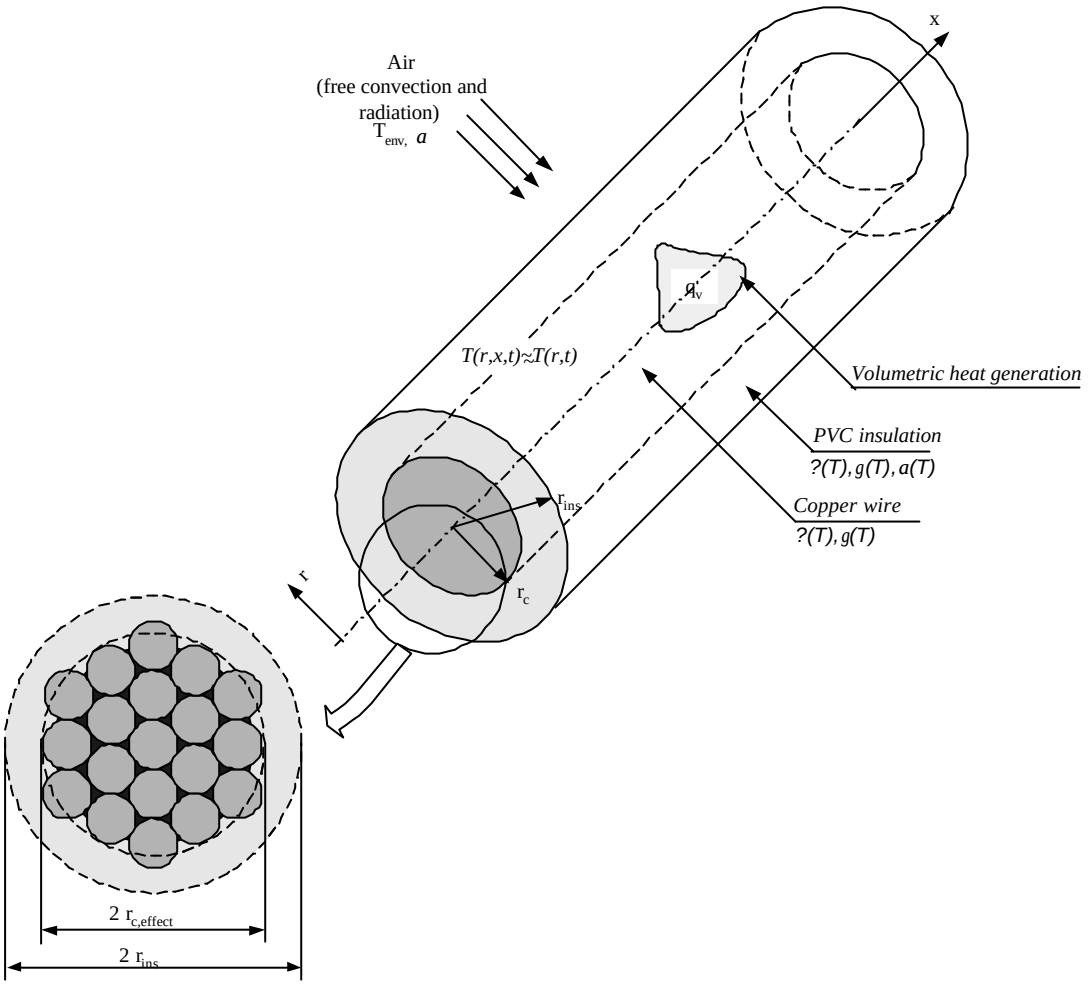

Figure 4.6 The model of heat conduction in round electrical wire
r_c – radius of the metallic conductor (copper), r_{ins} – radius of the insulation (PVC), $r_{c,effect}$ – effective radius of the conductor (pure copper without air gaps between single conductors)

In the heat transfer model of cylindrical wire we consider heat conduction in the cross section and neglect the conduction along the wire, assuming, that the end effects of the wire have no influence to the aimed calculation results. This approximation is reasonable *for* $L/r_{ins}>1000$, where L – length of the wire.

The numerical scheme is shown in Figure 4.7:

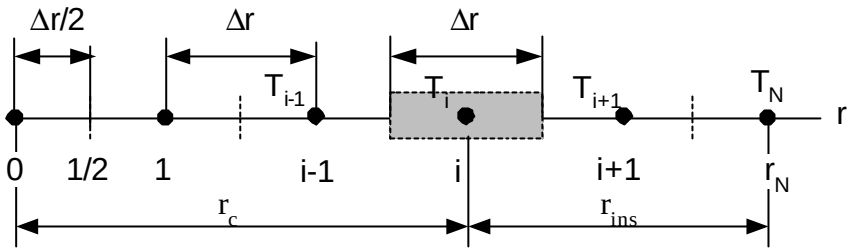

Figure 4.7 The finite volume grid of round wires

The governing equation is:

$$-\frac{1}{r}\frac{\partial}{\partial r}\left(l(r) r \frac{dT}{dr} \right) + g(T,r)\frac{\partial T}{\partial t} = q_v(T,r) \tag{4.9}$$

Equation (4.9) has discontinuous coefficients l and P:

$$\begin{cases} l = l_c,\ q_v \neq 0; & 0 < r \le r_c, \\ l = l_{ins}, q_v = 0; & r_c < r < r_{ins}; \end{cases} \tag{4.10}$$

After multiplication of the Equation (4.9) by *r*, the integral form of the governing equation for interior nodes of cylindrical wire becomes:

$$-\int_{\Delta V}\frac{\partial}{\partial r}\left(l(r) r \frac{dT}{dr} \right) dV + \int_{\Delta V} r g(T,r)\frac{\partial T}{\partial t} dV = \int_{\Delta V} r q_v(T,r) dV \tag{4.11}$$

Applying this integral form to the finite volume V_i= [i-0.5; i+0.5] (Figure 4.7) we can rewrite the Equation (4.12) as following:

$$-\int_{i-0.5}^{i+0.5}\frac{\partial}{\partial r}\left(r\, l(r)\frac{\partial T}{\partial r} \right) dr + \int_{i-0.5}^{i+0.5} r g(T,r)\Delta r \frac{\partial T}{\partial t} dr = \int_{i-0.5}^{i+0.5} r q_v(T,r)\Delta r dr \tag{4.12}$$

Integrating over [i-0.5; i+0.5] we get:

$$-r_{i+0.5}\, l(r)\frac{\partial T}{\partial r}\bigg|_{i+0.5} + r_{i-0.5}\, l(r)\frac{\partial T}{\partial r}\bigg|_{i-0.5} + g(T,r)\Delta r_i \frac{\partial T}{\partial t} = q_v(T,r)\Delta r_i \tag{4.13}$$

Replacing partial derivatives in space by central differences and derivative in time by backward difference, the Equation (4.13) takes the form:

$$-\frac{r_{i+1/2}\,l_{i+1/2}}{\Delta r_{i+1/2}}(T_{i+1}^{n}-T_{i}^{n})+\frac{r_{i-1/2}\,l_{i-1/2}}{\Delta r_{i-1/2}}(T_{i}^{n}-T_{i-1}^{n})+\frac{r_i g_i^{n}\Delta r_i}{\Delta t}(T_i^{n}-T_i^{n-1})=r_i q_i \Delta r_i \qquad (4.14)$$

Equation (4.14) is solved semi-implicitly in time. The space step *Dr* and time step *Dt* can be computed by these expressions:

$$\Delta r=\frac{r_{ins}}{N-0.5}\ \text{and}\ \Delta t=\frac{t}{K} \qquad (4.15)$$

here: r_{ins} the radius of insulated wire,
N number of nodes,
t the time needed to reach steady state in some y_i node,
K a number of time steps needed to reach steady state regime.

4.3.1.3 Electric fuse

Here, the problem deals with the axial heat transfer calculation in a copper (or brass) solid or hollow cylinder (fuse melting element prototype) with finite length (Figure 4.8). Axial temperature distribution in the fuse melting element must be computed in order to obtain the maximum temperature (melting temperature) of this element. In the mathematical model of heat transfer in the fuse, the non-homogenous geometry, heat convection and radiation is considered through the surface of the fuse element and prescribed temperature boundary conditions are applied. The temperature gradient in the radial direction is neglected, because heat conductivity coefficient of copper (or brass) is very large and gives a constant temperature distribution for the model geometry considered here. This model reduction reduces computational efforts considerably.

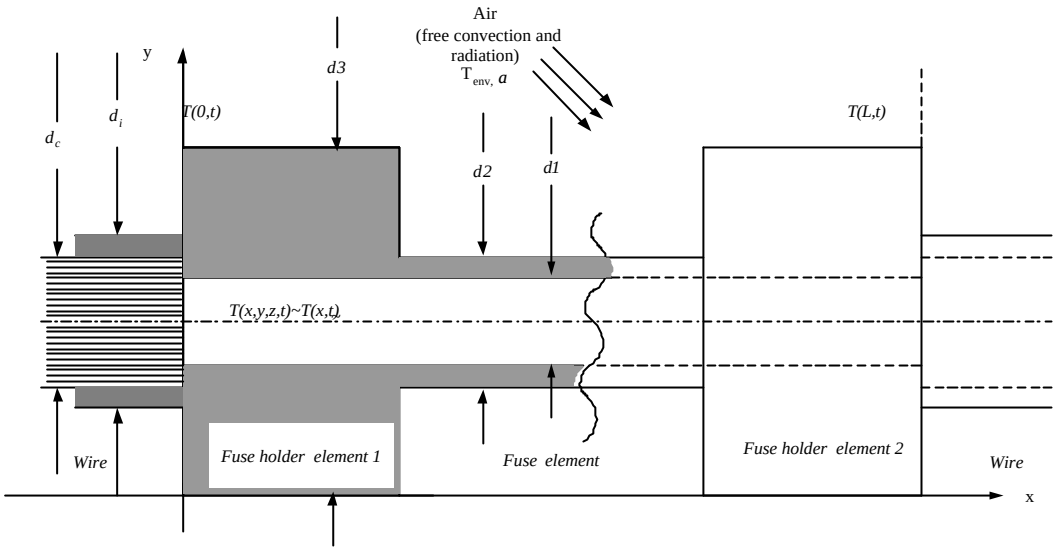

Figure 4.8 Physical model of the fuse melting element used for numerical computation

The heat transfer equation of the energy conservation law for a 1-D problem in the axial direction can be expressed as:

$$-\frac{\partial}{\partial x}\left(A(x)\,l\,\frac{\partial T}{\partial x}\right)+\left[a_c(T)\Delta T+a_r(T^4-T_{env}^4)\right]\cdot u + g(T,r)A(x)\frac{\partial T}{\partial t}=A(x)q_v(T) \tag{4.16}$$

here:

a_c	convection heat transfer coefficient	in W/m^{2}K,
DT	temperature difference between the temperature T on the surface and environment temperature T_{env}	in K,
$a_r = e\,s$	radiation heat transfer coefficient	in W/m^{2}K^4,
u	circumference of the fuse element	in m,
A	area (depends on the geometry of the fuse element)	in m^2.

Following the same procedure as in previous sections (4.3.1.1-2) we integrate Eq. (4.16) over [i-0.5; i+0.5] (Fig. 4.9). After integration equation yields:

$$-l\,A(x)\frac{dT}{dx}\bigg|_{i+0.5}+l\,A(x)\frac{dT}{dx}\bigg|_{i-0.5}+\left[a_c(T)\Delta T+a_r(T^4-T_{env}^4)\right]u + g(T,r)A(x)\Delta x\frac{dT}{dt}=A(x)q_v(T)\Delta x \tag{4.17}$$

Replacing the derivatives by central differences in space and derivative in time by backward difference, the Equation (4.17) gives:

$$\begin{aligned}&-\frac{l_{i+0.5}A_{i+0.5}}{\Delta x_{i+0.5}}(T_{i+1}^{n}-T_{i}^{n})+\frac{l_{i-0.5}A_{i-0.5}}{\Delta x_{i-0.5}}(T_{i}^{n}-T_{i-1}^{n})\\&+\left[a_{c}(T)(T_{N}^{n}-T_{env}^{n})+a_{r}((T_{N}^{n})^{4}-T_{env}^{4})\right]\mu_{i}T_{i}^{n}\\&+\frac{g_{i}^{n}A_{i}\Delta x_{i}}{\Delta t}(T_{i}^{n}-T_{i}^{n-1})=A_{i}q_{i}\Delta x_{i}\end{aligned} \tag{4.18}$$

The space step *Dx* and time step *Dt* is computed by:

$$\Delta x=\frac{L}{N-1}\ \text{and}\ \Delta t=\frac{t}{K} \tag{4.19}$$

here: L length of the fuse element,
N number of nodes in which the temperature is calculated,
T time needed to reach steady state in some x_i node,
K number of time steps needed to reach steady state regime.

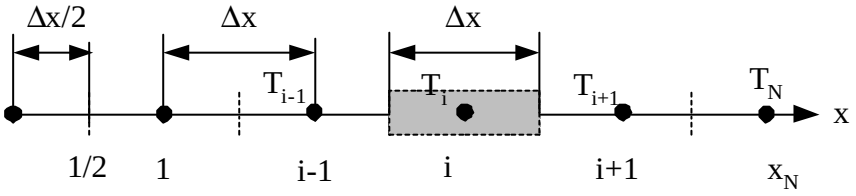

Figure 4.9 The finite volume grid of fuse

4.3.2. Numerical implementation of boundary conditions

4.3.2.1. Flat electric cable

The mathematical model of heat transfer in the flat cable consists of PDE and two boundary conditions. Therefore, the heat transfer problem must be considered as an initial-boundary value problem. Here we have to deal with mixed-type boundary conditions, which consist of Neumman type boundary conditions (second kind) and convective-radiative limit conditions (third kind). Since the flat cable model is a symmetrical system (see Fig. 4.4), we can use symmetry boundary condition at *y = 0*. The cable is placed in air in a horizontal position and affected only by laminar free convection and radiation to the environment. Due negligible difference between the heat convection on the upper and lower sides of the cable, this symmetry assumption is correct.

In this section we show how to approximate this type of boundary condition in order to have the same order of accuracy as the governing equation.

Initial and boundary condition is given as:

$$\begin{cases} T(y,0) = T_{env}(y), \quad y \in [0, y_N] \\ \lim\limits_{y\to 0} l_0(y)\dfrac{\partial T(y,t)}{\partial y} = 0, \quad t \ge 0 \\ -l_N \dfrac{\partial T(y,t)}{\partial y}\Big|_{y=y_N} = a_c(d,T)\big(T(y,t) - T_{env}\big) + e\,s\left(\big(T^*(y,t)\big)^4 - \big(T^*_{env}\big)^4\right), \; t \ge 0 \end{cases} \tag{4.20}$$

here T^*_{env} is the absolute temperature of environment in K.

The first boundary condition, which is derived from the symmetry of the physical model, has to be inserted into the main equation (4.5) and integrated over region $[r_0; r_{0.5}]$:

$$-\int_{y_0}^{y_{0.5}} \frac{\partial}{\partial y}\left(l(y)\frac{\partial T}{\partial y}\right)dy + g(T,y)\frac{\partial T}{\partial t}\int_{y_0}^{y_{0.5}} dy = \int_{y_0}^{y_{0.5}} q(T,y)dy \tag{4.20a}$$

Following the same procedure as in the derivation of the discrete form of the governing equation (4.8), the following discrete form of the first boundary condition is obtained:

$$-\frac{l_{0.5}}{\Delta y_{0.5}}(T_{i+1}^n - T_i^n) + \frac{\Delta y_0 g_{0.5}^n}{\Delta t}(T_i^n - T_i^{n-1}) = \Delta y_0 q_0 \tag{4.20b}$$

In order to describe heat conduction through the boundary of cable insulation and environment, we have to integrate Equation (4.3) over the region $[y_{N-0.5}; y_N]$:

$$-\int_{y_{N-0.5}}^{y_N} \frac{\partial}{\partial y}\left(l(y)\frac{\partial T}{\partial y}\right)dy + \int_{y_{N-0.5}}^{y_N} g\Delta y\frac{\partial T}{\partial t}dy = \int_{y_{N-0.5}}^{y_N} q\Delta y dy \tag{4.21}$$

Integrating Equation (4.21) over $[y_{N-0.5}; y_N]$ and considering convective – radiative phenomena at the boundary of insulation layer in the nod y_N we get heat conduction equation for the area $[y_{N-0.5}; y_N]$:

$$\begin{aligned}&(a(T_N^n - T_{env}^*) + b((T_N^n)^4 - (T_{env}^*)^4)) + \frac{l_{N-0.5}}{\Delta y_{N-0.5}}(T_N^n - T_{N-1}^n)\\&+ \frac{g_i^n \Delta y_N}{2\Delta t}(T_N^n - T_N^{n-1}) = \frac{1}{2} q_i^n \Delta y_N,\ i = N\end{aligned} \tag{4.22}$$

4.3.2.2. Round electric wire

The heat conduction equation of cylindrical electric wire has the same type of boundary conditions as flat cable (section 4.3.2.1): symmetry and convective-radiative boundary condition. The wire is placed in air in a horizontal position and affected by laminar free convection and radiation to the environment.

Initial and boundary conditions are given as following:

$$\begin{cases} T(r,0) = T_{env}(r), \quad r \in [0.5, r_N] \\ \lim\limits_{r\to 0} r\, l_0(r) \dfrac{\partial T}{\partial r} = 0, \quad t \ge 0 \\ -l_N \left.\dfrac{\partial T}{\partial r}\right|_{r=r_N} = a_c(d,T)(T_N - T_{env}) + e\, s\left((T^*)^4 - (T_{env}^*)^4\right), \ t \ge 0 \end{cases} \tag{4.23}$$

Here, the first boundary condition, which is also derived from the symmetry of the physical model, has to be inserted into the main equation (4.9) and integrated over region $[r_0; r_{0.5}]$:

$$-\int_{r_0}^{r_{0.5}} \frac{\partial}{\partial r}\left(r\, l(r) \cdot \frac{\partial T}{\partial r}\right) dr + \int_{r_0}^{r_{0.5}} r \Delta r g(T,r) \frac{\partial T}{\partial t} dr = \int_{r_0}^{r_{0.5}} r \Delta r q(T,r) dr \tag{4.23a}$$

Following the same procedure as in the derivation of the discrete form of the governing equation (4.12), the following discrete form of the first boundary condition is obtained:

$$-\frac{r_{0.5}\, l_{0.5}}{\Delta r_{0.5}}(T_{i+1}^n - T_i^n) + \frac{\Delta r_0\, r_{0.5} g_{0.5}^n}{\Delta t}(T_i^n - T_i^{n-1}) = \Delta r_0\, r_{0.5} q_0 \tag{4.23b}$$

In order to approximate the heat flux at $r=r_N$, we have to integrate Equation (4.9) over region $[r_{N-0.5}; r_N]$ and in r_N insert the second boundary condition of equation system (4.23):

$$-\int_{r_{N-0.5}}^{r_N} \frac{\partial}{\partial r}\left(r\, l(r) \cdot \frac{\partial T}{\partial r}\right) dr + g(T) \frac{\partial T}{\partial t} \int_{r_{N-0.5}}^{r_N} g(T,r) \frac{\partial T}{\partial t} \Delta r r dr = \int_{r_{N-0.5}}^{r_N} \Delta r r q(T,r) dr \tag{4.23c}$$

Integrating Equation (4.23c) over $[r_{N-0.5};r_N]$ and considering convective – radiative phenomena at the boundary of insulation layer in r_N point, we get the heat conduction equation for $[r_{N-0.5};r_N]$ area:

$$\boxed{\begin{aligned}&(a\,(T_N^n - T_{env}) + es\,(\left(T_N^{*n}\right)^4 - \left(T_{env}^*\right)^4) + \frac{r_{N-0.5}\,l_{N-0.5}}{\Delta r_{N-0.5}}(T_N^n - T_{N-1}^n) + \frac{g_i^n r_N \Delta r_N}{2\Delta t}(\Delta T_N^n - \Delta T_N^{n-1}) \\ &= \frac{1}{2} r_N \Delta r_N q_N^n,\ i = N\end{aligned}} \quad (4.23d)$$

4.3.2.3. Electric fuse

For axial heat transfer in the fuse element we consider Dirichlet (prescribed temperature) boundary conditions. The temperature on both fuse holders should be equal to the maximal permissible temperature of the electrical wire. Therefore, temperature of the electrical wire can be assigned to the boundaries of the fuse holders.

Initial – boundary conditions:

$$\boxed{\begin{cases} T(x,0) = T_{env}(x), & x \in [0, x_N] \\ T(0,t) = T_{m0}(t), & t \geq 0, \\ T(x_N,t) = T_{m1}(t), & t \geq 0, \end{cases}} \quad (4.24)$$

4.3.3 Solution of the equation system by Newton-Raphson method

4.3.3.1 Flat electric cable

Sections 4.3.1 and 4.3.2 have shown how to approximate differential equations by the finite volume approach. Thus, the heat transport problem in electrical cable, which is governed by a single differential equation and boundary conditions can be approximated by a system of algebraic equations. It is very important to understand what methods are best applicable to solve these systems of algebraic equations. If the number of equations to be solved is large and the equations are non-linear, one needs to examine the nature of the resulting system of equations. From sections 4.3.1 and 4.3.2 it can be seen, that we have to solve non-linear system of equations because heat capacity g of copper is

second order temperature dependent and the radiation boundary condition is fourth order temperature dependent. Other non-linearity problems like electrical resistance non-linear behavior and heat conductivity non-linear temperature dependence can be neglected since these phenomena have a small influence on computational results if the temperature does not exceed about 150°C.

The objective of this section is to illustrate how to solve a non-linear system of algebraic equations obtained from the governing single differential equation and its boundary conditions in order to determine unknown temperature variables

Since we have to deal with a one-dimensional heat transfer problem, the Gauss elimination method [19] can be further simplified by taking advantage of the zeros of the tridiagonal coefficient matrix. This modified procedure, generally referred to as *Thomas Algorithm*, is an extremely efficient method for solving a large number of such equations [19]. Using this algorithm, the number of basic arithmetic operations for solving a tridiagonal set is of the order N, in contrast to $O(N^3)$ operations required for solving with Gauss Elimination. Therefore, not only are the computation times much shorter, but the round off errors are also significantly reduced.

In the Equation system (4.25) a Newton-Raphson iteration Method used to linearise equations. The Newton-Raphson method is an algorithm for finding the roots of systems of nonlinear algebraic equations by iteration. If a good initial guess is made, Newton-Raphson iteration process converges extremely fast. Iterations are terminated when the computed changes in the values of $\left|P^n - P^{n-1}\right|$ become less than some specified quantity ε.

$$\begin{cases} c_0 P_0^n - b_0 P_1^n = f_0^n = q_0^n - c_0 T_0^n + b_0 T_1^n; \\ -a_1 P_0^n + c_1 P_1^n - b_1 P_2^n = f_1^n = q_1^n + a_1 T_0^n - c_1 T_1^n + b_1 T_2^n; \\ ------------ \\ -a_j P_{j-1}^n + c_j P_j^n - b_j P_{j+1}^n = f_j^n = q_j^n + a_j T_{j-1}^n - c_j T_j^n + b_j T_{j+1}^n; \\ j = 1..N-1; \\ -a_N P_{N-1}^n + (c_N + a_c + es\ 4(T_N^n)^3) P_N^n = f_N^n = q_N^n + a_N T_{N-1}^n ... \\ +(-c_N - a_c) T_N^n - es\ (T_N^n)^4 + a_c T_{env} + es\ (T)_{env}^4. \end{cases} \tag{4.25}$$

here: P unknown temperature variables;
T initially guessed values.

Temperature variables P are found by following expressions:

$$\begin{cases} alpha_0 = \dfrac{b_0}{c_0}; beta_0 = \dfrac{f_0}{c_0} \\ alpha_j = \dfrac{b_j}{c_j - a_j alpha_{j-1}} \\ beta_j = \dfrac{f_j + a_j beta_{j-1}}{c_j - a_j alpha_{j-1}} \\ T_N^n = \dfrac{f_N + a_N beta_{N-1}}{c_N - a_N alpha_{N-1}} \\ T_i^n = alpha_i T_{i+1}^n + beta_i, \qquad i = 1...N-1 \end{cases} \tag{4.26}$$

here: $b_0 = \dfrac{l_{0.5}}{\Delta y_{0.5}}$; $c_0 = \dfrac{l_{0.5}}{\Delta y_{0.5}} + \dfrac{\Delta r_0 g_{0.5}}{\Delta t}$; $q_0 = \Delta y_0 EJ + g_{0.5}\Delta y_0 \dfrac{T_i^{n-1}}{\Delta t}$, $i=0$;

$$a_j = \frac{l_{i-0.5}}{\Delta y_{i-0.5}};\ b_j = \frac{l_{i+0.5}}{\Delta y_{i+0.5}};\ c_j = \frac{2l_i}{\Delta y_i} + \frac{g_i}{\Delta t},\ q_j = EJ + g_i \frac{T_i^{n-1}\Delta y_i}{\Delta t};$$

$1 < i < N$;

$$a_N = \frac{l_{N-0.5}}{\Delta y_{N-0.5}}; c_N = \frac{l_{N-0.5}}{\Delta y_{N-0.5}} + \frac{g_{N-0.5}\Delta y_{N-0.5}}{2\Delta t};\ q_N = \frac{1}{2} EJ\Delta y_N + g\frac{T_N^{n-1}\Delta y_N}{2\Delta t};$$

$i=N$.

4.3.3.2 Round electric wire

The way of solving the system of algebraic equations is analogous to the method described in the section (4.3.3.1):

$$\begin{cases} c_0 P_0^n - b_0 P_1^n = f_0^n = q_0^n - c_0 T_0^n + b_0 T_1^n; \\ -a_1 P_0^n + c_1 P_1^n - b_1 P_2^n = f_1^n = q_1^n + a_1 T_0^n - c_1 T_1^n + b_1 T_2^n; \\ ---------- \\ -a_j P_{j-1}^n + c_j P_j^n - b_j P_{j+1}^n = f_j^n = q_j^n + a_j T_{j-1}^n - c_j T_j^n + b_j T_{j+1}^n; \\ j = 2...N-1; \\ -a_N P_{N-1}^n + (c_N + a_c + es\ 4(T_N^n)^3) P_N^n = f_N^n = q_N^n + a_N T_{N-1}^n ... \\ +(-c_N - a_c) T_N^n - es\ (T_N^n)^4 + a_c T_{env} + es\ (T)_{env}^4. \end{cases} \tag{4.27}$$

Temperature variables P are found from the Eq. (4.27), where the coefficients a, b, c and f are calculated by:

$$b_0 = \frac{r_{0.5}\, l_{0.5}}{\Delta r_{0.5}};\ c_0 = \frac{r_{0.5}\, l_{0.5}}{\Delta r_{0.5}} + \frac{\Delta r_0 r_{0.5} g_{0.5}}{\Delta t};\ q_0 = r_{0.5}\Delta r_0 EJ + g_{0.5}\Delta r_0 \frac{T_i^{n-1}}{\Delta t}, \qquad i=0;$$

$$a_j = \frac{r_{i-0.5}\, l_{i-0.5}}{\Delta r_{i-0.5}};\ b_j = \frac{r_{i+0.5}\, l_{i+0.5}}{\Delta r_{i+0.5}};\ c_j = \frac{2 r_i\, l_i}{\Delta r_i} + \frac{\Delta r_i g_i}{\Delta t},$$

$$q_j = r_i \Delta r_i EJ + g_i \Delta r_i \frac{T_i^{n-1}}{\Delta t}, \qquad 1 < i < N;$$

$$a_N = \frac{r\, l}{\Delta r}; c_N = \frac{r\, l}{\Delta r} + \frac{\Delta r g r}{2\Delta t};\ q_N = \frac{1}{2} r \Delta r EJ + g_N \frac{T_N^{n-1}}{\Delta t}, \qquad i=N.$$

4.3.3.3 Electric fuse

In order to calculate the temperature distribution in the fuse system a non-linear system of equations has to be solved because of the radiation term in the equation (4.16). We use, as in previous cases a Newton-Raphson method to solve the problem.

The system of algebraic equations is given as follows:

$$\begin{cases} c_0 T_0^n - b_0 T_1^n = T_{m0}; \\ -a_1 P_0^n + (c_1 + au + es\ 4(T_1^n)^3 u) P_1^n - b_1 P_2^n = q_1^n + a_1 T_0^n - (c_1 + au) T_1^n \\ -es\,(T_1^n)^4 u + auT_{env} + esT_{env}^4 u + b_1 T_2^n; \\ ---------- \\ -a_j P_{j-1}^n + (c_j + au + es\ 4(T_j^n)^3 u) P_j^n - b_j P_{j+1}^n = q_j^n + a_j T_{j-1}^n - (c_j + au) T_j^n \\ -es\,(T_j^n)^4 u + auT_{env} + es\,(T)_{env}^4 u + b_j T_{j+1}^n; \\ j = 1..N-1; \\ -a_N T_{N-1}^n + c_N T_N^n = T_{m1}. \end{cases} \tag{4.28}$$

Here the coefficients a, b, c and p are calculated as follows:

$$c_0 = 1;\ b_0 = 1;\ T_{m0} = 105; \qquad \text{i = 0;}$$

$$a_j = \frac{A_{i-0.5}\, l_{i-0.5}}{\Delta x_{i-0.5}};\ b_j = \frac{A_{i+0.5}\, l_{i+0.5}}{\Delta x_{i+0.5}};\ c_j = \frac{2 A_i\, l_i}{\Delta x_i} + \frac{\Delta x_i g_i}{\Delta t},$$

$$q_j = AEJ + g_i \frac{T_i^{n-1} \Delta x_i}{\Delta t}, \qquad \text{i = 1,2,…,N-1;}$$

$$a_N = 1; c_N = 1;\ T_{m1} = 105, \qquad \text{i = N.}$$

Results of numerical simulation using the approach developed in this chapter together with a validation procedure are presented in Chapter 6. Flat electrical cables of different conductor size supplied by the company Technology & Innovation GmbH and round

electrical wires supplied by the company Leoni Bordnetze GmbH were used. Fuse element samples were provided by DaimlerChrysler AG.

CHAPTER 5

BASIC CONSIDERATIONS OF THE EXPERIMENT AND EXPERIMENTAL SETUP

This chapter presents the theory of the experimental procedure used in this work together with the measurement setup and the data acquisition. The aim of the experiments was to investigate the electrical load capacities of various electrical wires and cables. For this, two types of measurements were required:

a) Current versus voltage measurement,
b) Resistance versus temperature measurement

The investigation commenced with the measurement of power dissipation as function of temperature of the wire surface, called *"current versus voltage measurement"*,(a). The next step was to validate the linear temperature coefficient α_T, called *"resistance versus temperature measurement"*,(b). Later the information from both experiments was used to correct the theoretical model, if necessary.

First, some information on how properly the measurements have to be performed will be given. The theoretical background for the measurement specification was developed extensively during this research work. Then, a figure detailing the experimental set up for both cases will be shown. The procedure of parameter acquisition using GPIB (General Purpose Interface Bus) devices and the appropriate software will be also presented. The programme is given in the Appendix C.

5.1 Basic considerations of the experiment

5.1.1 Resistance versus temperature measurement

The aim of this experiment is to determine the linear temperature coefficient α_T of copper wires and cables. Later, this temperature coefficient α_T is used to calculate the wire and cable temperature from the current versus voltage relationship obtained from the second experiment: the current versus voltage measurement.

The electrical resistance R_i of the wire has to be determined for different applied temperature T_i values of the wire. These temperatures are achieved by heating up the cable in a heat chamber. Chamber temperature T_{ch} should be increased in equal steps from environment temperature T_{env} up to max. cable temperature T. In order to avoid errors

caused by an unsteady state during the measurement, the resistance of cable should be also measured for decreasing temperature values down to T_{env}.

During the measurement process, the cable is not heated electrically. For the qualitative measurement, the following three conditions must be fulfilled:

a) For every resistance measurement step, temperature steady-state condition must be obtained,
b) The measurement error due to material restraints must be estimated,
c) Thermo voltages must be avoided.

A. Requirements for a steady-state temperature condition

Here, the most important parameter is a steady-state time t, after which temperature difference between T_{ch} and cable temperature T_0 becomes zero. The time t is influenced by a time constant t , which is different for every wire type. In order to calculate steady-state time t, one should determine the factor n, i.e. the number of time constants t needed to reach a steady-state:

$$t = nt \tag{5.1}$$

To calculate factor n, we can consider the precision of the heating chamber temperature. We can assume that the temperature difference dT_{L} between the cable temperature and chamber temperature should be equal to the temperature error of the chamber dT_{ch}:

$$dT_L = JTe^{-n} = dT_{ch} \tag{5.2}$$

From there, the factor n is given by:

$$\boxed{n = \ln \frac{JT}{dT_{ch}}} \tag{5.3}$$

where:	dT_L	temperature difference between cable and chamber temperatures	in K
	dT_{ch}	temperature measurement error of the heating chamber	in K
	t	thermal time constant of the cable	in s
	JT	step size of temperature interval	in K
	n	time constant factor	
	t	steady-state time	in s

Here we consider dT_{ch} from the technical specification of heating chamber 0.5 K. Step size of temperature interval for resistance measurement is JT = 10 K. Then, the n factor is calculated:

$$\boxed{n \geq \ln 10 / 0.5 = 2.996 \approx 3} \tag{5.4}$$

this means, that only after $3t$ cable resistance can be measured.

B. Permissible measurement error of cable resistance.

In order to estimate permissible measurement error of cable resistance, we ought to use the following formula:

$$R(t) = R_0\left[1 + a_T(T - T_0) + b_T(T - T_0)^2\right] = R_0\left[1 + a_T(\Delta T) + b_T(\Delta T)^2\right] \tag{5.5}$$

After differentiation, we obtain:

$$dR(t) = R_0\left[a_T + 2b_T\Delta T\right]d\Delta T \tag{5.6}$$

For $ß_T = 0$, equation (5.6) simplifies to:

$$\frac{dR}{dT} = R_0 a_T \tag{5.7}$$

If we apply a small difference to the resistance dR and temperature dT, we get a temperature error based on reference resistance $R_0(T_0)$ at reference temperature T_0:

$$\left|\frac{dR}{R_0}\right| = \frac{R_2 - R_1}{R_0} = a_T dT \tag{5.8}$$

In the case that measurement error of temperature does not exceed a value of $|dT| < 0.5\,\mathrm{K}$, we get maximal permissible relative resistance error dR/R_0 for copper:

$$\left|\frac{dR}{R_0}\right| = \leq 0.19\% \approx \leq 0.2\% \tag{5.9}$$

The total measurement error consists of measured cable temperatures dT_{c1} (heating up), dT_{c2} (cooling down) and error of heating chamber temperature dT_{ch}:

$$dT = dT_{c1} + dT_{c2} + dT_{ch} \tag{5.10}$$

Inserted in the equation (5.8) we obtain the following maximal allowed resistance error:

- linear part: $2b_T\Delta T << a_T$

$$\left|\frac{dR}{R_0}\right| = 3a_T dT_{ch} \tag{5.11}$$

- linear and square part:

$$\left|\frac{dR}{R_0}\right| = 3(a_T + 2b_T \Delta T) dT_{ch} \tag{5.12}$$

here: $\left|\frac{dR}{R_0}\right|$ - maximal permissible resistance error.

For the temperature interval *DT=0* to *120K* (or considering environment temperature T_{env}*= 20°C, T=20* to *140°C*) we get:

$$\left|\frac{dR}{R_0}\right| = (\le 1.14... \le 1.19\%) dT_{ch} \tag{5.13}$$

Considering the temperature error of the chamber $dT_{ch} \le 0.5$K we obtain maximal permissible resistance error $\left|\frac{dR}{R_0}\right|$:

$$\left|\frac{dR}{R_0}\right| = (\le 0.57... \le 0.60\%) \approx 0.6\% \tag{5.14}$$

C. Measurement error due to thermo voltages.

Thermo voltages occur if two different metals at different temperatures come into contact. It is critical to perform the experiment by measuring voltage drop on the cable rather than doing a four-pole resistance measurement. This is obvious from the following example:

Thermo voltage for Cu vs Cu-Fe contact is about 5 µV/K whereas for 100 K it makes 0.5 mV. In case of 4-pole resistance measurement for 1 mm^2 copper wire thermo voltage is:

at 1 mA current – only 17.5 µV/m,
for 3 m wire - ≈ 50 µV

Experiment results are presented in the table 5.1. Here are evaluated linear and square temperature coefficients α_{65} and ß$_{65}$ at 65°C reference temperature respectively.

Experiment Nr.	Cable type	α_{65} in 1/K	$ß_{65}$ in 1/K^2
1.	Round cable FLYR-B 2.5mm^2	$3.364 \cdot 10^{-3}$	$- 2.8 \cdot 10^{-9}$
1.	Extruded PET flat cable, b=50mm	$3.350 \cdot 10^{-3}$	$- 2.8 \cdot 10^{-8}$
2.	Extruded PET flat cable, b=50mm	$3.360 \cdot 10^{-3}$	$- 9.0 \cdot 10^{-8}$
1.	PET flat cable b=20mm	$3.340 \cdot 10^{-3}$	$- 7.0 \cdot 10^{-8}$
2.	PET flat cable b=20mm	$3.000 \cdot 10^{-3}$	$- 7.8 \cdot 10^{-8}$
1.	PET flat cable b=50mm	$3.360 \cdot 10^{-3}$	$- 2.0 \cdot 10^{-8}$

Tab. 5.1 Linear and square temperature coefficients of round and flat electric cables

It can be seen that square temperature coefficient $ß_{65}$ is negative while theoretical value is $+ 6.0 \cdot 10^{-7}$ 1/K^2. This phenomenon is difficult to explain. Therefore, only the linear temperature coefficient α_{65} was taken into consideration for the whole model validation.. Since, temperature of the cables does not exceed 140°C, linear approximation of the resistance as a function of temperature is sufficiently precise.

5.1.2 Current versus voltage measurement

The aim of the second experiment is the determination of the current-voltage characteristic of wires and cables. From this characteristic, the relationship between wire resistance and its temperature can be determined. This information is very important in order to validate the mathematical model of wires and cables presented in Chapters 3 and 4. This model validation is given in Chapter 6, where experimental curves are compared with those from numerical calculation. The experiment is performed by measuring the voltage drop U_i for different current values I_i. It is advisable to increase the current I_i stepwise from 0 to maximal permissible cross section current I_{max} in 10 equal intervals JI. The same procedure should be repeated whilst reducing the current down from I_{max} to 0.

Ambient temperature of the experiment environment should be kept constant and any forced air movement should also be avoided.

In order to perform qualitative experiment almost the same requirements as in (5.1.1) have to be stated:

a) For every voltage-current measurement step, steady-state condition must be obtained.
b) Measurement errors due to restraint of materials must be estimated.
c) Thermo voltages must be avoided.
d) A minimum required distance between current and voltage drop on the cable contacts must be kept.

The first two requirements (a) and (b) have the same definition as in the resistance-temperature experiment. The third requirement (c) should be reconsidered, since the thermo voltage influence is not critical in this case due to high current induced higher voltage drop.

The thermo voltage for Cu vs. Cu-Fe pair is 5 μV/K, that is for 100 K – 0.5 mV. Considering the voltage drop in 1 mm^2 copper wire:

> For 10 A measurement current, the voltage drop leads to 0.175 V/m. For a 10 m length copper wire (which is a minimum requirement to avoid the influence of the boundary temperature decay) the voltage drop results in 1.75 V. This is about 300 times bigger value as the thermo voltage for 100 K.

From this explanation follows that thermo voltages do not significantly influence to measurement error.

The distance between current and voltage measurement contacts of non-insulated wire can be calculated according to equations (3.51, Chapter 3) is given by:

$$c = \sqrt{\frac{lA^2}{a\,uA - a_r I^2 r_0}} \tag{5.15}$$

Denoting $A = \frac{pd^2}{4}$ and $u = pd$ we obtain:

$$c = \frac{pd^2}{2}\sqrt{\frac{l}{ap^2d^3 - 4a_r I^2 r_0}} = \sqrt{\frac{ld}{4a - a_r dI^2 r_0}} \tag{5.16}$$

We can rewrite equation (5.16) in the following form:

$$\boxed{c = \frac{1}{2}\sqrt{\frac{ld}{a\left(1 - \frac{a_r I^2 r_0}{ap^2 d^3}\right)}}} \tag{5.17}$$

For a small current density, the Eq. (5.17) can be simplified as follows:

$$c = \frac{1}{2}\sqrt{\frac{ld}{a}}, \quad nc = \frac{n}{2}\sqrt{\frac{ld}{a}} \tag{5.18}$$

here: n is the number of length constants, which may be applied ranging from any given temperature to the cable temperature of an infinite length with an acceptable error.

For application in this study a factor n = 3, leading to an error of 5 %, is sufficiently precise:

$$\boxed{3c = \frac{3}{2}\sqrt{\frac{ld}{a}} = 0.897\sqrt{\frac{d_{/mm}}{a}}} \tag{5.19}$$

here: d cable diameter in mm.

If we consider a critical heat convection coefficient a = 16 and wire diameter of 1.0 mm we get:

3χ = 224 mm $\approx$ 22 cm

Following equations are used to compute cable temperature T as a function of current I:

1. Determination of cable temperature T:

$$R(T) = R_0\left[1 + \alpha_0(T - T_0) + \beta_0(T - T_0)^2\right] = R_0\left[1 + \alpha_0(DT) + \beta_0(DT)^2\right] \qquad (5.20)$$

here: a_0 linear temperature coefficient of copper at reference temperature T_0 in 1/K

b_0 square temperature coefficient of copper at reference temperature T_0 in $1/K^2$

Material constants a_0 and b_0 have been determined by the experiment described in (5.1.1), however only linear temperature coefficients will be used to calculate cable temperature. Cable temperature T is found from Eq. (5.15):

$$\boxed{T_i = \frac{1}{a_0}\left(\frac{R_i}{R_0} - 1\right) + T_0} \qquad (5.21)$$

here: i number of measurements within one experiment

2. Determination of cable resistance R_i:

From voltage drop measurement on the cable at current I_i according to Ohm's law the resistance is:

$$\boxed{R_i = \frac{U_i}{I_i}} \qquad (5.22)$$

here: I_i current calculated by voltage drop on the shunt U_{si} with constant resitance R_s:

$$\boxed{I_i = \frac{U_{si}}{R_s}} \qquad (5.23)$$

5.2 Experimental setup

5.2.1 Determination of the cable conductor temperature coefficient

Figure 5.1 shows experimental setup for cable resistance / temperature measurement. The cable is placed in a liquid silicon bath, which is situated in a heating chamber (Type: Nixon 815, ISOTECH). The liquid was used as a heat transferring media in order to ensure very constant and homogeneous temperature in the cable. The heat chamber has its own temperature control, which however is not precise enough for this kind of experiment. Therefore, an additional Pt10 sensor was used to measure the liquid and cable temperature.

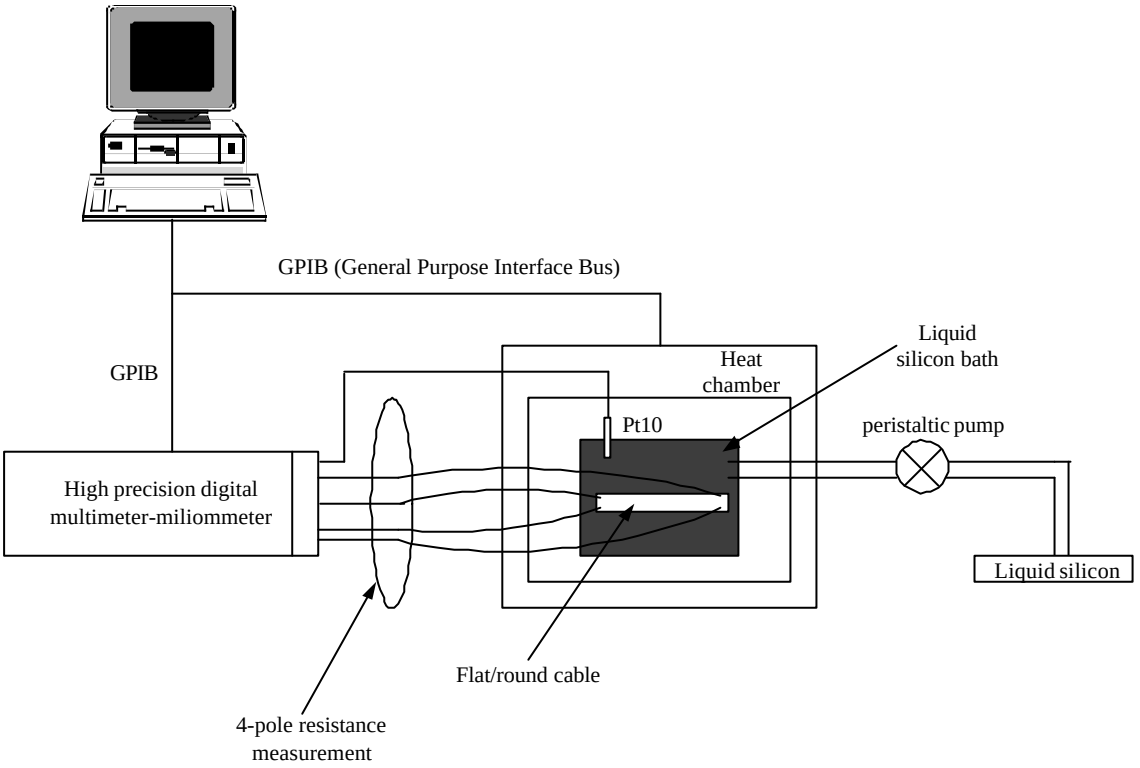

Fig. 5.1 Experimental setup for the cable conductor resistance measurement at different temperatures for the determination of the temperature coefficient

The voltage and the current measurement connection wires were soldered to the cable and sealed with temperature resistant insulating epoxy adhesive. This insulation is very important in order to avoid short circuits in the fluid. Resistance measurement was performed by the $8^{1/2}$ digits precision digital multimeter PREMA 6040S. This multimeter as well as the heat chamber was controlled by a GPIB (General Purpose Interface Bus) controller, which allows the automation of the whole experiment. The liquid silicon is circulated by a pump, which allows more precise temperature control. All input data

(control of experiment equipment) and output data (measurement results) are handled by a LabView program, which was specifically developed for this purpose.

5.2.2 Determination of the cable conductor temperature

In figure 5.2, the experimental setup is given to measure cable voltage drop at different load currents. In this experiment, the cable is placed in free air without touching anything. The laboratory room has constant ambient temperature of 24°C and no significant air currents. Under these laboratory conditions, a precise measurement of the cable power dissipation is possible.

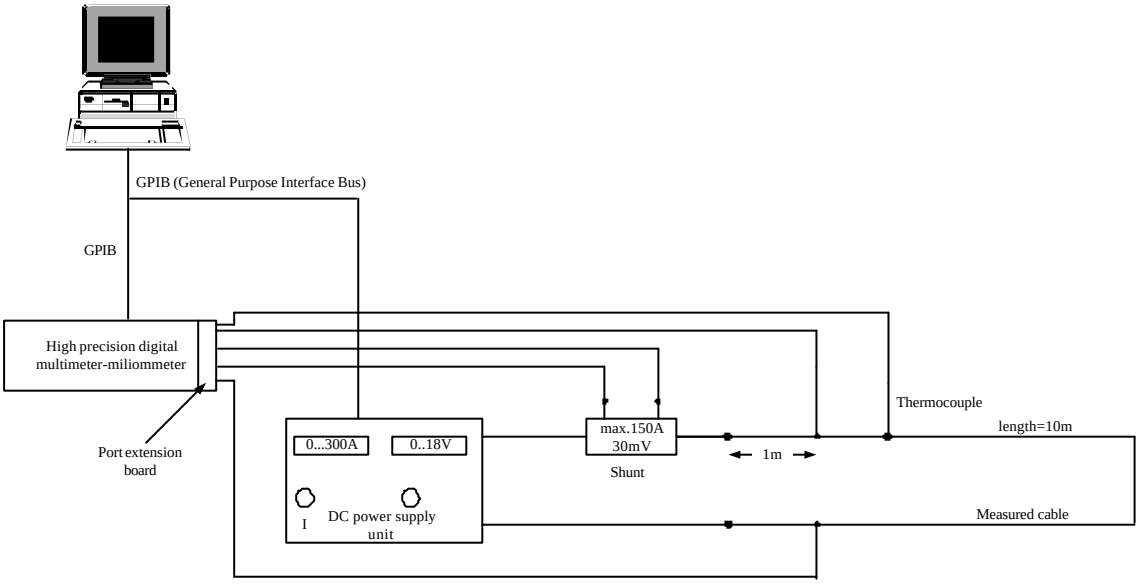

Fig. 5.2 Experimental setup for the cable conductor voltage measurement at different currents for the determination of the conductor temperature

All experimental equipment was controlled by a computer via GPIB interface and in-house developed LabView software (Appendix C), which enabled data acquisition. The whole experiment is fully automated, avoiding any interference of an operator with the experiment environment.

The voltage drop and the current of the power supply unit EA-PS 9018-300 are indicated by the unit, however it was more accurate to use a high precision digital voltmeter and a shunt (precision class 0.2) in order to measure the voltage drop and the load current.

The cable resistance is obtained by the division of the voltage drop through the load current. Here, it is very important to take the temperature drop at the end of the cable into account. Therefore, the measuring points of the voltage on the cable must have a required minimum distance (see Eq. 5.19) from the current supply connections. Finally,

the cable temperature is calculated from the cable resistance with the help of the conductor temperature coefficient.

For the sake of redundancy, a second independent method to receive cable temperature has been applied by using a nickel-constantan thermocouple sensor, which was attached to the cable surface. This sensor was also used for safety to cut off the power supply unit if the maximum allowed temperature of the cable is exceeded.

Thermocouple sensors measure very precisely even if only very small surfaces are available. This is very important for small size electric cables. It would not be possible to measure the temperature of such cables with a Pt100 sensor. The disadvantage of thermocouples is however, that a very precise reference temperature of zero degrees is required. For this purpose, a water-ice mixture was used.

5.3 Measuring process and parameter acquisition

5.3.1 Determination of the cable conductor temperature coefficient

The measuring algorithm of the resistance vs. temperature characteristic of the cable is given in by P. Mack [24]. During this measuring process the cable resistance was measured by 4-pole measurement and its results saved in the computer. Temperature of the cable was measured by Pt10 sensor, which had been placed as close as possible to the cable. The resistance of Pt10 was also measured by the same digital multimeter (DMM) and later, resistance values were converted to the temperature. This conversion is possible by the empirical equation:

$$T = T' + 0.045\frac{T'}{100°C}\left(\frac{T'}{100°C}-1\right)\left(\frac{T'}{419.58°C}-1\right)\left(\frac{T'}{630.74°C}-1\right) \tag{5.19}$$

here T' is given by the equation:

$$T' = \frac{1}{a}[W(T)-1] + d\,\frac{T'}{100°C}\left(\frac{T'}{100°C}-1\right) \tag{5.20}$$

or,

$$T' = \frac{\left(1+\frac{d}{100}\right) - \sqrt{\left(-1+\frac{d}{100}\right)^2 - \frac{4d}{10000}\frac{W(T)-1}{a}}}{\frac{2d}{10000}} \tag{5.21}$$

here: $W(T) = R(T) / R(0°C)$,

R(T)	measured resistance of Pt10 sensor	in Ω,
R(0°C)	= 10.62796	in Ωm,
α	= $3.925870 \cdot 10^{-3}$	in 1/K,
d	= 1.496225	in °*C*.

5.3.2 Determination of the cable conductor temperature

The measuring process and data acquisition of the voltage vs. current experiment had been implemented in Pascal language by T. Roida [25] and later improved in LabView by the author of this study (see also Fig. 5.3, 5.4).

The idea of the measuring process is illustrated in the following table:

Set the power supply unit to 15 VDC		
The user defines the step size and interval of currents from i = 1 to n + 1 (n = number of currents)		
	The user sets the number of measurements for a single current value from i = 1 to m (m = number of measurements of one current value)	
		The user sets one waiting time for all the measurements in s
Steady state = Number of measurement times (Waiting time for one measurement)		
Reset the power supply to 0 A		
Close the files		

Tab 5.1 Algorithm of the measurement program

The visualisation of the measurement data is given in the figures 5.5 and 5.6. The time scale (Fig. 5.5) illustrates the measurement procedure and gives information about the transient state regime. In Fig. 5.6 the temperature of an insulated copper wire is depicted as function of the load current.

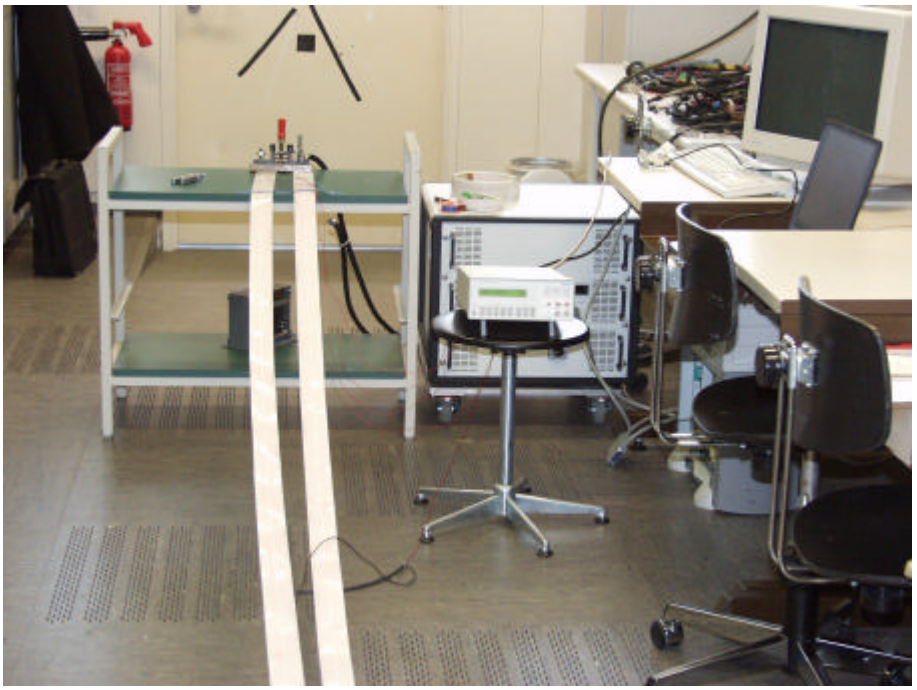

Fig. 5.3 Experimental setup of flat electric cable (FFC)

Fig. 5.4 Experimental setup of round electric cable

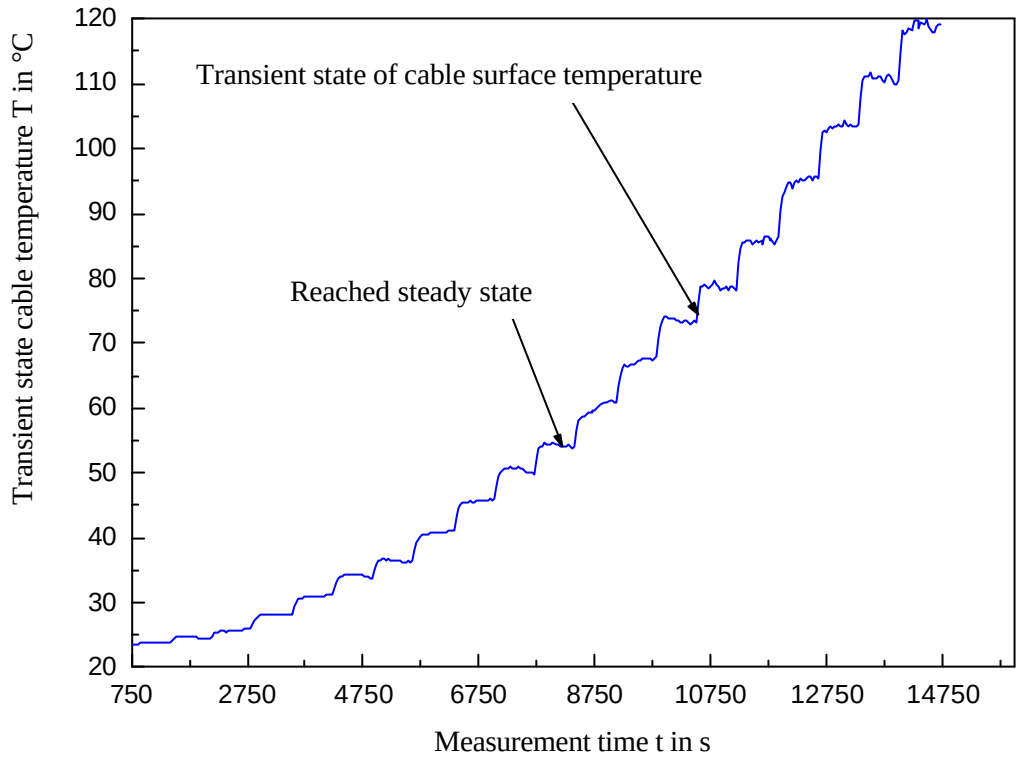

Fig. 5.5 Experimental transient temperature -time characteristic of electrical cable

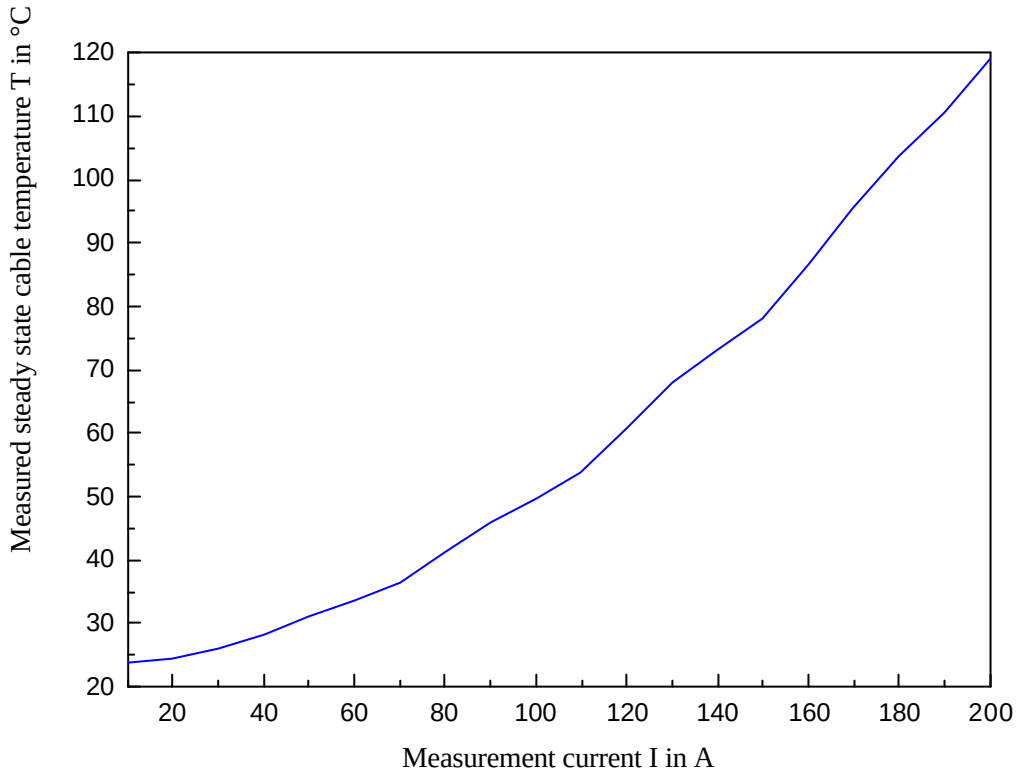

Fig. 5.6 Experimental steady-state temperature-current characteristic of electrical cable

CHAPTER 6

MATHEMATICAL MODEL VALIDATION AND INTERPOLATION OF THE NUMERICAL RESULTS

This chapter starts with the validation of the numerical simulation by the measurement results. Section 6.2 presents a least-square interpolation of the validated results. The theoretical model is determined by the thermal conductivity of insulating materials, the temperature coefficient of copper resistance and the convection and radiation coefficients. The numerical results are fitted by polynomial or logarithmic functions, where the coefficients of those functions are obtained by applying the least-square technique.

6.1 Mathematical model validation

Before starting the comparison of the theoretical (numerical) results with the experimental ones, the quality of the model equations and the evaluation procedure for fitting them to the experimental data should be checked.

The quality of derived heat equations can be understood as the reduction of a 3-D model to a 1-D model. During experimental work, the model reduction to 1-D problem turned out to be sufficient with a negligible error between the theoretical and the physical model.

In addition, boundary conditions can be considered as the quality factor. Implemented limit conditions must be as close to realistic conditions as possible. In our model, the boundary conditions represent laminar free convection to the air while the effects caused by turbulent convection were neglected. In reality, the experiments were performed in an environment where the forced convection was minimised. In addition, convection caused by turbulence was negligible.

The first step was to the validate linear temperature coefficient of the conductor resistance α_ρ, since this parameter is important for the conductor electrical resistance behaviour in the theoretical model. The basic material for the production of stranded conductors for automotive wires is oxygenic copper according to DIN 40500, part 4. The DIN designation of this conductor type is E-CU 58 F21. Since this material does not consist of pure copper, and the manufacturing process might have changed the properties, it

was necessary to measure and validate temperature coefficient of copper resistance again.

Below the measurement results of conductor resistance as a function of temperature are given:

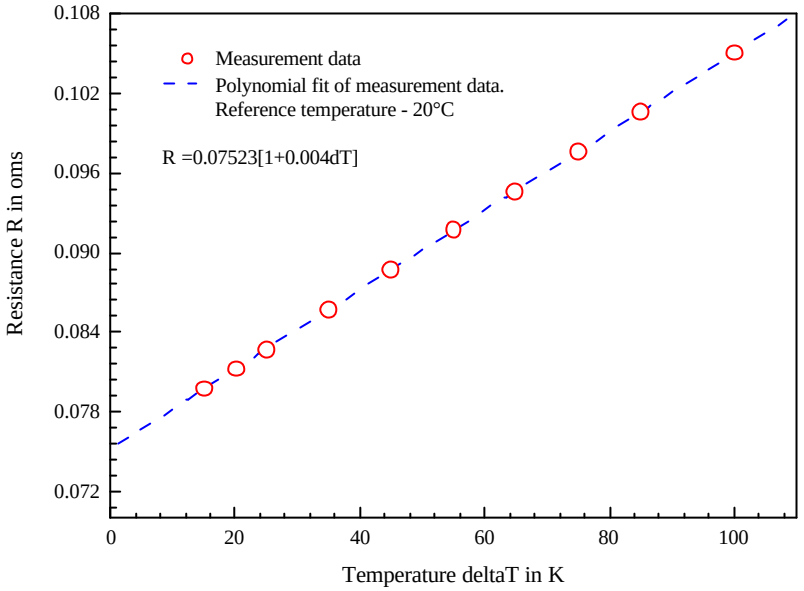

Fig. 6.1 Measured resistance R of round wire for temperature range from 0 to 100 K. Measured temperature coefficient of copper resistance is a_r = 0.004 1/K (based on 20 °C)

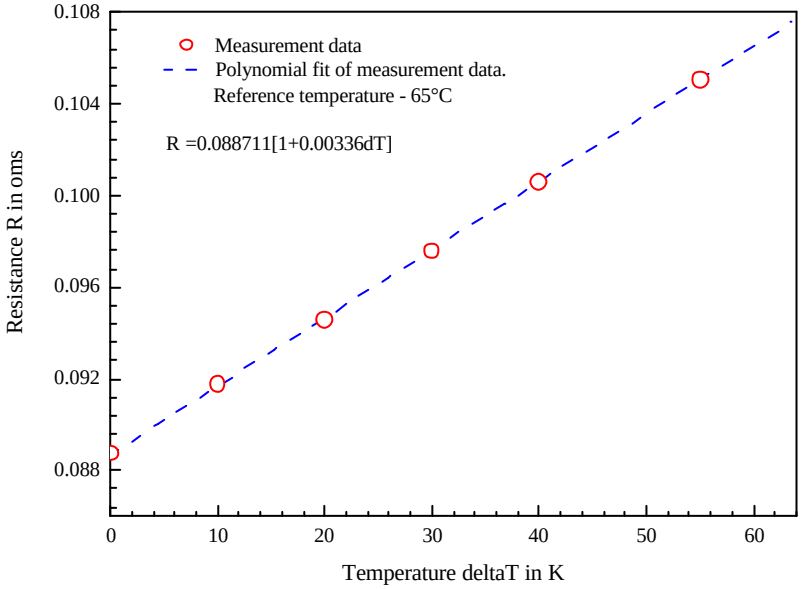

Fig. 6.2 Measured resistance R of round wire for a temperature range from 0 to 60 K. Measured temperature coefficient of copper resistance is a_r = 0.0036 1/K (based on 65 °C)

From the measurement results (Fig.6.1) it can be seen that α_ρ has a value of 0.004 1/K instead of 0.0038 1/K as given in the literature for pure copper material.

Figure 6.2 shows a temperature coefficient of 0.0036 1/K (based on 65 °C), which corresponds the value of 0.004 1/K (based on 20 °C). The value of 0.0036 1/K is also useful, since all our calculations are based on the environment temperature of 65°C.

Below are equations for the conversion of the temperature coefficient α_ρ to any reference temperature. For the derivation, the following functions of the electrical resistance R(T) through the points T_1 and T_2 are considered:

$$\begin{cases} R(T) = R_1\left(1 + a_1\Delta T_1 + b_1\Delta T_1^2\right) \\ R(T) = R_2\left(1 + a_2\Delta T_2 + b_1\Delta T_2^2\right) \end{cases} \tag{6.1}$$

here: $\Delta T_n = T - T_n$

The aim is to obtain a relationship between α_2 and α_1.

First and second order derivatives of Eq. (6.1) are:

$$R'(T) = R_1\left(a_1 + 2b_1\Delta T_1\right) \tag{6.1a}$$

$$R'(T) = R_2\left(a_2 + 2b_2\Delta T_2\right) \tag{6.1b}$$

$$R''(T) = 2b_1R_1 \tag{6.1c}$$

$$R''(T) = 2b_2R_2 \tag{6.1d}$$

$$b_2R_2 = b_1R_1 \tag{6.1e}$$

$$a_2R_2 = a_1R_1 + 2b_1R_1(T_2 - T_1) \tag{6.1f}$$

$$R_2 = R_1 + a_1R_1(T_2 - T_1) + b_1R_1(T_2 - T_1)^2 \tag{6.1g}$$

Then the result is the following:

$$R_2 = R_1\left[1 + a_1(T_2 - T_1) + b_1(T_2 - T_1)^2\right] \tag{6.2}$$

$$a_2 = \frac{a_1 + 2b_1(T_2 - T_1)}{1 + a_1(T_2 - T_1) + b_1(T_2 - T_1)^2} \tag{6.3}$$

$$b_2 = \frac{b_1}{1 + a_1(T_2 - T_1) + b_1(T_2 - T_1)^2} \tag{6.4}$$

Since the non-linear part of the temperature coefficient ß is very small, for temperature up to 140 °C ß can be assumed zero (ß = 0). In that case, the equations are simplified as follows:

$$R_2 = R_1[1 + a_1(T_2 - T_1)] \tag{6.5}$$

$$\boxed{a_2 = \frac{a_1}{1 + a_1(T_2 - T_1)}} \tag{6.6}$$

The next step of the model validation is to estimate the heat conductivity coefficient ? of the insulation material. It should be noted that during this research work the heat conductivity coefficient was not investigated experimentally. Here, in order to save investigation time and costs, the coefficient ? was obtained by fitting of the temperature measurement results with theoretical ones. Of course, it would have been possible to use the coefficient from the literature, however the available values were only given in a very narrow temperature range. Therefore, the ? coefficient was varied in order to fit to the experimental curves of the conductor surface temperature.

Below the measured conductor surface temperature of round and flat electrical cables are compared with the computed ones.

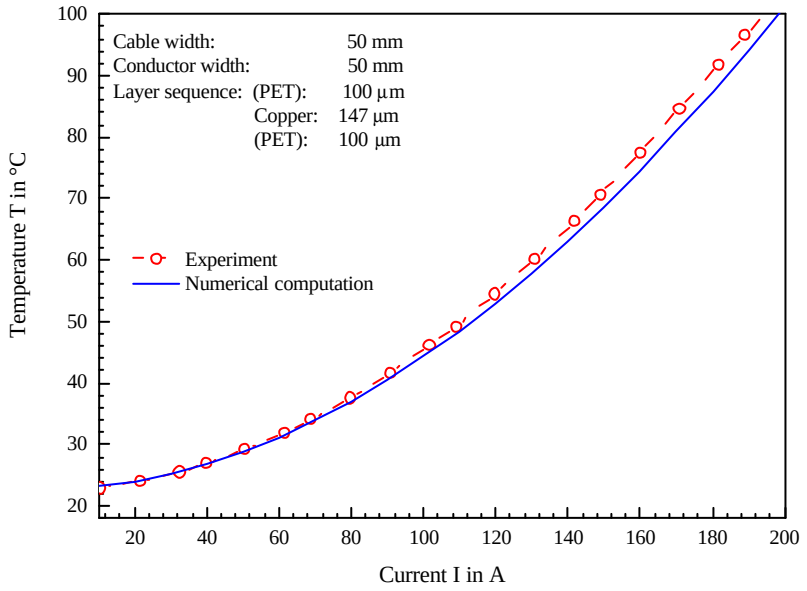

Fig. 6.3 Measured temperature of a flat cable conductor (conductor width 50 mm) as function of the electric load

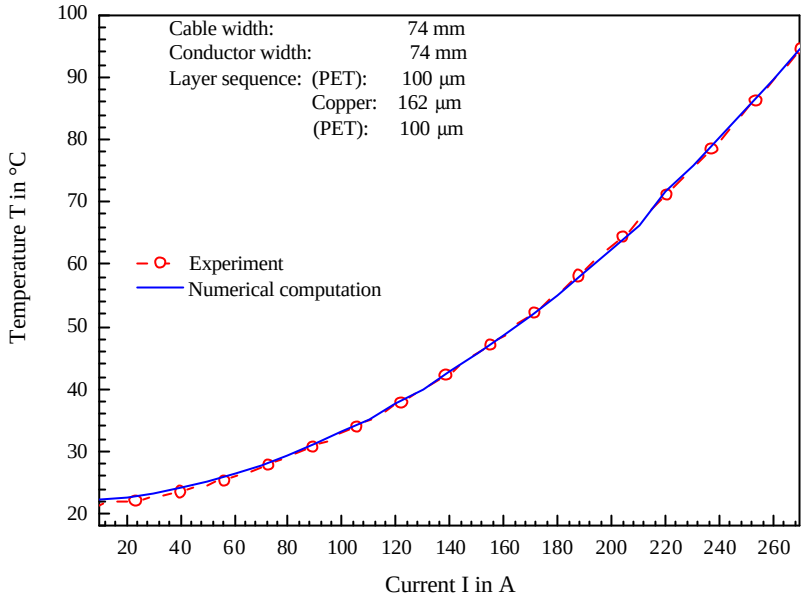

Fig.6. 4 Measured temperature of a flat cable conductor (conductor width 74 mm) as function of the electric load

Fig. 6. 5 Flat cable (FFC) examples

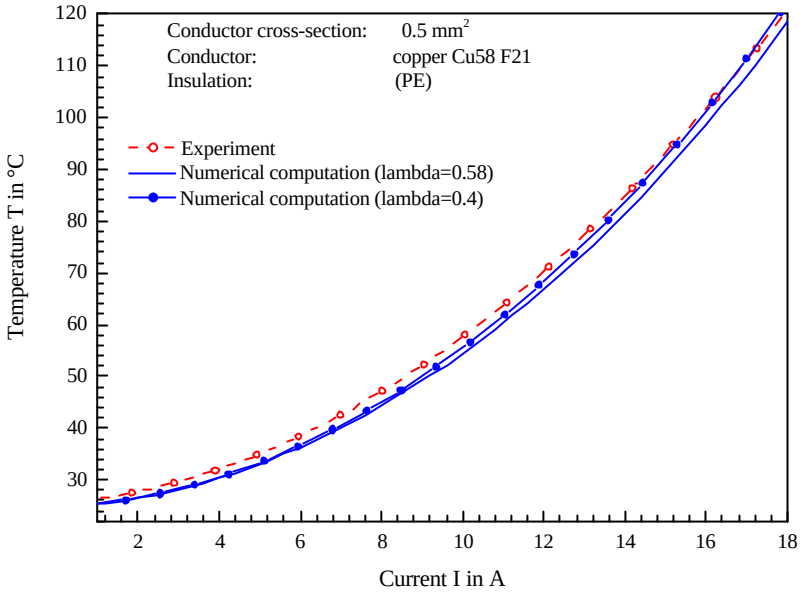

Fig. 6. 6 Measured temperature of a round wire conductor (cross section 0.5mm^2) as function of the electric load

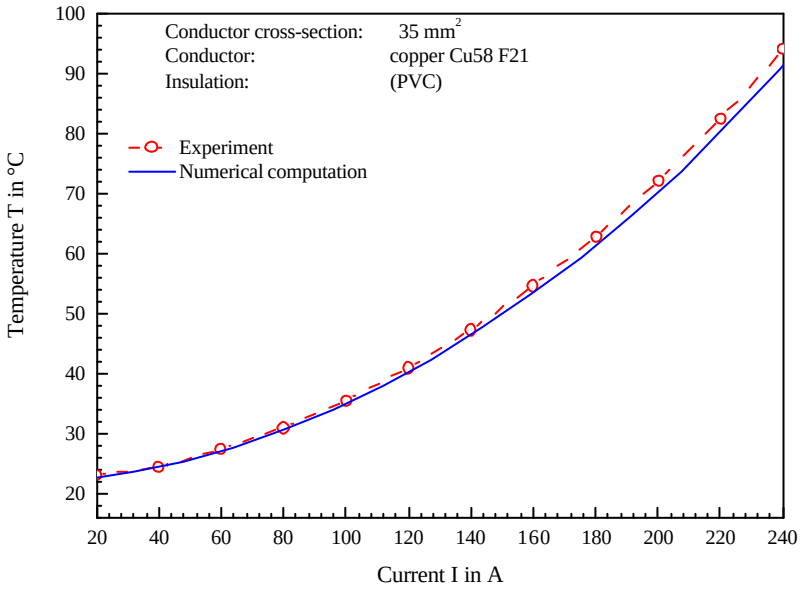

Fig. 6. 7 Measured temperature of a round wire conductor (cross section 35mm^2) as function of the electric load

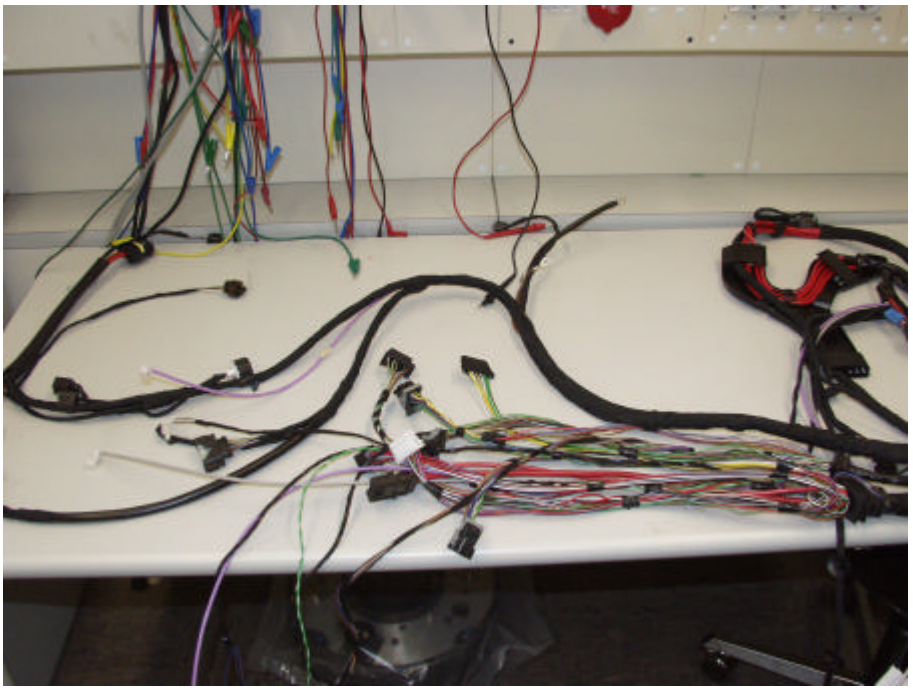

Fig. 6. 8 Round cable examples

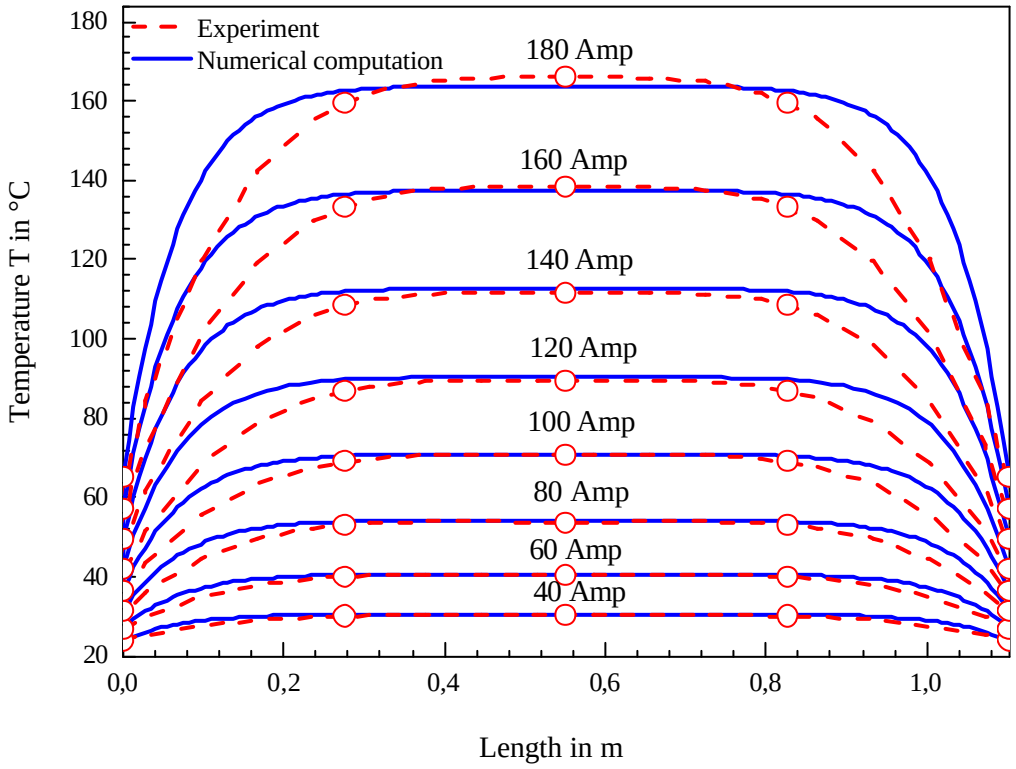

Fig. 6.9 Measured temperature of a fuse element as function of the electric load

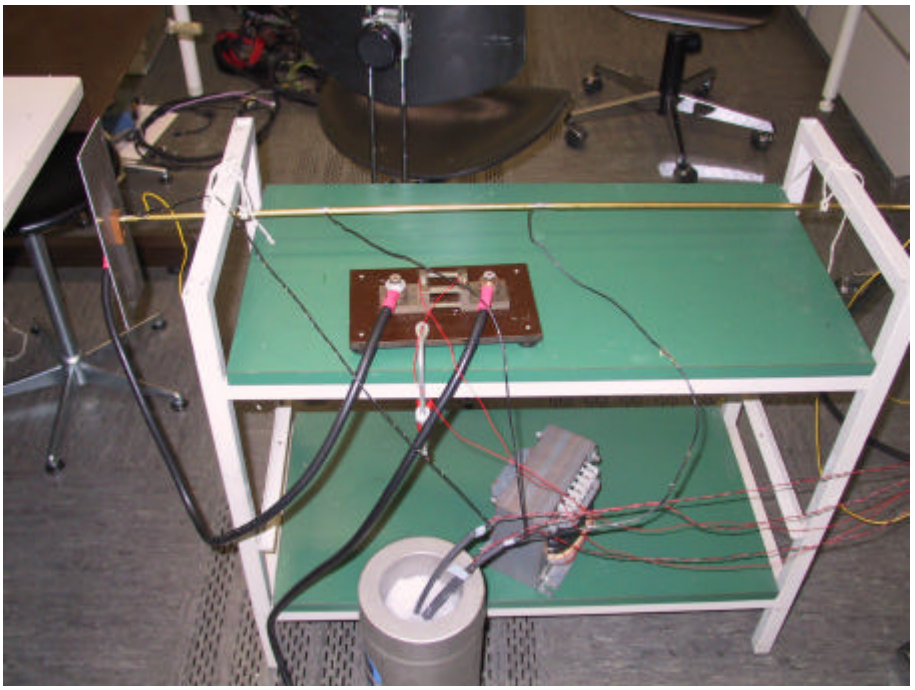

Fig. 6.10 Fuse element prototype with temperature sensors (thermocouples). Fuse element (hollow cylinder) dimensions: inner diameter – 6mm, outer diameter 8mm. Material type of the fuse element: Bras 58 (CuZn39Pb3).

Finally, the heat convective and radiative coefficients had to be validated. During separate experimental work [18] a number of measurements of various round wires was carried out in order to validate the empirical heat convection and radiation formulas, which were presented in the section (2.5). The results of this experimental work have shown that the evaluation procedure of convection and radiation coefficients is correct.

Since, it has already been described how the model was validated, now the obtained results can be studied. The following three models, which differ by the geometry and type of materials are presented:

1. Figures 6.3 and 6.4 show the **flat cable** conductor temperature as function of the electrical current. These results are obtained for a cable, which is placed free in air, in a horizontal position. The temperature is taken after the steady state has been reached. Both, numerical simulation and measurement data, gives a very good agreement.

2. Figures 6.6 and 6.7 show the **round wire** conductor temperature as function of the electrical current. By altering of the conductivity coefficient l of PE (Polyethylene) in figure 6.6, a better agreement of both curves can be achieved.

3. Figure 6.9 shows the temperature distribution along the **fuse element**. The length of the whole system was about 1 meter, since the influence of the fuse holders and contacts must be considered. Also electrical wire, which is protected by this fuse had to be taken into consideration too. The temperature distribution is presented for different electrical current values. The calculated curves in all figures match with the measured data ac

ceptably well. At the boundaries of the fuse holders and contacts, a larger error is present. This can be explained by the limited performance of the experiment setup. Temperature of the fuse system was measured only by three thermocouple sensors. Later, three measurement points were interpolated. However, high accuracy of temperature gradient on the boundaries is not of primary importance. Only the fuse element maximal temperature is of interest, because this temperature causes the required interruption of the fuse-melting element.

Discussed results show the fact that the approximation made for the derivatives of the equations (Chapter 2: 2.4, 2.6, 2.8) as well as the validation of the physical model constants are applicable under the experimental conditions, which are interested in this context.

6.2 Interpolation of the numerical results to reduce heat transfer equations

Throughout the entire study, the heat transfer analysis algorithm was derived using analytical / numerical methods. This algorithm allows the determination of the thermo-electrical characteristic of electrical conductors in both a steady- and transient-state regimes. The proposed approach provides very good accuracy between theory and experimental results, is applicable for different conductor geometries, and can be extended from a 1-D to a 2-D problem. However, very often, numerical simulation of heat transfer requires a lot of computation time that is not acceptable if the numerical simulation routine has to be integrated into another complex simulation system. This leads finally to a situation, where the whole performance of a complex simulation system becomes very poor. Another disadvantage of pure numerical simulation of heat transfer problem is that very often in a real life, the calculations have to be done very quickly and in a simple manner

Therefore, our intension in this study is not only to present fully-developed numerical models but also to develop simple, with the minimum number of physical constants, analytical equations, which describe best the steady-state and transient-state heat transfer regimes in any type of conductors. These equations should have the advantage of producing a manageable relationship having only two or three constants, which can be obtained easily by the least-square (LS) algorithm. Finally, having those simple equations, an operator can perform the calculations in an easy way.

In this section we will present polynomial and logarithmical equations of thermo-electrical characteristics and show how to apply the LS algorithm [8,9] for the calculation of the "simplified-equation" coefficients. It is very important to predict correctly the correct equations with a minimum number of unknown constants. Basically, two type of functions are of interest: polynomial regression and logarithmical functions. With these two functions, all important thermo-electrical characteristics can be described.

The following functions are considered, whose physical meaning will be given later:

- thermo-electrical characteristic *DT(I)* (Fig.6.11)

- heating-up time characteristic *tg(I)* (Fig.6.12)
- time constant characteristic *t(I)* (Fig.6.13)
- electric-field strength characteristic *E(I)* (Fig.6.14)

It is worth to emphasise that these four functions are valid for any kind of conductor (flat cables, fuses or cable bundles), where heat generation by electrical current takes place. For the illustration of the LS algorithm, a round insulated wire of FLRY-B - 2.5mm^2 type is used. Here the maximal final temperature of the wire is 105 °C and environment temperature 65 °C.

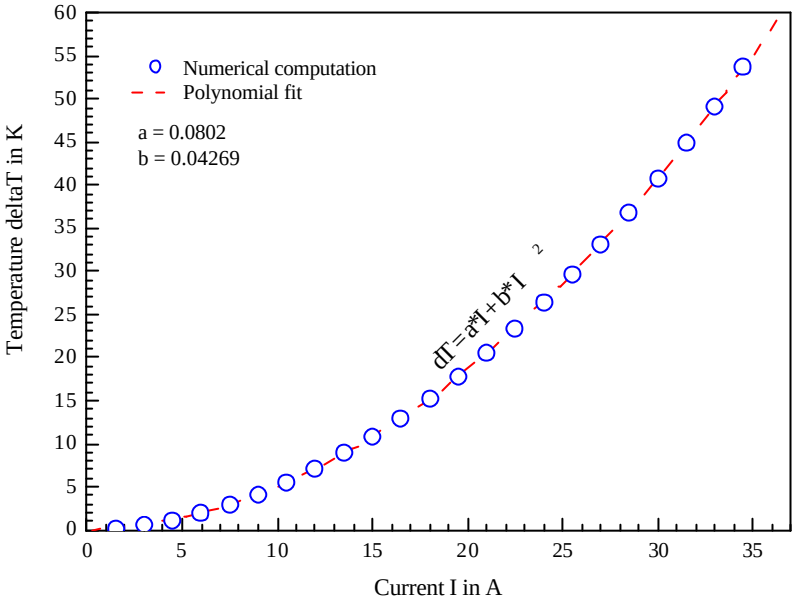

Fig. 6.11. Thermo-electrical characteristic *DT(I)* of round insulated wire (FLRY-B, 2.5mm^2) obtained from numerical calculation and approximated by polynomial function

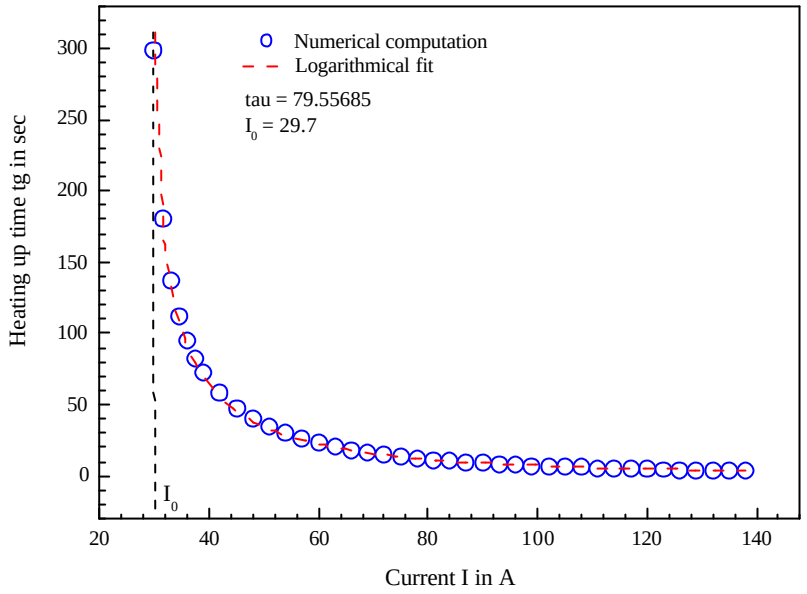

Fig. 6.12. Heating-up time *tg(I)* characteristic of round insulated wire (FLRY-B, 2.5mm^2) obtained from numerical calculation and approximated by logarithmical function

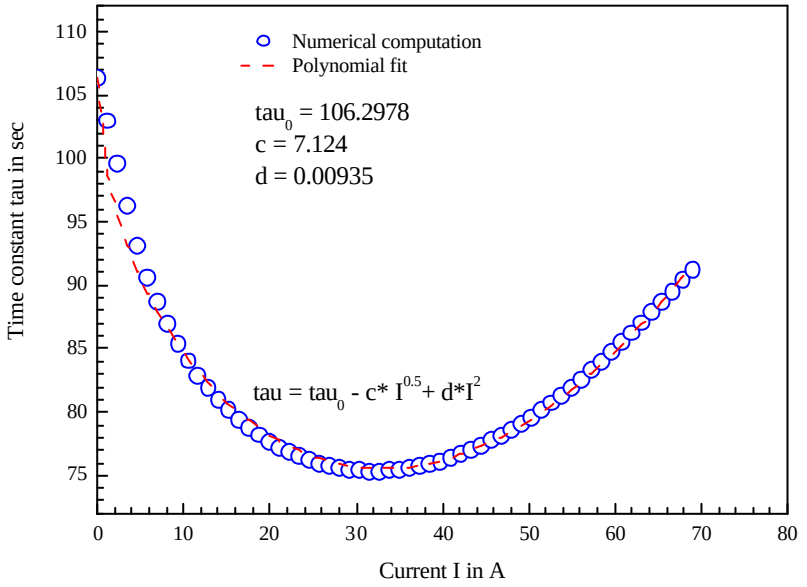

Fig. 6.13. Time constant *t (I)* characteristic of round insulated wire (FLRY-B, 2.5mm^2) obtained from numerical calculation and approximated by polynomial function

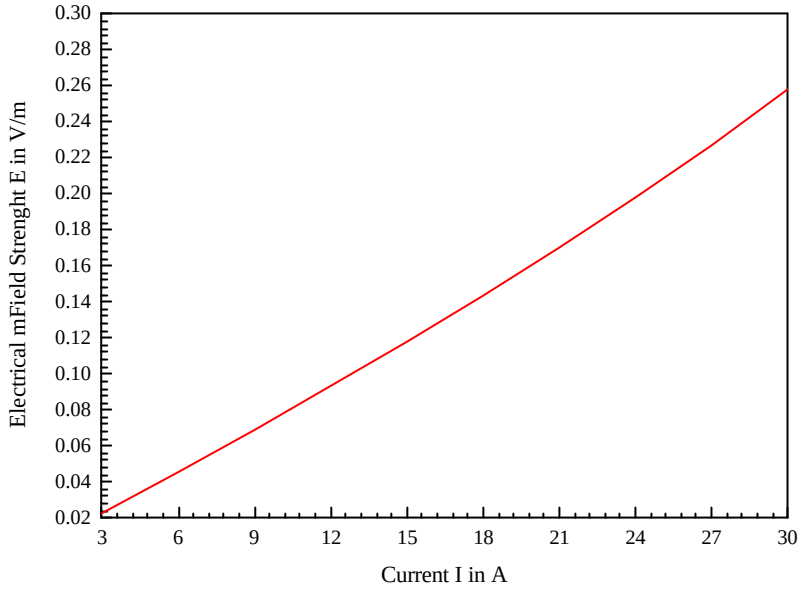

Fig. 6.14 Electric field strength *E(I)* characteristic of round insulated wire (FLRY-B, 2.5mm^2) obtained from Eq. (6.10)

The curves presented in figures 6.11, 6.12, 6.13 and 6.14 can be described by the following equations:

- thermo-electrical characteristic (here $I \geq 0$):

$$\boxed{\Delta T\left(I \leq I_0\right) = a\, I + b\, I^2} \tag{6.7}$$

- heating-up time characteristic:

$$\boxed{t_g\left(I > I_0\right) = t_g \ln \frac{I^2}{I^2 - I_0^2}} \tag{6.8}$$

- time constant characteristic:

$$\boxed{t = t_0 - c\, I^{0.5} + d\, I^2} \tag{6.9}$$

- electrical field strength characteristic:

$$E = \frac{Ir}{A} = \frac{Ir_0(1 + a_r \Delta T + b_r(\Delta T^2))}{A} \tag{6.10}$$

In equation (6.10) temperature difference ΔT is calculated by Eq. (6.7)

The coefficients of the equations (6.7, 6.8, 6.9) *a, b, I_0, t_g, t_0, c, d,* are valid only for one specific type of wire. If another wire type has to be investigated, the coefficients have to be re-computed. The Least-Square Method (LS) can be used to obtain these coefficients.

Applying LS method and solving the linear system of the equations leads to the following required coefficients:

- final temperature per current coefficient *a*:

$$a = \frac{\sum_1^n I_n^4 \times \sum_1^n I_n \times DT_n - \sum_1^n I_n^3 \times \sum_1^n I_n^2 \times DT_n}{\sum_1^n I_n^2 \times \sum_1^n I_n^4 - \left(\sum_1^n I_n^3\right)^2} \tag{6.11}$$

- final temperature per current square coefficient *b*:

$$b = \frac{\sum_1^n I_n^2 \times \sum_1^n I_n^2 \times DT_n - \sum_1^n I_n^3 \times \sum_1^n I_n \times DT_n}{\sum_1^n I_n^2 \times \sum_1^n I_n^4 - \left(\sum_1^n I_n^3\right)^2} \tag{6.12}$$

- heating-up time constant t_g

$$\tau_g = \frac{\sum_1^n t_n \ln \frac{I_n^2}{I_n^2 - I_0^2}}{\sum_1^n \left(\ln \frac{I_n^2}{I_n^2 - I_0^2}\right)^2} \tag{6.13}$$

- time constant per square root current coefficient *c*

$$c = \frac{\tau_0 \sum_1^n I_n^{0.5} \times \sum_1^n I_n^2 - \tau_0 \sum_1^n I_n^2 \times \sum_1^n I_n^{2.5} - \sum_1^n I_n^2 \times \sum_1^n I_n^{0.5}\tau_n + \sum_1^n I_n^{2.5} \times \sum_1^n I_n^2\tau_n}{\sum_1^n I_n \times \sum_1^n I_n^4 - \left(\sum_1^n I_n^{2.5}\right)^2} \tag{6.14}$$

- time constant per square current coefficient *d*

$$d = \frac{\tau_0 \sum_1^n I \times \sum_1^n I_n^2 - \tau_0 \sum_1^n I_n^{2.5} \times \sum_1^n I_n^{0.5} - \sum_1^n I_n \times \sum_1^n I_n^2\tau_n + \sum_1^n I_n^{2.5} \times \sum_1^n I_n^{0.5}\tau_n}{\left(\sum_{n=1}^n I_n^{2.5}\right)^2 - \sum_1^n I_n \times \sum_1^n I_n^4} \tag{6.15}$$

here: $\forall = 1, n$; where n is the number of calculating points in the wire characteristics;

I_n – the electrical current values, which are used in the characteristics of Fig. 6.11-6.14

DT – temperature values, which are used in the characteristic of Fig. 6.11

t_n – heating up time values, which are used in the characteristic of Fig. 6.12

t_n – time constant values, which are used in the characteristic of Fig. 6.13

The relationship presented in Fig. 6.11 is a steady-state load characteristic of electric cables. Here the temperature represents the steady-state for a particular load current value. Normally, this characteristic ends with the maximum allowed temperature of the wire or cable after infinite time.

In Fig. 6.12 heating up time is given as a function of the load current. This relationship is well known from the fuse time-current characteristic and it makes sense to apply the same characteristic to any electric wire or cable.

The heating up time is the time to reach maximal permissible temperature with a current greater than the nominal load. For example, in Fig. 6.12 105 °C degrees are given as maximal permissible temperature. Having available the time-current characteristics for both: wires and fuses, it is possible to model the geometry of the fuse to match the heating-up time function of the wire. Finally, having a fuse with such a characteristic, it is possible to protect the wire with good accuracy.

Fig. 6.13 gives the time constant as a function of load current. This curve gives the possibility to obtain any t constant as a function of only one variable; the current. It is also straightforward to compute the transient state analytically, having t as the known parameter.

Fig. 6.14 represents the electric field strength dependence on load current. Here, the non-linear curve behaviour is due to non-linear electric resistance dependence on temperature.

CHAPTER 7

CALCULATION OF THE HEAT TRANSFER IN A MULTI-WIRE BUNDLE

Contrary to previous chapters, where the heat transfer was modelled for a single electric cable, in this chapter possible methods to calculate the heat conduction in a multi-cable bundle will be shown. The main effort to solve this problem is devoted to the linear co-ordinate transformation in order to simplify the model geometry and to the determination of an averaged heat conductivity coefficient of the multi-cable material media. This chapter deals with a one-dimensional radial steady state heat conduction problem, where the heat transfer equation is solved analytically. In analogy to a single insulated conductor (see Fig. 7.1a), the multi-insulated cable conductor (see Fig. 7.1b) is considered as an insulated "mixed" conductor.

7.1 Coordinate transformation of the multi-wire bundle geometry

The calculation of heat transfer in a multi-cable bundle belongs to the heat conduction problems for anisotropic multi-layered media [28]. The heat conductivity coefficient has been determined using *conservative averaging method for layered media* [78], where heat conductivity of single cables are transformed to a common mixed property or mixed heat conductivity coefficient. The algorithm of temperature determination using a conservative averaging method can be found in Chapter 8, (3)

The calculation method considers an anisotropic material that is homogeneous and has constant thermo-physical properties. It also considers radial symmetry, i.e. no angular temperature gradient $\partial T / \partial f = 0$. Then, the governing partial differential equation for the heat conduction problem in a cylindrical coordinate system becomes:

$$-\frac{1}{r}\frac{\partial}{\partial r}\left(l r \frac{\partial T(r)}{\partial r} \right) = q_V(r) \tag{7.1}$$

here: $?$ thermal conductivity coefficient,
T temperature field,
q_v volumetric heat generation.

This leads to a temperature drop in the cable bundle, which is obtained in a similar way as in Chapter 3 (analytical analysis of heat transfer in cylindrical wires):

$$\Delta T = \frac{p}{p}\left[\frac{1}{a(D+2S)} + \frac{1}{2\lambda_I}\ln\left(1+\frac{2S}{D}\right) + \frac{1}{4\lambda_L}\right] \tag{7.1a}$$

here: λ_I, λ_L heat conductivity of insulation and of mixed conductor in W/mK,
D diameter of the cable without insulation in m,
I the current in A,

$$p = \sum_1^n p_n$$

describes the electrical power per length EI, i.e. a sum of all single wires in W/m,
S thickness of insulation in m.

In a mathematical sense, Eq. (7.1) is transformed by the linear coordinate transformation as shown in figure 7.1. In a physical sense, the governing equation (7.1) of an anisotropic heat conduction problem is converted into an equivalent isotropic problem by replacing different material coefficients by mixed material properties.

This transformation has the following characteristics:

a) it is linear and continuous,
b) an anisotropic problem is converted to an isotropic problem after transformation,
c) there is no stretch and the rotation in radial direction,
d) no gaps or overlaps are generated along the interface,
e) no sliding and mismatches occur along the interface.

These features offer advantages in dealing with straight boundaries and interfaces in the multi-layered system.

In this study the conversion of round insulated wires into a square ones with the same conductor, insulation and air cross section is proposed (see Fig. 7.2).

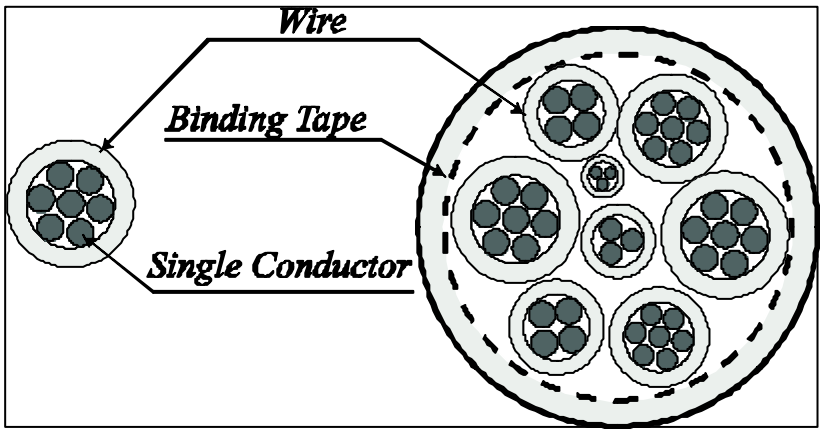

a) **b)**

Fig. 7.1 Insulated single (a) and insulated multi-wire conductor (b)

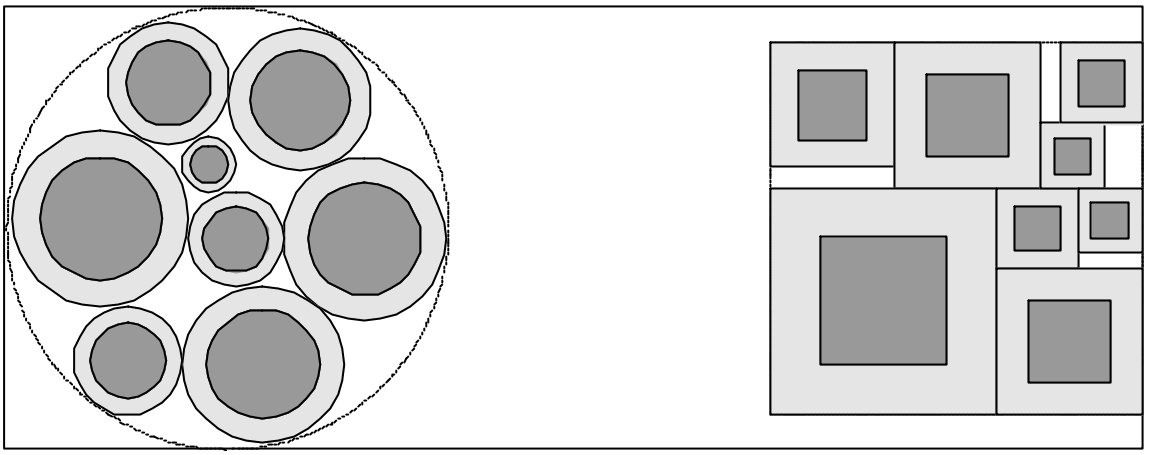

a) **b)**

Fig. 7.2 Transformation of insulated round conductors (a) into squares of same area (b)

The square structure can be now calculated easily as a thermal serial-parallel switched model of similarly covered areas. In order to simplify the calculation, the complete solid material was separated from the air and combined in three layers. The influence of the lower heat conductivity of air will be considered later with a so-called "filling factor".

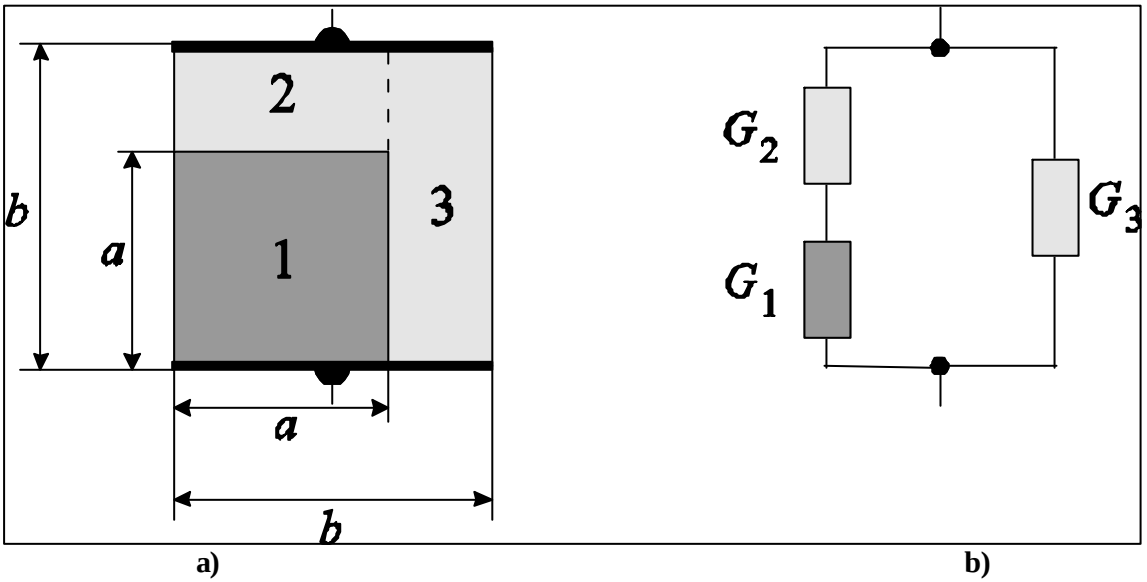

a) **b)**

Fig. 7.3 Determination of the mixed area conductivity: (a) assembly, (b) circuitry

For long (compared to their thickness) wires, the whole material can be treated two-dimensionally with a so-called "area conductivity" *?l* and which is proportional to the known heat conductivity *?*. The heat conductance *G* is given by

$$G = \frac{l\,lx}{y}$$

and for each layer given in Fig.3 one obtains:

$$G = ll\,,\; G_1 = l_1 l\,,\; G_2 = l_2 l \frac{a}{b-a}\,,\; G_3 = l_3 l \frac{b-a}{b} \tag{7.2}$$

Finally, a "Mixed Material Equation" of the following form is obtained:

$$l = l_2 \left(\frac{1}{\frac{l_2}{l_1} + \frac{b}{a} - 1} - \frac{a}{b} + 1 \right) \tag{7.3}$$

where the heat conductance are replaced by their heat conductivities.

here:	?	radial mixed heat conductivity,	
	$?_1$	heat conductivity of the conductor,	
	$?_2$	heat conductivity of the wire insulation (see Fig.7.1),	
	a	edge of heat conductor material 1 ($?_1$),	in mm,
	b	edge of mixed heat conductor material 1 and 2 (?)	in mm.

The next step is to determine the relationship of b/a which is calculated from the area a^2 of the materials 1 and 2 (which is the cross section of the conductor and the isolator).

Since the conductor consists of single wire veins with air gaps in between, the real conduction cross section a^2 has still to be multiplied with the so-called filling factor f, which is the relationship of the real conducting cross section to the cross section to be determined by its measured diameter: $A_1 = a^2 f$. The cross section of the conductor and the isolator together results in:

$$\frac{A_1}{f} + A_2 = b^2 \tag{7.4}$$

from which finally b/a can be calculated, whereby the areas A_2 and A_1 may be replaced by the sums of the diameter squares of the conductor d and of the wire veins d:

$$\frac{b}{a} = \sqrt{\left(\frac{fA_2}{A_1} + 1 \right)} = \sqrt{\frac{f \sum_1^i d_i^2}{\sum_1^i n_i d_i^2}} = \sqrt{\frac{f}{\Sigma}} \tag{7.5}$$

The model described by the equation 7.3 is only valid for materials with similar heat conductivity. If one part diverts as far as air compared to copper, the model is no longer applicable. In this case, the assumption is made, that the conductor consists of two different conducting materials, which are switched in parallel as follows:

$G = G_a + G_b$.

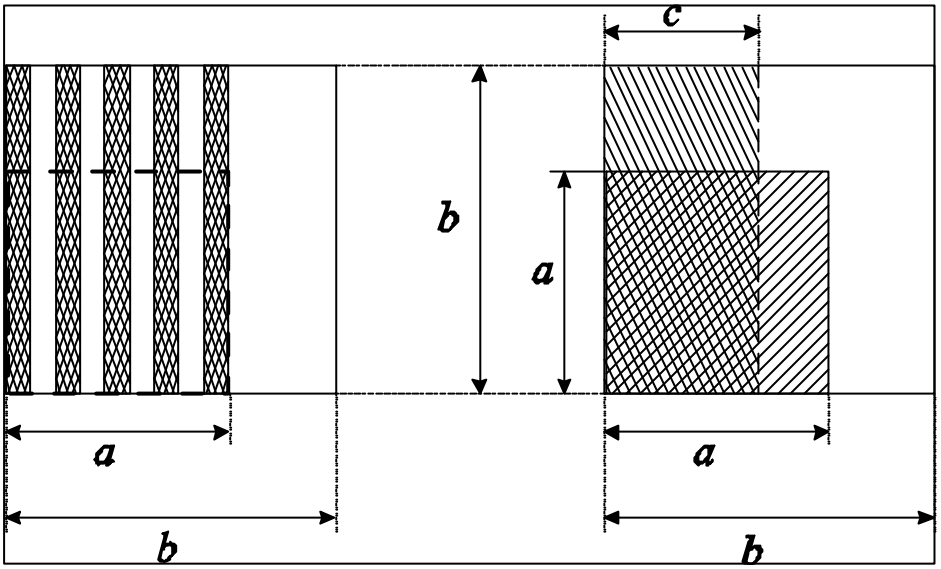

Fig. 7.4 Volume change due to empty spaces, in accordance with the filling factor *f* or *F*

In accordance with Fig. 7.4 the heat conductivities can be calculated as follows:

$$G = l\ ,\ G_a = l_a \frac{c}{b}, G_b = l_a \frac{b-c}{b} \tag{7.6}$$

here: $?$ mixed heat conductivity,
$?_a$, $?_b$ heat conductivity of area a^2 and b^2, respectively,
a, b virtual length of all conductors and of mixed conductor,
c virtual length c/b of b^2.

Replacing a square element by two rectangular elements with different heat conductivity, (see Fig. 7.4) leads to the mixed heat conductivity:

$$l = l_a \frac{c}{b} + l_b \frac{b-c}{b}.$$

Using the filling factor:

$$f = \frac{c}{b}$$

for the air between veins in a wire and

$$F = \frac{b-c}{b}$$

for the air between wires in a cable gives the thinning equations:

$$\boxed{l = l_a f + l_b(1-f) \approx l_a f,\ l = l_a F + l_b(1-F) \approx l_a F} \tag{7.7}$$

Assuming the application of the first model (Eq. 7.3) is more suited for insulated conductors and the second model (Eq. 7.7) is more suited for non-insulated conductors with gaps in between, the two equations can be combined as follows. In this case, the heat conductivity *?* of the mixed material without air can be replaced by the heat conductivity *?F* of the mixed material with air, whereby *F* is the insulated wire filling factor.

Assuming, that the conductor material has much higher heat conductivity than the air in between, the equation may be simplified even further, e.g. for $?_1 f >> ?_2 F$ one obtains:

$$\boxed{l = l_2 F\left(1 + \frac{1}{\sqrt{\frac{f}{\Sigma} + \frac{l_2}{l_1 f} - 1} - \sqrt{\frac{f}{\Sigma}}}\right) \approx l_2 F\left(1 + \frac{1}{\frac{f}{\Sigma} - \sqrt{\frac{f}{\Sigma}}}\right)} \tag{7.8}$$

7.2 Calculation of temperature distribution in the real multi-wire bundle

Considering the following cable bundle structure, (see picture 7.6):

Wire type	Cross section	Number of single wires (veins)	Diameter of the single wire (vein)	Wire (vein) diameter	Number of wires in the bundle
		n_i	d_i	∂_i	m_i
	mm^2		mm	mm	
FLRY-A	0,35	7	0,26	0,80	10
FLRY-A	0,5	19	0,19	1,0	10
FLRY-A	0,75	19	0,23	1,20	10
FLRY-A	1,5	19	0,32	1,70	5
FLRY-B	2,5	50	0,26	2,20	5
FLRY-B	4	56	0,31	2,75	2

Tab 7.1. Physical data of the cable bundle

First, calculating the fill factor *f* of the wire:

$$f = \frac{nd^2}{\partial^2} \tag{7.9}$$

here: ? wire diameter in mm

From the conductor and wire vein squared sum data, a cross section quotient Σ of cable bundle is calculated:

$$\Sigma = \frac{\sum_1^i n_i d_i^2}{\sum_1^i d_i^2} = \frac{\sum_1^i m_i n_i d_i^2}{\sum_1^i m_i d_i^2} \tag{7.10}$$

Since, experiment data are available of the cable bundle presented in the 7.1 table, the bundle fill factor of cable bundle *F* empirically can be calculated:

$$F = \frac{4p\ r_1 l I}{\Sigma \cdot U\left(U_S - 2p\ S\right)^2} \tag{7.11}$$

Finally, having all required information to calculate radial averaged heat conduction coefficient ?, Eq. (7.8) can be used to obtain this coefficient:

$$l = l_2 F \left(1 + \frac{1}{\sqrt{\frac{f}{\Sigma}} - 1} - \frac{1}{\sqrt{\frac{f}{\Sigma}}} \right) \tag{7.8}$$

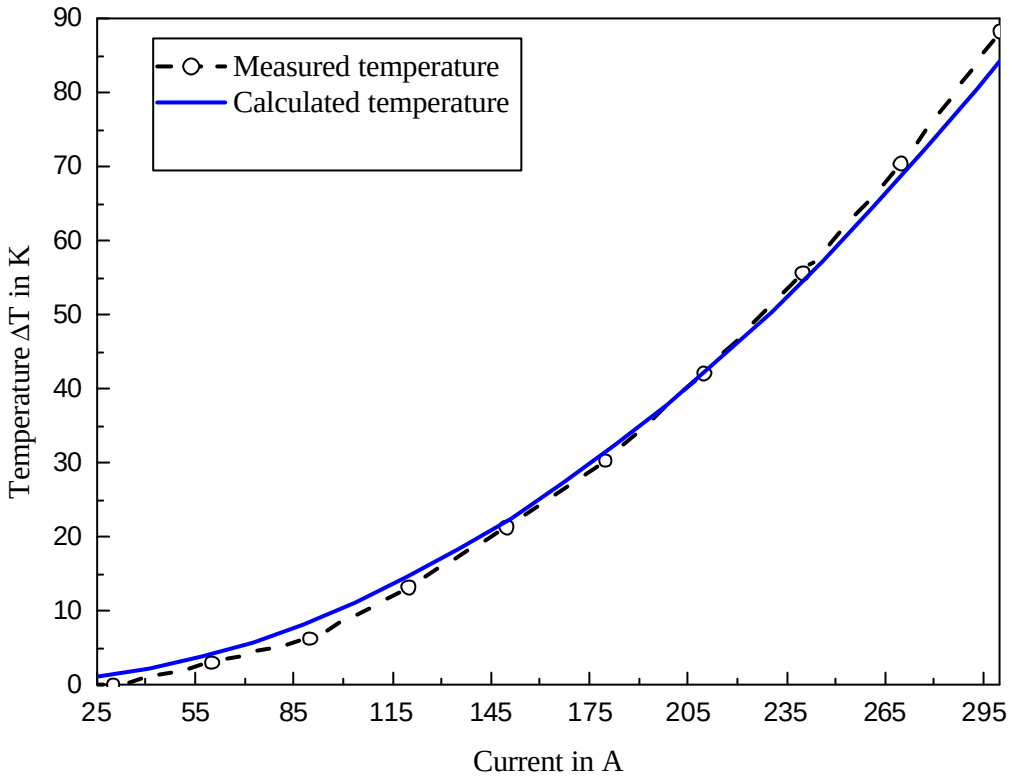

Fig. 7.5 Experimental versus theoretical results of the cable bundle. Environment temperature 23°C

In Fig. (7.5) the temperature dependence on load current of the presented cable bundle (see Tab. 7.1) is given. Here the experimental results are compared with the results obtained using the new derived *averaged heat conductivity coefficient ?*.

There is some error between two curves, which can not be fully explained yet. It seems that the applied model for the bundle does not completely describe the reality in every case. The reason for this observation might be geometrical differences between the reality and the model. Another reason could come through a difference between the real and the calculated heat radiation from the bundle surface. The relevant emissive coefficient is not known precise enough for this application.
All these observations are an area of further consideration if necessary.

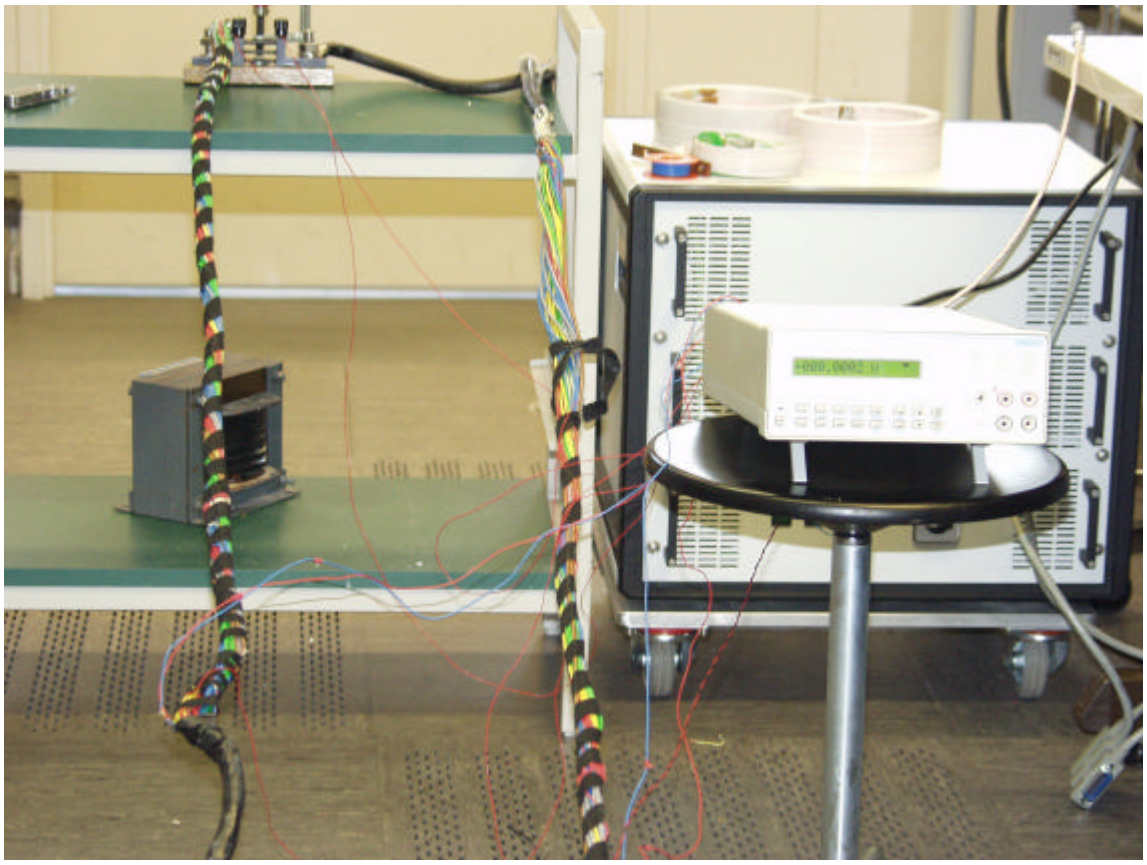

Fig. 7.6 Experimental setup of multi-wire bundle

Despite of all these small errors, the results of the calculations are more than sufficient for practical applications.

CHAPTER 8

SUMMARY AND CONCLUSIONS

8.1 Summary

Heat transfer and temperature distribution in electrical cables and fuses have been studied analytically and numerically in the present research work. Obtained results from numerical simulation are interpolated by the Least-Square method that led to simple polynomial and logarithmical functions of the main thermo-electrical characteristics.

The geometries of physical models and appropriate heat transfer equations are presented in Chapter 2. Analytical solutions of the heat equations for different conductor types have been obtained in Chapter 3. A numerical approach based on a finite volume method has been studied in Chapter 4. A new computational algorithm to compute transient state thermo-electrical characteristics of electrical cables was also described in Chapter 4. The experimental setup and the execution procedure of the experiments is explained in Chapter 5. The achieved computational results of the developed mathematical model were verified by laboratory experiments. Interpolation using Least-squares technique of numerical results in order to reduce the amount of numerical data is given in Chapter 6. Finally, a new approach to calculate heat conduction coefficient of multilayer cable bundles is presented in Chapter 7.

The ultimate goal of this work is to develop a methodology of the analysis of heat transfer in electrical cables and fuses. The main result of this analysis is: temperature distribution in the conductors and transient state thermo-electrical characteristics. To obtain these steady- / transient-state characteristics a numerical algorithm had to be employed, since most materials are temperature dependant. Another reason for a use of numerical algorithm is that the heat transfer calculation is much easier to perform by a numerical approach instead of applying analytical Fourier series solutions.

A one-dimensional model for different kinds of electric conductors is presented in section 2.2. The physical models of three different types of conductors: flat cable, round wire and fuse melting element are taken as physical examples for mathematical modelling, simulation and analysis of heat transfer. When creating the mathematical models (section 2.3) the heat transfer equations were reduced to one-dimensional problems (Eq. 2.3, 2.6, 2.7). In order to have a clear understanding about the modelling of the heat transfer in electric conductors the entire second chapter is devoted to the derivation of a mathematical model. Therefore, sections 2.4, 2.5 describe the analysis of heat conduction and thermal convection respectively. Since, one has to deal with an initial-boundary

value problem, boundary conditions are described in section 2.6. Here are the first kind (Dirichlet) and mixed type (symmetry and convective-radiative) limit conditions are presented. Additionally, numerical implementation of the same kind of boundary conditions is given in section 4.3.2.

After creation and preparation of the mathematical model of electric conductors the following Chapters 3 and 4 give detailed analysis of analytical and numerical calculation procedures of temperature distribution in the conductors.

In the analytical analysis (Chapter 3), exact solutions of steady state heat transfer equations were obtained. These solutions are given for temperature independent material coefficients as well as for temperature dependent coefficients. Different boundary conditions (symmetry or derived from energy balance equation) were implemented for analytical expressions. A very important property was obtained from the heat equation with temperature dependant coefficients. This property is called “avalanche effect” and can be described by the following equation:

if,

$$au = a_r IE_0 = \frac{a_r r_0 I^2}{A} \tag{3.53}$$

then,

$$c_A = \infty, \hat{T}_A = \infty .$$

The next step of heat transfer analysis in the electric conductors was to develop a numerical model to compute steady- and transient-state temperature behaviour in the conductors. The numerical model was created using a finite volume method. The integral form of the heat equation was discretised using central differences in space and a backward difference scheme in time. Thus, second order accuracy scheme in space and first order accuracy in time was achieved. Discretisation of the equations in time were made implicitly in order to achieve unconditional stability and increase computational efficiency. All finite volume schemes were developed on structured grids, however this method is straightforward applicable on unstructured grids too. Systems of algebraic equations were solved by the iterative Newton-Raphson method, which has fast convergence if a suitable initial guess is made.

As computational results, following characteristics were obtained (Fig. 6.10, 6.11-6.14, Chapter 6):

a) conductor surface temperature as a function of load current,
b) heating up time as a function of load current,
c) time constant as a function of load current,
d) electric field strength as a function of load current (considering non-linear electric resistance dependence on temperature)
e) temperature distribution in the fuse element.

Chapter 5 details how the theoretical model of electric cables and fuses has been tested. For this purpose, two different experiments (section 5.1.1 and 5.1.2) were made.

The first experiment deals with the determination of the temperature coefficient of copper resistance. This coefficient is an important parameter for the determination of the cable resistance dependence on temperature. Three different cables were placed in a heated liquid silicon bath. The cable conductor resistance change due to temperature was measured. Necessary theory was developed and described in the section 5.1.1. The experimental set up is described in section 5.2.

The second experiment was designed to measure the cable power dissipation. Here, all available wires and cables as well as fuses and cable bundles were connected to the direct current power supply source and loaded with the power from 0 to the maximal allowed value. The whole experiment was controlled by the software developed for this purpose. The necessary theory of this experiment and experimental setup are given in the sections 5.1.2 and 5.2 respectively. The measuring process and the parameter acquisition procedure was described in the section 5.3.

Chapter 6 describes the validation of the mathematical model of electric conductors and the interpolation procedure of the numerical results by simple polynomial functions.
The validation of the model was based on estimating the parameters, which most influence the heat transfer in electric cables. Therefore, considerable attention was paid to the validation of the heat convection coefficient, a, and the temperature coefficient of copper resistance, a_r.

From section 6.1 one could see that the mathematical model was properly derived and approximated, since characteristics presented in figures 6.3, 6.4, 6.6, 6.7, 6.9 have good agreement with experimental data.

In section 6.2 an algorithm was developed to interpolate numerical results. All thermoelectrical characteristics were interpolated by simple polynomial functions using the Least-Square method. These functions are very useful for practical calculation problems of electric cables. Also, if such equations are implemented in the computer programme to calculate thermal performance of electric cables, the programme gives very good computational efficiency in time. The polynomial functions are given in Eq. (6.7-6.9).

The final chapter concludes this study with a newly developed approach of heat transfer calculation in the multi-wire cable bundle. This chapter applies the principles, which have been derived for single conductors to multi-wires. Only after detailed research of heat transfer models for single wires and cables was it possible to derive the methodology for the cable bundle. The key of this methodology is to calculate averaged heat conductivity coefficient of multi-wire layers. Therefore, it was proposed to use the linear coordinate transformation in order to simplify cable bundle geometry. An averaging method for layered media was then used to determine a mixed or averaged heat conductivity coefficient. The cable bundle model is given in Fig. 7.1 and its transformation to square frames of the same area in Fig. 7.2. Developed “mixed material equations” for thermal conductivity coefficient is given by the Eq. 7.3. In the following section 7.2 the comparison of the results was given. They were obtained with the calculated mixed heat

conductivity coefficient and compared with measurements from the cable bundle. From the figure 7.5, one could see that the developed method to calculate the averaged heat conductivity coefficient gives sufficient accuracy for practical applications.

8.2 Conclusions

Four different one-dimensional analytical and numerical models were successfully developed in this research work, which are able to simulate heat transfer in any kind of electric conductors such as flat cables, round electric wires, electric fuses or multi-wire cable bundles. The new analytical-numerical approach, which has been proposed in this work, allows analysis of the thermo-electrical characteristics of electric conductors.

From this study, several other conclusions are as follows:

- Analytical solutions for steady-state temperature distribution in a single conductor were obtained. These solutions are valid for temperature independent material constants as well as temperature dependant material constants. An "avalanche effect" has been obtained from these analytical solutions (section 3.3.3). It was also observed that transient heat transfer equations require very complicated techniques which are time and space dependent in order to obtain exact solutions. Therefore it is not worth making too much effort to solve transient heat transfer equations. Instead, a numerical approach should be used.

- A numerical model as developed to simulate heat transfer in the conductors, which is based on the finite volume method. This simulates heat transfer very precisely due to the scheme of second order in space. Also implicit schemes in time proved to have better computational performance than explicit ones if time accuracy is not of primary importance.

- Experiments delivered qualitative data and enabling an estimate of the quality of the mathematical model.

- A new method to calculate heat transfer in the multi-wire cable bundle was created. Original equations of heat conductivity coefficient were used by transforming the complicated wire bundle geometry to more simple squares. Equations of "mixed material properties" produce averaged heat conductivity coefficients for a cable bundle, which consist of materials as copper, PVC and air.

- An analytical-numerical approach was developed to simulate heat transfer in electric conductors. This was implemented into a computer aided design program to optimise thermal performance of the cables.

- The developed software allows analysis of thermo-electric properties of both wires and fuses. This analysis is very important for fuse manufacturing processes in order to obtain better time-current characteristics for wire and cable protection against overload and short-circuit currents. In the future, companies

could design fuse materials, using the developed software. The result would be very narrow time-current characteristic of a fuse (close to wire time-current characteristic). Finally, wires and cables can be loaded with 100% load while being protected by the fuses in a reliable way.

- The main results of this study were presented in three international conferences (Lithuania, 2003) and published in three international journals.

List of publications:

1. A. Ilgevicius, H.D. Liess. Thermal Analysis of Electrical Wires by Finite Volume Method. *Electronics and Electrical Engineering.* Nr. 4 (46), Kaunas, 2003.
2. A. Ilgevicius, H.D. Liess. Calculation of the Heat Transfer in Cylindrical Wires and Fuses by Implicit Finite Volume Method. *Mathematical Modelling and Analysis*, 8(3), 217-227, 2003.
3. H.D.Liess, A. Ilgevicius. Analytical versus Numerical Solutions of Physical Problems. The Benefits of its Combination. *Mathematical Modelling and Analysis*, 8(4), 291-302, 2003.

8.3 Suggestions for future research

In the present research a one-dimensional model for different geometries of physical models have been developed. However a two-dimensional model would be appreciable for heat transfer simulation in complicated fuse element geometries and multi-wire bundles. Also, a mesh generation tool for Cartesian and radial coordinates is desirable.

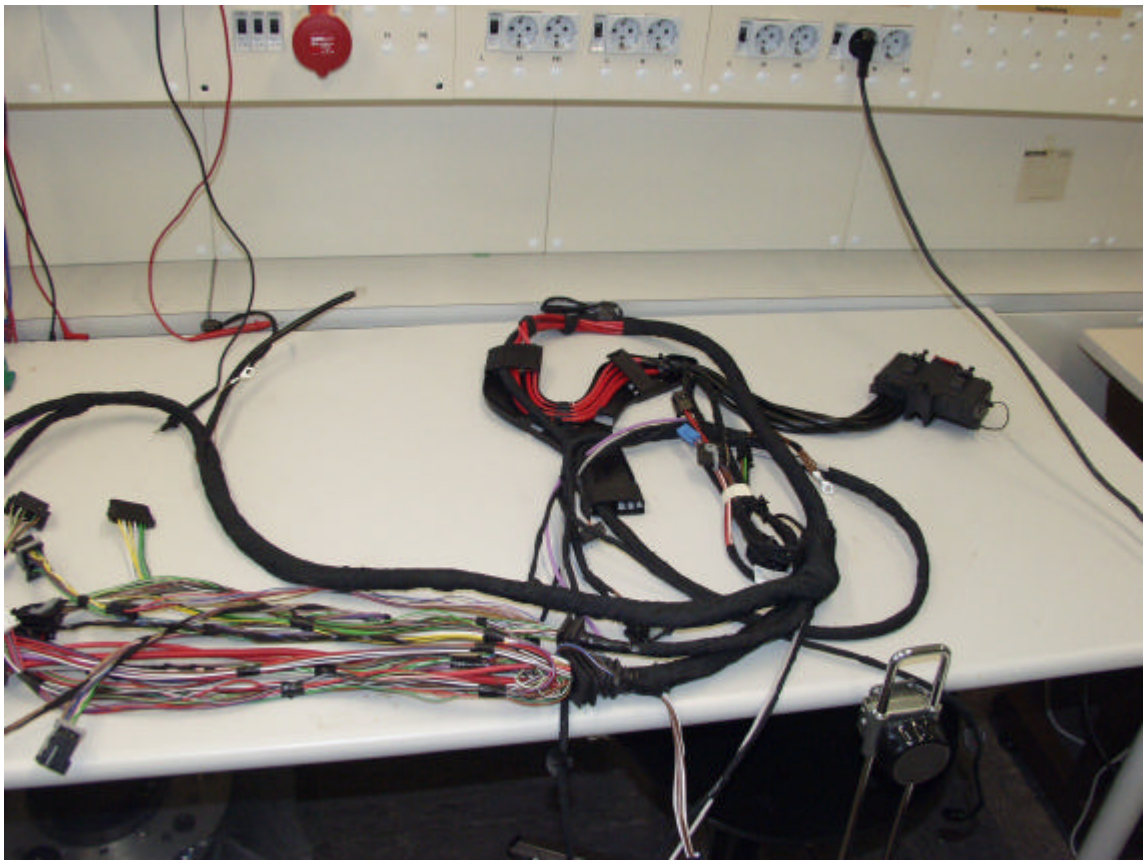

Fig. 8.1. Multi-wire tree of on-board electrical system

More research work should be undertaken developing mathematical models of cable bundles or even cable trees (see Fig. 8.1). Heat conductivity inside the bundle has to be estimated by further experimental works in order to validate the numerical model. Studies should also be made to ascertain which numerical method is more appropriate for the model for cables bundle and cable trees: finite volume or finite element method.

APPENDIX A

HEAT TRANSFER EQUATIONS FOR ELECTRIC CONDUCTORS

A.1 Heat transfer equations for flat electric cable

The aim of this appendix is to give the derivation of heat transfer equations from the physical point of view. It will be shown how to obtain one-dimensional transient state heat equations for different heat transfer directions in electrical conductors.

In order to derive the heat equation for vertical heat transfer applicable for heat transfer in a flat cable, two assumptions have to be formulated:

1. The heat flux q is a vector. This vector is *normal* to the cross section area. More generally, the heat flows in an isotropic media with some heat conductivity *?* against the vector of temperature gradient:

$$\vec{q} = -l \; gradT \tag{A.1}$$

2. The change of heat flux div q is a vector. This vector describes the heat flux change in space per volume and time and is proportional to the heat capacity g and to the rate of temperature change:

$$div\vec{q} = -g \frac{\partial T}{\partial t} \tag{A.2}$$

or,

$$div\left(l \, gradT\right) = g \frac{\partial T}{\partial t} \tag{A.3}$$

For *?* = const. and since div grad $U=\Delta U$,

differential equation for any media is of the following form:

$$\boxed{\Delta \cdot T = \frac{g}{l} \frac{\partial T}{\partial t}} \tag{A.4}$$

here:

?	Heat capacity	in Ws/m^3K
?	Heat conductivity	in W/mK
?	Operator	in $1/m^2$
q	Heat flux	in W/m^2
T	Temperature	in K oder °C

The operator ? is given by:

for Cartesian coordinates:

$$\Delta = \frac{\partial^2}{\partial x^2} + \frac{\partial^2}{\partial y^2} + \frac{\partial^2}{\partial z^2}$$

for cylindrical coordinates:

$$\Delta = \frac{\partial^2}{\partial x^2} + \frac{\partial^2}{\partial r^2} + \frac{1}{r}\frac{\partial}{\partial r} + \frac{1}{r^2}\frac{\partial^2}{\partial j^2}$$

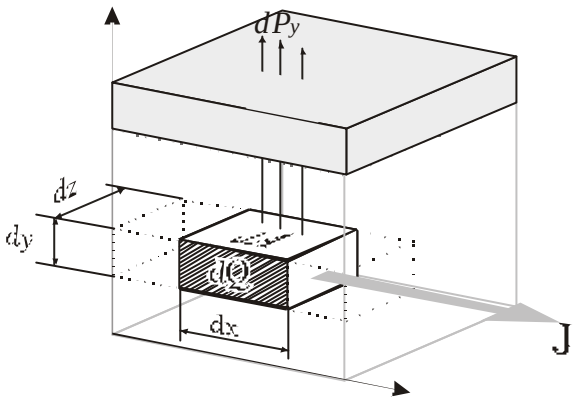

Fig. A.1 Vertical heat transfer in the flat cable

According to the picture in A1, electric power P_e is given by:

$$dP_e = O\ E\ J\ dy \tag{A.5}$$

In z- direction the heat power P_z can be neglected:

$$P_z = 0 \tag{A.6}$$

In y- direction the heat power through the cable surface is as follows:

$$P_y = -l\ O\frac{dT(y,t)}{dy} \tag{A.7}$$

In the cable accumulated heat energy Q:

$$dQ = g\ O\Delta T(y,t)dy \tag{A.8}$$

here: $O = a\ l$ is the surface area in m^2

From the energy balance equation, P_e is given by:

$$P_e = P_y + \frac{dQ}{dt} \quad \text{or} \quad dP_e = dP_y + d\left(\frac{dQ}{dt}\right) \tag{A.9}$$

By inserting the equations A5, A.7 and A.8 to the equation A.9, we obtain a differential equation for transient temperature distribution in the flat cable:

$$O E J\, dy = -l\, O \frac{d^2T(y,t)}{dy} + g\, O\, d\left(\frac{T(y,t)}{dt}\right) dy \tag{A.10}$$

dividing by $O \cdot dy$:

$$l \frac{\partial^2 T(y,t)}{\partial^2 y} + E J - g \cdot \frac{\partial T(y,t)}{\partial t} = 0 \tag{A.11}$$

or,

$$\boxed{\frac{\partial^2 T(y,t)}{\partial^2 y} + \frac{E J}{l} - \frac{g}{l} \cdot \frac{\partial T(y,t)}{\partial t} = 0} \tag{A.12}$$

A.2 Heat transfer equations for round electric wire

For radial heat transfer, differential equations with cylindrical coordinates have to be used. In figure A.2 heat conduction is given.

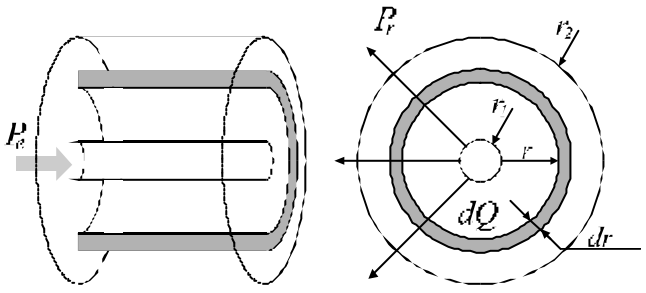

Fig. A.2 Radial heat transfer in the round wire

Electric power P_e is given by:

$$dP_e = O E J\, dr \tag{A.13}$$

where: $O = l\,u = 2\,p\,l\,r$ - the surface

$$dP_e = 2\,p\,l\,r\,E\,J\,dr \tag{A.13a}$$

Radial heat power of the wire P_r is given by:

$$P_r = -l\,O\frac{dT(r,t)}{dr} = -2p\;l\,l\,r\frac{dT(r,t)}{dr} \tag{A.14}$$

$$dP_r = -2p\;l\,l\frac{dT(r,t)}{dr}dr - 2p\;l\,l\,r\frac{d^2T(r,t)}{dr}$$

In the wire accumulated heat energy Q:

$$d^2Q = g\,l\,u\,dT(r,t)dr = 2p\,g\,l\,r\,dT(r,t)\,dr \tag{A.15}$$

From the energy balance equation, for radial heat conduction, the power P_r is given by:

$$P_e = P_r + \frac{dQ}{dt} \quad \text{or} \quad dP_e = dP_r + d\left(\frac{dQ}{dt}\right) \tag{A.16}$$

After insertion of the equations A.13a, A.14 and A.15 into the equation A.16, the differential equation for transient temperature distribution in the cylindrical wire follows:

$$2p\,l\,r\,E\,J\,dr = -2p\;l\,l\,dT(r,t) - 2p\,l\,r\,l\frac{d^2T(r,t)}{dr} + 2p\;l\,r\,g\frac{T(r,t)}{dt}dr \tag{A.17}$$

divided by $2p\;l\,r\,dr$ we have,

$$l\frac{\partial^2T(r,t)}{\partial r^2} + l\frac{\partial T(r,t)}{r\,\partial r} + E\,J - g\cdot\frac{\partial T(r,t)}{\partial t} = 0 \tag{A.17a}$$

or,

$$\boxed{\frac{\partial^2T(r,t)}{\partial r^2} + \frac{\partial T(r,t)}{r\,\partial r} + \frac{E\,J}{l} - \frac{g}{l}\cdot\frac{\partial T(r,t)}{\partial t} = 0} \tag{A.18}$$

A.3 Heat transfer equations for an electric fuse element

Here we consider axial heat transfer in a cylindrical or flat body electric fuse with constant cross section. The axial heat conduction in a cylindrical fuse element is given in picture A.3.

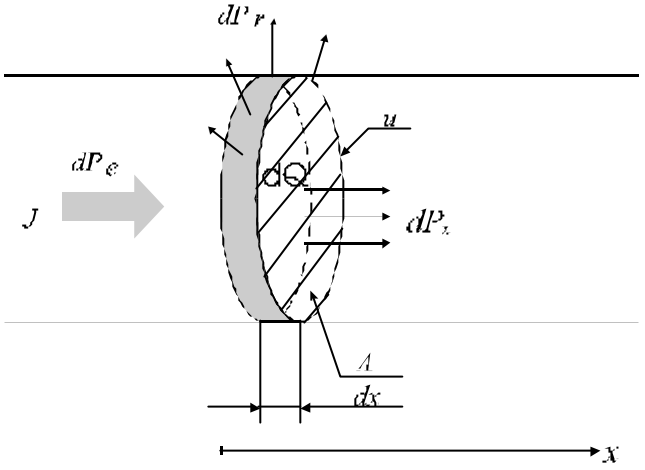

Fig. A.3 Axial heat transfer in the fuse

According to Fig. A3, electric power P_e is given by:

$$dP_e = A\,E\,J\,dx \tag{A.19}$$

Radial heat conduction P_r through the surface is:

$$dP_r = a\,u\,T(x,t)\,dx \tag{A.20}$$

Axial heat conduction P_x along the fuse is::

$$P_x = -l\,A\frac{dT(x,t)}{dx} \tag{A.21}$$

In the wire accumulated heat energy Q is:

$$dQ = g\,AT(x,t)dx \tag{A.22}$$

From the energy balance equation, P_r is given by:

$$P_e = P_r + P_x + \frac{dQ}{dt} \quad \text{or} \quad dP_e = dP_r + dP_x + d\left(\frac{dQ}{dt}\right) \tag{A.23}$$

Repeating the same procedure for the fuse element as was applied for flat and cylindrical cables. Equations A.19, A.20, A.21 and A.22 are inserted into the equation A.23. Finally the differential equation for transient temperature distribution in the fuse element leads to:

$$A E J\, dx = a\, u T(x,t) dx - l\, A \frac{d^2 T(x,t)}{dx} + g\, A d\left(\frac{T(x,t)}{dt}\right) dx \tag{A.24}$$

divided by $A \cdot dx$,

$$l \frac{d^2 T(x,t)}{dx^2} - \frac{a\, u}{A} T(x,t) + E\, J = g\, d\left(\frac{T(x,t)}{dt}\right) \tag{A.24a}$$

or,

$$\boxed{\frac{\partial^2 T(x,t)}{\partial^2 x} - \frac{a\, u}{l\, A} \cdot \Delta T(x,t) + \frac{E\, J}{l} - \frac{g}{l} \cdot \frac{\partial T(x,t)}{\partial t} = 0} \tag{A.25}$$

APPENDIX B

NUMERICAL ALGORITHM APPLICATION FOR HEAT TRANSFER SIMULATION

B.1 Numerical heat transfer simulation and interpolation of the results

The aim of this appendix is to illustrate the practical implementation of a numerical algorithm (Chapter 4) in order to simulate the heat transfer in electric conductors and the implementation of the interpolation algorithm (Chapter 6). In the figure B.1 the graphical interface to input pre-processing data for the numerical simulation of heat transfer in cylindrical wires is given. Here the user has the possibility to choose any geometry of the wire in cylindrical coordinates, environment temperature and to apply different types of materials. The boundary conditions are, however, fixed, and expose free convection and radiation to the air. As post-processing information, numerical representation in an ASCII file (see Fig. B.2). Interpolation results are saved in the binary file (see Fig. B.3)

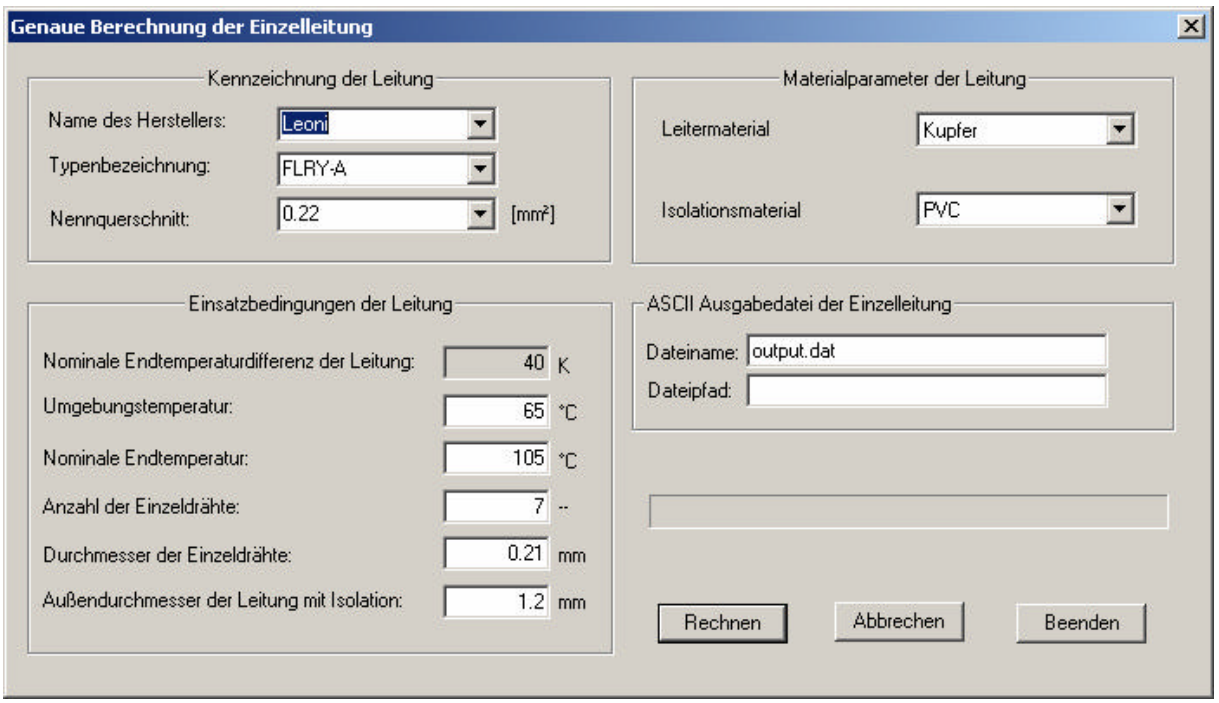

Fig. B.1 Window of pre-processing information for the heat transfer simulation program in cylindrical wires

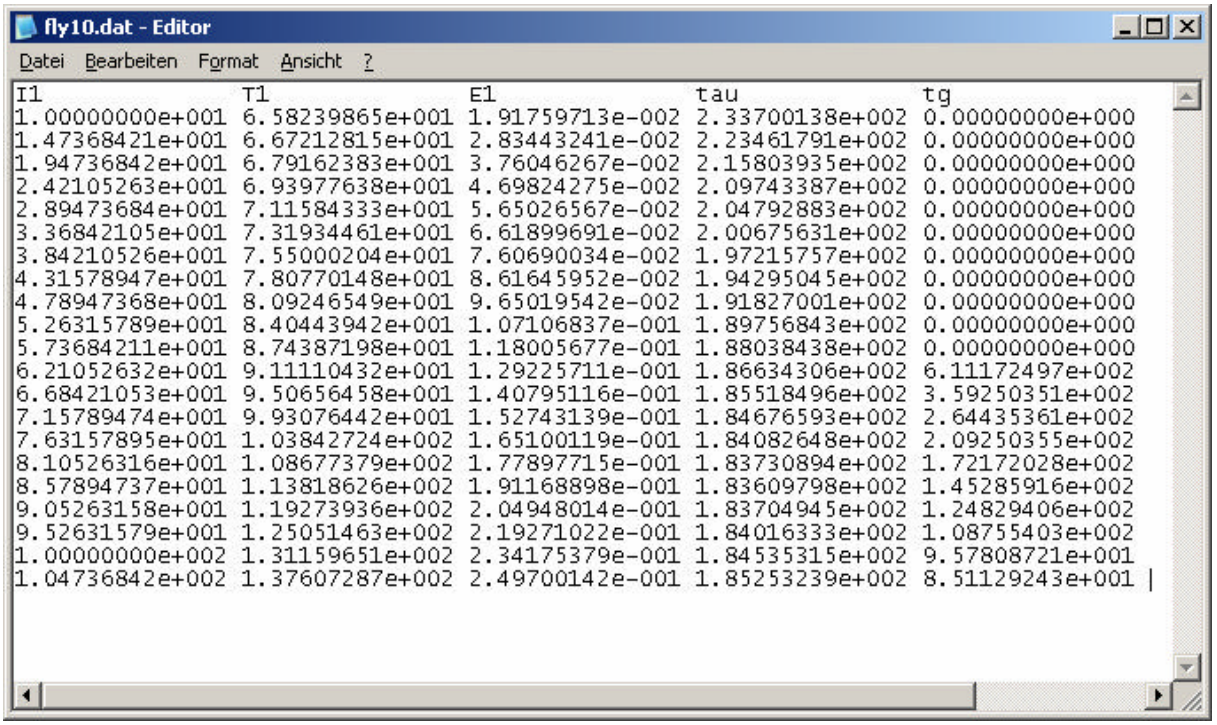

fly10.dat - Editor

Datei Bearbeiten Format Ansicht ?

I1	T1	E1	tau	tg
1.00000000e+001	6.58239865e+001	1.91759713e-002	2.33700138e+002	0.00000000e+000
1.47368421e+001	6.67212815e+001	2.83443241e-002	2.23461791e+002	0.00000000e+000
1.94736842e+001	6.79162383e+001	3.76046267e-002	2.15803935e+002	0.00000000e+000
2.42105263e+001	6.93977638e+001	4.69824275e-002	2.09743387e+002	0.00000000e+000
2.89473684e+001	7.11584333e+001	5.65026567e-002	2.04792883e+002	0.00000000e+000
3.36842105e+001	7.31934461e+001	6.61899691e-002	2.00675631e+002	0.00000000e+000
3.84210526e+001	7.55000204e+001	7.60690034e-002	1.97215757e+002	0.00000000e+000
4.31578947e+001	7.80770148e+001	8.61645952e-002	1.94295045e+002	0.00000000e+000
4.78947368e+001	8.09246549e+001	9.65019542e-002	1.91827001e+002	0.00000000e+000
5.26315789e+001	8.40443942e+001	1.07106837e-001	1.89756843e+002	0.00000000e+000
5.73684211e+001	8.74387198e+001	1.18005677e-001	1.88038438e+002	0.00000000e+000
6.21052632e+001	9.11110432e+001	1.29225711e-001	1.86634306e+002	6.11172497e+002
6.68421053e+001	9.50656458e+001	1.40795116e-001	1.85518496e+002	3.59250351e+002
7.15789474e+001	9.93076442e+001	1.52743139e-001	1.84676593e+002	2.64435361e+002
7.63157895e+001	1.03842724e+002	1.65100119e-001	1.84082648e+002	2.09250355e+002
8.10526316e+001	1.08677379e+002	1.77897715e-001	1.83730894e+002	1.72172028e+002
8.57894737e+001	1.13818626e+002	1.91168898e-001	1.83609798e+002	1.45285916e+002
9.05263158e+001	1.19273936e+002	2.04948014e-001	1.83704945e+002	1.24829406e+002
9.52631579e+001	1.25051463e+002	2.19271022e-001	1.84016333e+002	1.08755403e+002
1.00000000e+002	1.31159651e+002	2.34175379e-001	1.84535315e+002	9.57808721e+001
1.04736842e+002	1.37607287e+002	2.49700142e-001	1.85253239e+002	8.51129243e+001

Fig. B.2 Simulation data of a cylindrical wire with 10mm^2 cross section. Here: I1 – load current in amps, T1 – conductor surface temperature in °C, E1 – electrical field strength in V/m, tau – time constant after n=5 in sec, tg – heating up time to reach 90°C in sec.

B.2 Calculation of thermo-electric characteristics by the polynomial functions

In order to be able to work with an interpolated mathematical model or with simplified polynomial functions, another programme was created (see Fig. B4). Here, using equations (6.7-6.10) given in section 6.2, thermo-electrical characteristics can be calculated.

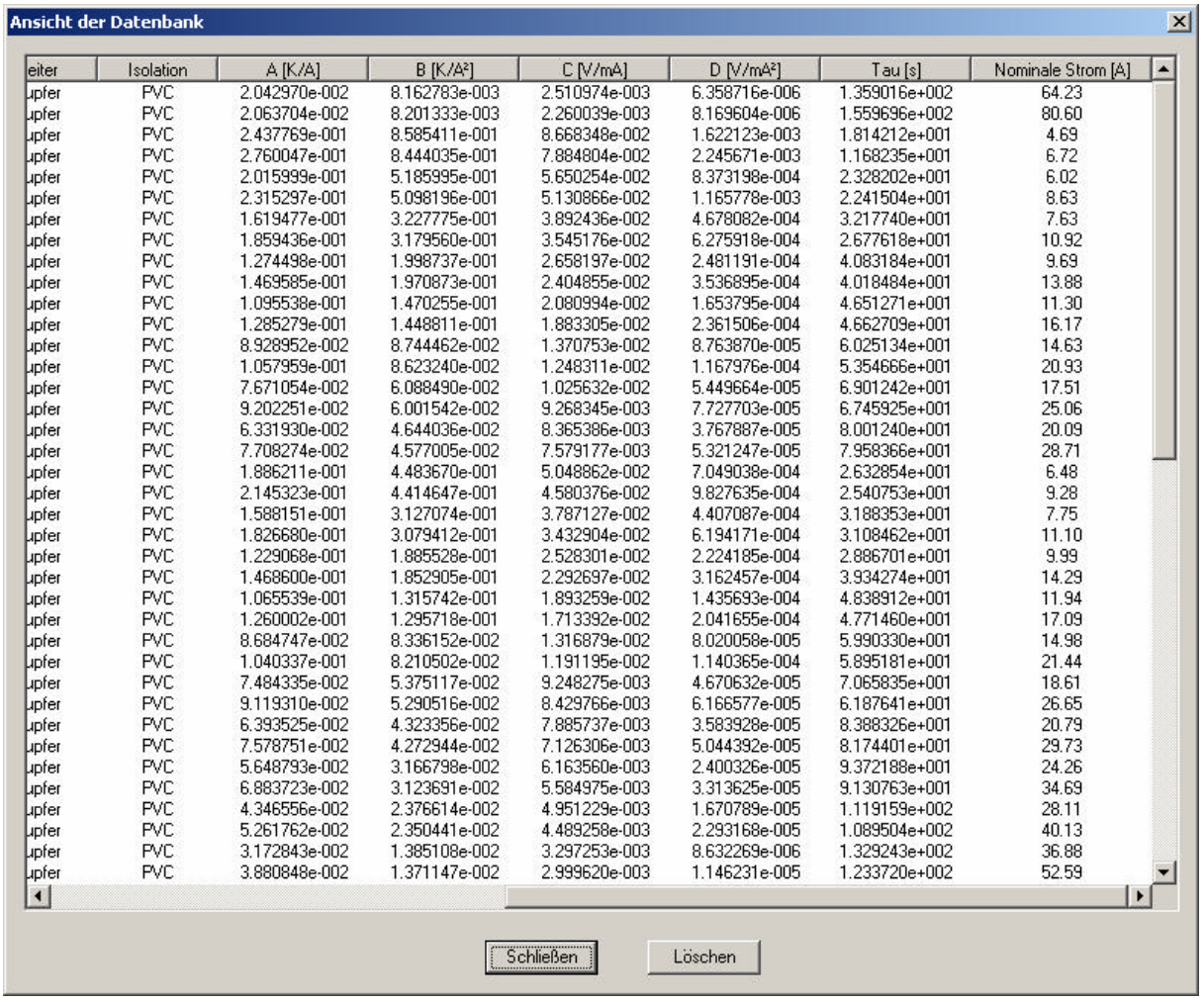

eiter	Isolation	A [K/A]	B [K/A²]	C [V/mA]	D [V/mA²]	Tau [s]	Nominale Strom [A]
upfer	PVC	2.042970e-002	8.162783e-003	2.510974e-003	6.358716e-006	1.359016e+002	64.23
upfer	PVC	2.063704e-002	8.201333e-003	2.260039e-003	8.169604e-006	1.559696e+002	80.60
upfer	PVC	2.437769e-001	8.585411e-001	8.668348e-002	1.622123e-003	1.814212e+001	4.69
upfer	PVC	2.760047e-001	8.444035e-001	7.884804e-002	2.245671e-003	1.168235e+001	6.72
upfer	PVC	2.015999e-001	5.185995e-001	5.650254e-002	8.373198e-004	2.328202e+001	6.02
upfer	PVC	2.315297e-001	5.098196e-001	5.130866e-002	1.165778e-003	2.241504e+001	8.63
upfer	PVC	1.619477e-001	3.227775e-001	3.892436e-002	4.678082e-004	3.217740e+001	7.63
upfer	PVC	1.859436e-001	3.179560e-001	3.545176e-002	6.275918e-004	2.677618e+001	10.92
upfer	PVC	1.274498e-001	1.998737e-001	2.658197e-002	2.481191e-004	4.083184e+001	9.69
upfer	PVC	1.469585e-001	1.970873e-001	2.404855e-002	3.536895e-004	4.018484e+001	13.88
upfer	PVC	1.095538e-001	1.470255e-001	2.080994e-002	1.653795e-004	4.651271e+001	11.30
upfer	PVC	1.285279e-001	1.448811e-001	1.883305e-002	2.361506e-004	4.662709e+001	16.17
upfer	PVC	8.928952e-002	8.744462e-002	1.370753e-002	8.763870e-005	6.025134e+001	14.63
upfer	PVC	1.057959e-001	8.623240e-002	1.248311e-002	1.167976e-004	5.354666e+001	20.93
upfer	PVC	7.671054e-002	6.088490e-002	1.025632e-002	5.449664e-005	6.901242e+001	17.51
upfer	PVC	9.202251e-002	6.001542e-002	9.268345e-003	7.727703e-005	6.745925e+001	25.06
upfer	PVC	6.331930e-002	4.644036e-002	8.365386e-003	3.767887e-005	8.001240e+001	20.09
upfer	PVC	7.708274e-002	4.577005e-002	7.579177e-003	5.321247e-005	7.958366e+001	28.71
upfer	PVC	1.886211e-001	4.483670e-001	5.048862e-002	7.049038e-004	2.632854e+001	6.48
upfer	PVC	2.145323e-001	4.414647e-001	4.580376e-002	9.827635e-004	2.540753e+001	9.28
upfer	PVC	1.588151e-001	3.127074e-001	3.787127e-002	4.407087e-004	3.188353e+001	7.75
upfer	PVC	1.826680e-001	3.079412e-001	3.432904e-002	6.194171e-004	3.108462e+001	11.10
upfer	PVC	1.229068e-001	1.885528e-001	2.528301e-002	2.224185e-004	2.886701e+001	9.99
upfer	PVC	1.468600e-001	1.852905e-001	2.292697e-002	3.162457e-004	3.934274e+001	14.29
upfer	PVC	1.065539e-001	1.315742e-001	1.893259e-002	1.435693e-004	4.838912e+001	11.94
upfer	PVC	1.260002e-001	1.295718e-001	1.713392e-002	2.041655e-004	4.771460e+001	17.09
upfer	PVC	8.684747e-002	8.336152e-002	1.316879e-002	8.020058e-005	5.990330e+001	14.98
upfer	PVC	1.040337e-001	8.210502e-002	1.191195e-002	1.140365e-004	5.895181e+001	21.44
upfer	PVC	7.484335e-002	5.375117e-002	9.248275e-003	4.670632e-005	7.065835e+001	18.61
upfer	PVC	9.119310e-002	5.290516e-002	8.429766e-003	6.166577e-005	6.187641e+001	26.65
upfer	PVC	6.393525e-002	4.323356e-002	7.885737e-003	3.583928e-005	8.388326e+001	20.79
upfer	PVC	7.578751e-002	4.272944e-002	7.126306e-003	5.044392e-005	8.174401e+001	29.73
upfer	PVC	5.648793e-002	3.166798e-002	6.163560e-003	2.400326e-005	9.372188e+001	24.26
upfer	PVC	6.883723e-002	3.123691e-002	5.584975e-003	3.313625e-005	9.130763e+001	34.69
upfer	PVC	4.346556e-002	2.376614e-002	4.951229e-003	1.670789e-005	1.119159e+002	28.11
upfer	PVC	5.261762e-002	2.350441e-002	4.489258e-003	2.293168e-005	1.089504e+002	40.13
upfer	PVC	3.172843e-002	1.385108e-002	3.297253e-003	8.632269e-006	1.329243e+002	36.88
upfer	PVC	3.880848e-002	1.371147e-002	2.999620e-003	1.146231e-005	1.233720e+002	52.59

Fig. B.3 Binary file, where all interpolation coefficients are saved (A, B, C, D, Tau).

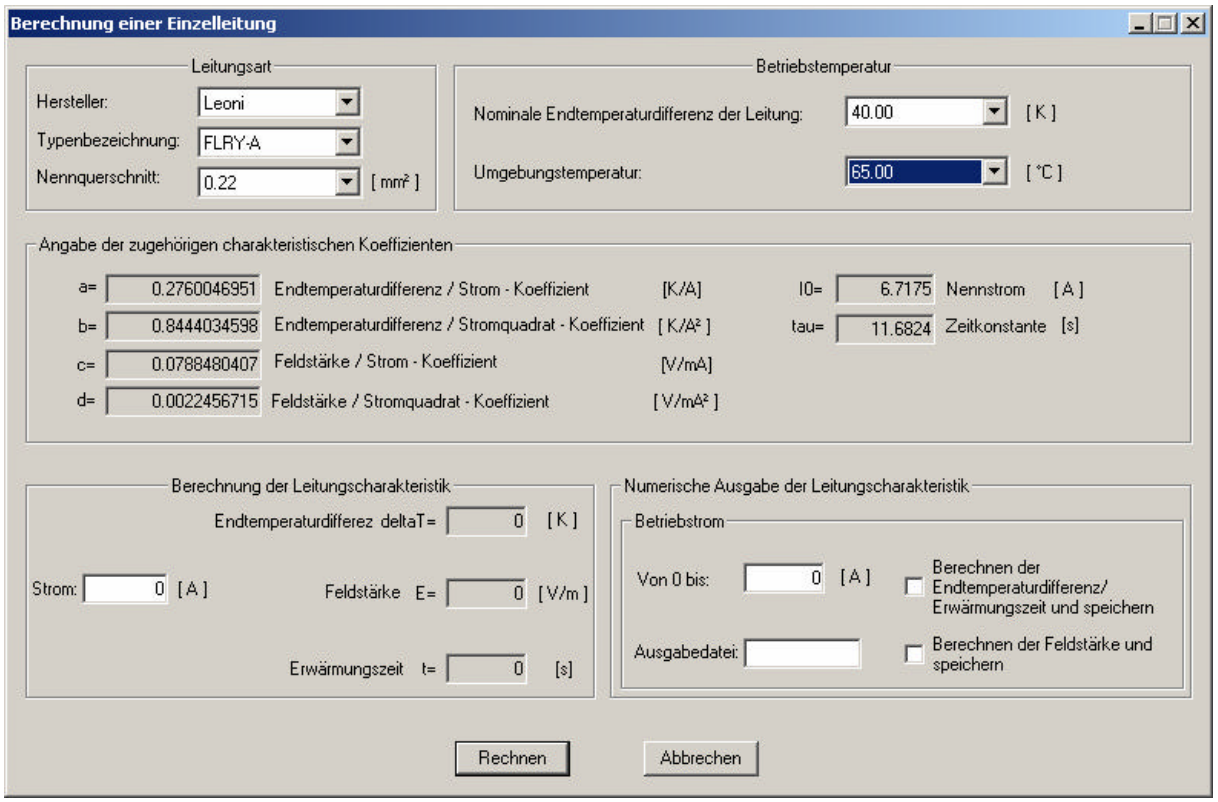

Fig. B.4 Programme, which calculates thermo-electrical characteristics of cylindrical wire by simplified polynomial functions.

APPENDIX C

SOFTWARE FOR MEASUREMENT DATA ACQUISITION

C.1 Algorithm description and measurement program

In the section 5.3 two different measurement procedures of electric cables to validate the mathematical model were explained. In this appendix, a closer look at the measurement software will be given. Both experiments were run by the same type of software, implemented in the LabView 6.1 environment. For the explanation in this chapter, only the second experiment software will be presented. This program controls the power supply of direct current and digital multimeter, to which the measurement sensors were attached. The control of measurement equipment is implemented by a GPIB controller.

The program has the following structure:

- set the voltage to 15V;
- open the files needed to save the results and the computations;
- reset the multimeter;
- write into the files the date and the time;
- compute R_{65} – in order to do this: apply a 1 amp current for 60 seconds, read the voltage drops on the cable and on the shunt, read the environment temperature and finally compute it;
- for all current values (**for** i = 0 **to** number of currents **do**):
    - compute the present current and apply it to the cable;
    - **for** j = 'number of measurements' – 4 **to** 'number of measurements' **do**:
        - set the multimeter scale to DC voltage range;
        - read the voltage drop on the shunt and wait for 4 seconds – also save the value in a variable;
        - read the voltage drop on the cable and wait for 4 seconds – also save the value in a variable;
        - read the sensor temperature - read actually a voltage drop and then compute the temperature with the following formula:
          Ts = 2.83668 + 15.5669 * **VoltageDrop** * 1000.
          Remark: this thermocouple sensor is a safety sensor, which cuts off the power supply if the conductor temperature exceeds maximal allowed value.
        - read the environment temperature and save the value in a variable for later use.
        - based on the saved values compute the cable resistance, the cable temperature, the cable power.
        - write the results in the file dedicated to computed values.

- write into both files the date and the time (the measurement has finished at this point);
- reset both power supply and multimeter;
- close both files;

The program interface is shown in the picture C.1.

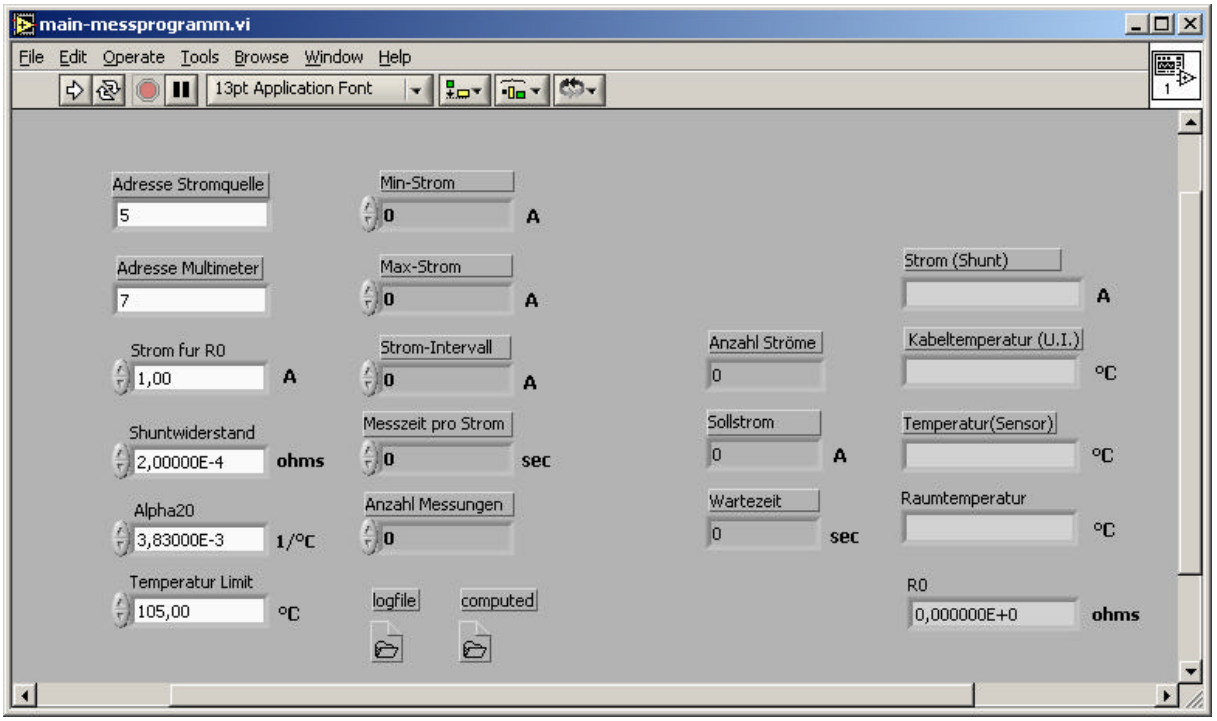

Fig. C.1 Measurement programme to measure cable voltage drop, resistance, electric power and temperature

The measurement of cable resistance, voltage drop, electric power and temperature can be started if all measurement equipment defined in the programme is switched on. The program should initialise the available GPIB controller, power supply source, temperature sensors and the digital multimeter, which serves as a data acquisition device. Whenever the hardware is correctly initialised, the user should give initial data into the program. First, *"Strom für R0"* box has to be filled in, where some current value required in order to measure cold resistance R0 of the cable. Next, in the box *"Shuntwiderstand"* shunt resistance should be defined in order to compute exact load current produced by the power supply. *"Alpha20"* box defines the temperature coefficient of copper resistance. This value is required for the temperature computation of the cable. *"Temperatur Limit"* required for the safety reasons, if the cable temperature exceeds this value, the power supply source is cut off. *"Min. Strom"* and *"Max. Strom"* are required to specify the starting current load value and the end current value respectively. Next, the step size of measurement interval should be given. For this, the box *"Strom-Intervall"* should be used. The measurement time, after which the steady state should be reached is given in the box *"Messzeit pro Strom"*. The box *"Anzahl Messungen"* means, how many intermediate values for every measurement interval should be measured and saved in the file. This information is important in order to record the transient state of cable temperature.

The measurement procedure then begins, and the whole experiment runs automatically. In order to observe the measurement data online, the computer with measurement software should be connected to the Ethernet network, and using "Remote Desktop Connection" application, the measurement computer can be controlled via the Ethernet network. On the right hand side of the program, online measurement information is presented: actual load current, actual cable temperature obtained by measuring cable voltage drop, cable surface temperature

obtained by thermocouple sensor, environment temperature obtained by Pt100 sensor and the cold cable resistance R0.

C.2 Measurement results

The measurement programme produced numerical results, saved in the ASCII type file (see Fig. C.2)

Measurement Time	Special Events	Measured Cable Temp in °C	Wanted Current in A	Current measured by PowerSupply in A	calculated current in A	Cable Power in W	Shunt Voltage Drop in V	Cable Voltage Drop in V	Cable Resistan in ohm
48	16:11 - Extra file initiated as: C:\CPOW\testfin.log								
48	16:11 - Environment temperature: 20.00000 deg C								
0	16:11 - User Tom Roida startet a new Measurement! Date: 2001-4-2								
16	16:11 - Setting new current to 0.00 A								
515		33,76	0	0,36	0,12250	0,00039	2,45000E-05	3,19790E-03	
616		33,61	0	0,36	0,12150	0,00039	2,43000E-05	3,19450E-03	
716		33,47	0	0,29	0,12300	0,00039	2,46000E-05	3,19430E-03	
816		33,29	0	0,29	0,12050	0,00038	2,41000E-05	3,19080E-03	
876	16:26 - Setting new current to 10.00 A								
1416		33,17	10	9,87	9,68050	1,89056	1,93610E-03	1,95296E-01	2,01741E-02
1516		33,17	10	9,87	9,67950	1,89034	1,93590E-03	1,95293E-01	2,01760E-02
1616		33,17	10	9,94	9,67950	1,89036	1,93590E-03	1,95295E-01	2,01762E-02
1716		33,13	10	9,94	9,67950	1,89017	1,93590E-03	1,95276E-01	2,01741E-02
1736	16:40 - Setting new current to 20.00 A								
2316		33,98	20	19,96	19,72500	7,85852	3,94500E-03	3,98404E-01	2,01979E-02
2416		34,15	20	19,96	19,72500	7,86177	3,94500E-03	3,98569E-01	2,02063E-02
2516		34,31	20	19,96	19,72400	7,86573	3,94480E-03	3,98790E-01	2,02185E-02
2615		34,46	20	19,96	19,72300	7,86993	3,94460E-03	3,99023E-01	2,02314E-02
2649	16:55 - Setting new current to 30.00 A								
3216		36,24	30	29,91	29,69550	17,95414	5,93910E-03	6,04608E-01	2,03603E-02
3315		36,33	30	29,98	29,69650	17,95839	5,93930E-03	6,04731E-01	2,03637E-02
3416		36,38	30	29,98	29,69550	17,96082	5,93910E-03	6,04833E-01	2,03678E-02
3516		36,46	30	29,98	29,69500	17,96533	5,93900E-03	6,04995E-01	2,03736E-02
3616		36,50	30	29,91	29,69300	17,96810	5,93860E-03	6,05129E-01	2,03795E-02
3616	17:11 - Setting new current to 40.00 A								
4316		37,73	40	40	39,74350	32,25896	7,94870E-03	8,11679E-01	2,04229E-02
4416		37,47	40	40	39,74350	32,23397	7,94870E-03	8,11050E-01	2,04071E-02
4516		37,27	40	40	39,74500	32,22366	7,94900E-03	8,10760E-01	2,03990E-02
4615		37,18	40	40	39,74700	32,21542	7,94940E-03	8,10512E-01	2,03918E-02
4636	17:28 - Setting new current to 50.00 A								
5315		38,61	50	49,94	49,72800	50,73365	9,94560E-03	1,02022E+00	2,05161E-02
5416		38,48	50	49,94	49,72700	50,72164	9,94540E-03	1,02000E+00	2,05120E-02
5516		38,62	50	50,02	49,72800	50,75503	9,94560E-03	1,02065E+00	2,05247E-02
5616		38,73	50	49,94	49,72750	50,78436	9,94550E-03	1,02125E+00	2,05370E-02
5716		38,83	50	49,94	49,72650	50,83431	9,94530E-03	1,02228E+00	2,05580E-02
5716	17:46 - Setting new current to 60.00 A								
6516		42,00	60	60,04	59,78150	74,50084	1,19563E-02	1,24622E+00	2,08462E-02
6616		42,07	60	60,04	59,78200	74,51892	1,19564E-02	1,24651E+00	2,08509E-02
6715		42,08	60	59,96	59,78100	74,53166	1,19562E-02	1,24675E+00	2,08552E-02
6816		42,17	60	60,04	59,78150	74,54066	1,19563E-02	1,24689E+00	2,08574E-02
6843	18:05 - Setting new current to 70.00 A								
7716		44,92	70	69,98	69,76700	102,64526	1,39534E-02	1,47126E+00	2,10882E-02
7816		44,94	70	69,98	69,76750	102,66071	1,39535E-02	1,47147E+00	2,10910E-02
8015		45,01	70	69,98	69,76800	102,67282	1,39536E-02	1,47163E+00	2,10932E-02
8023	18:25 - Setting new current to 80.00 A								
8916		48,16	80	80	79,81350	136,04219	1,59627E-02	1,70450E+00	2,13560E-02
9016		48,07	80	80	79,81350	136,03437	1,59627E-02	1,70440E+00	2,13548E-02
9116		48,31	80	80	79,81250	136,07361	1,59625E-02	1,70492E+00	2,13615E-02
9216		48,17	80	80,08	79,81300	136,06273	1,59626E-02	1,70477E+00	2,13595E-02
9256	18:45 - Setting new current to 90.00 A								
10216		51,48	90	89,95	89,74750	174,35920	1,79495E-02	1,94278E+00	2,16471E-02
10316		51,50	90	89,95	89,74750	174,40156	1,79495E-02	1,94325E+00	2,16524E-02
10416		51,45	90	89,95	89,74900	174,38087	1,79498E-02	1,94298E+00	2,16491E-02
10516		51,48	90	89,95	89,74800	174,38144	1,79496E-02	1,94301E+00	2,16496E-02
10543	19:07 - Setting new current to 100.00 A								
11516		54,99	100	99,97	99,86350	219,14446	1,99727E-02	2,19444E+00	2,19744E-02
11616		55,12	100	100,04	99,86500	219,07785	1,99730E-02	2,19374E+00	2,19671E-02
11716		55,14	100	100,04	99,86400	219,10461	1,99728E-02	2,19403E+00	2,19702E-02
11816		55,10	100	100,04	99,86600	219,06106	1,99732E-02	2,19355E+00	2,19649E-02
11883	19:29 - Setting new current to 110.00 A								
12922		58,88	110		109,84300	269,33833	2,19686E-02	2,45203E+00	2,23230E-02
13016		58,81	110	109,99	109,84450	269,30137	2,19689E-02	2,45166E+00	2,23194E-02
13116		58,81	110	110,06	109,84200	269,27327	2,19684E-02	2,45146E+00	2,23181E-02

Fig. C.2 Saved experimental data in ASCII type file

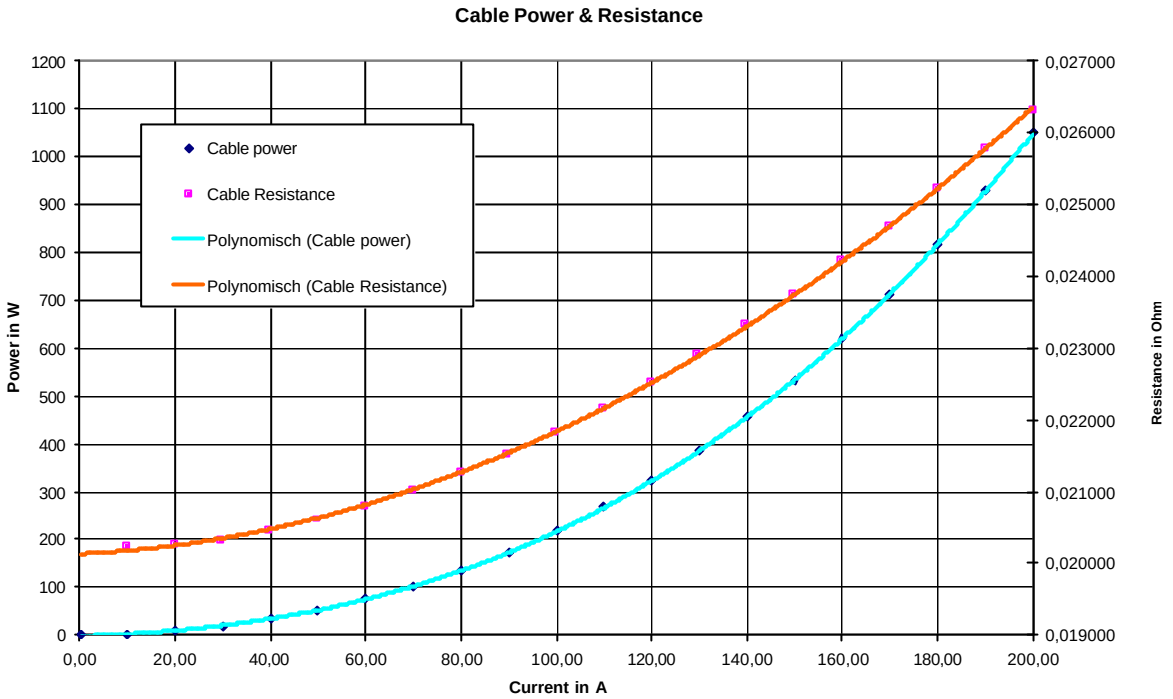

Fig. C.3 Measured cable power and resistance after steady state regime

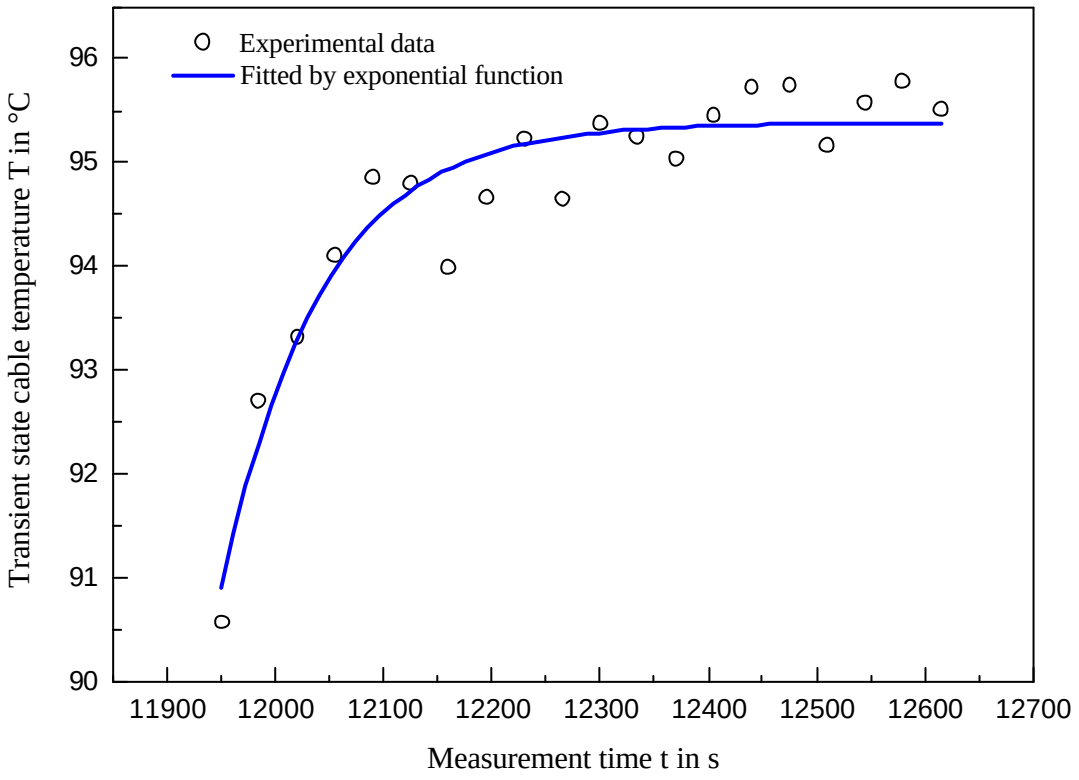

Fig. C.4 Measured cable surface temperature in transient state regime at the current I = 170 A

Bibliography

[1] Hiranandani, Ajit. *Calculation of Conductor Temperatures and Ampacities of Cable Systems Using a Generalized Finite Difference Model*. IEEE Transactions on Power Delivery, Vol. 6, No. 1, 15-21, January 1991.

[2] Haskew, Tim, A., Carwile, Regina F., Grigsby, L., L. *An Algorithm for Steady-State Thermal Analysis of Electrical Cables with Radiation by reduced Newton-Raphson Techniques*. IEEE Transactions on Power Delivery, Vol. 9, No. 1, January 1994.

[3] Harshe, B.L., Black, W.Z. *Ampacity of cables in single open-top cable trays.* IEEE Transactions on Power Delievery, Vol. 9; No. 4, October 1994.

[4] El-Kady, M.A. *Calculation of the power cable ampacity to variations of design and environment parameters*. IEEE transactions on power and systems. Vol. PAS-103; No.8, 2043-2050, 1984.

[5] Ryan, C., Leen, G. and Heffernan, D. *A Prototype Steer-by-Wire and Brake-by-Wire System for Educational Research Projects.* Proceeedings U.K. Institute of Physics - Sensors&Applications XII. Sept. 2003.

[6] Neher, J.H, McGrath, M.H. *The Calculation of temperature Rise and Load Capability of Cable Systems.* AIEE Transactions, Vol. 76, 752-772, October 1957.

[7] George J. Anders. *Rating of electric power cables*. IEEE Press Power Engineering Series. McGraw-Hill, 1997. ISBN 0-7803-1177-9.

[8] Schulz, Thomas. *Grundsatzuntersuchung zum Temperaturverhalten elektrischer Leitungen und æren Schutzelemente auf Schmelztleiterbasis in Kfz-Bordnetzen.* Dissertation, Universität der Bundeswehr München, 2002.

[9] Das, S., Knapp, R. H. and Shimabukuro, T.A. *Finite Element Analysis - A New Tool for Cable Design*. Proc 50th Intl. Wire and Cable Symposium, Paper 11-4, Lake Buena Vista, FL, Nov. 12-15, 2001.

[10] Groth, C., Müller, G. *FEM für Praktiker-Temperaturfelder*. Band 463, Expert Verlag, 2. Auflage, 1997.

[11] Incropera, Frank, P., DeWitt, David P. *Introduction to heat transfer*. John Willey & Sons, USA, 1985. ISBN 0-471-80126-7.

[12] Buikis, A., Kalis, H. *The mathematical modelling of nonlinear heat transport in thin plate.* Mathematical modelling and analysis, Vol. 4, 44-50, 1999.

[13] Kalis, H. Lasis, A. *Simple algorithms for calculation of the axial – symmetric heat transport problem in a cylinder*. 6(2), 262-269, 2001.

[14] Buikis, A., Kalis, H. *Calculation of electromagnetic fields, forces and temperature in a finite cylinder*. Mathematical modelling and analysis, 7(1) 21-32, 2002.

[15] Zurbau, O. *Optimizing the wire system package in automobile industry.* Diplom thesis, Universität der Bundeswehr München, 2002.

[16] Tslaf, Avraham. *Combined properties of conductors*. Physical science data Vol. 9, Elsevier, Netherlands, 1981. ISBN 0-444-41959-4.

[17] *VDI-Wärmeatlas*, 8. Auflage, Springer-Verlag, Berlin, New York, 1997. ISBN 3-540-62719-7.

[18] Wongyala, Nawin. *Erwärmung elektrischer Leiter*. Diplomarbeit, Universität der Bundeswehr München, 1999.

[19] Özsik, M.,N. *Finite difference methods in heat transfer*. CRC Press, Inc., USA, 1994. ISBN 0-8493-2491-2.
[20] Zienkewic, O.C. *The finite element method in Engineering Science*. New York: McGraw-Hill. 1971.
[21] Gottlieb, D., Orszag, S. A. *Numerical Analysis of Spectral Analysis: Theory and Applications, Society for Industrial and Applied Mathematics.* Philadelphia, PA, 1977.
[22] Versteeg, H.K, Malalsekera, W. *An introduction to computational fluid dynamics. The finite volume method*. Longman Group, 1995. ISBN 0-582-21884-5.
[23] Hirsch, C. Numerical computation of internal and external flows. Vol.1: Fundamentals of numerical discretization. ISBN 0-471-91762-1.
[24] Mack, *P. Bestimmung des linearen und quadratischen Temperaturkoeffizienten ausgewählter elektrischer Leiter*. Studienarbeit, Universität der Bundeswehr München, 2001.
[25] Roida, T. *Automatisierte Messung der Wärmeableitung von elektrisch beheizten Leitern*. Studientarbeit, Universität der Bundeswehr München, 2001.
[26] Lancaster, P., Šalkauskas. K. *Curve and surface fitting. An introduction*. Academic press, UK, 1986. ISBN 0-12-436060-2.
[27] Cuthbert, D., Fred, S.W. *Fitting equations to data.* John Wiley & Sons, USA, 1980. ISBN 0-471-05370-8.
[28] Chien-Ching, Shin-Wen Chang. *Analytical exact solutions of heat conduction problems for anisotropic multilayered media*. International journal of heat and mass transfer 47, 1643-1655, 2004.
[29] Fletcher, C.A. *Computational Galerkin methods*. New York, Berlin, Heidelberg, Tokyo, Springer Verlag, 1984.
[30] Munoz-Cobo, J.L, Corberan, J.M, Chiva, S. *Explicit formulas for laminar natural convection heat transfer along vertical cylinders with power-law wall temperature distribution*. Heat and Mass Transfer 39, 215-222, 2003.
[31] Kays, W.M., Crawford, M.E. Convective Heat Transfer. Mc Graw Hill, 1993.
[32] Anders, G.J., Roiz, J., Moshref, A. *Advanced computer programs for power cable ampacity calculations*. IEEE Comput. Appl. Power, Vol. 3, No. 3, 42-45, 1996.
[33] El-Kady, M.A. *Calculation of the sensitivity of power cable ampacity to variations of design and environmental parameters*. IEEE Trans. Power App. Syst., Vol. PAS-103, No. 8, 2043-2050, 1985.
[34] Flatabo, N. *Transient heat conduction problem in power cables solved by the finite element method*. IEEE Trans. Power App. Syst. Vol. PAS-92, 161-168, 1973.
[35] Hanna, M.A., Chikhani, A.Y., Salama, M., M., A. *Thermal analysis of power cables in multi-layered soil*. Parts 1 and 2. IEEE Trans. Power Delivery, Vol. 8, No. 3, 761-778, 1993.
[36] Kellow, M.A. *A numerical procedure for the calculation of temperature rise and ampacity of underground cables*. IEEE Trans. Power App. Syst., Vol. PAS-100, No. 7, 3322-3330, 1981.
[37] Mushamalirwa, D., Germay, N., Steffens, J.C. *A 2-D finite element mesh generator for thermal analysis of underground power cables*. IEEE Trans. Power Delivery, Vol. 3, No. 1, 62-68, 1988.
[38] Cannon, J.R. *The one-dimensional heat equation*. Addison-Wesley Publishing Company, USA, 1984, ISBN 0-201-13522-1.
[39] Shneider, P.J. *Conduction heat transfer*. Addison-Wesley,Reading, MA, 1955.

[40] Burmeister, L.,C. *Convective Heat Transfer*. 2nd Ed., Wiley, New York, 1995.
[41] Simson, J.R. *Engineering heat transfer*. The Macmillan Press Ltd, 1975. ISBN 0 333 18757 1.
[42] Shih, Tien-Mo. *Numerical properties and methodologies in heat transfer*. Springer-Verlag, Berlin, 1983. ISBN 0-89116-309-3.
[43] Lisejkin, V.D. *Grid generation methods*. Springer-Verlag Berlin Heidelberg New York. 1999. ISBN 3-540-65686-3.
[44] Heinhold, L. *Kabel und Leitungen für Starkstrom. Teil 1 und 2.* Siemens Verlag, 4. Auflage 1987.
[45] Bauer, H. *Kraftfahrtechnisches Taschenbuch*. Bosch, 22. Auflage-VDI-Verlag, 1995. ISBN 3-18-419122-2.
[46] Al-Khafaji, Amir Wadi. *Numerical methods in engineering practice*. Saunders College Publishing, 1986. ISBN 0-03-001757-2.
[47] Morton, Keith W. *Numerical solution of convection-diffusion problems.* Chapman&Hall, 1996. ISBN 0 412 56440 8.
[48] Jaluria, Y. *Computational heat transfer*. Springer-Verlag, 1986. ISBN 3-540-16879-6.
[49] Müller, G. *FEM für Praktiker*. Expert Verlag,1993. ISBN 3-8169-0800-4.
[50] Lax, P. D. *Calculus with application and computing Vol.1*. Springer-Verlag. 1976. ISBN 3-540-90179-5.
[51] Minkowycz, W.J. *Handbook of numerical heat transfer*. John Wiley & Sons, Inc,1988, ISBN 0-471-83093-3.
[52] Ansorge, R. *Iterative solution of nonlinear system equations*. Proceedings of a Meeting held at Oberwolfach, Germany, Jan. 31-Feb. 5. Springer-Verlag, 1982. ISBN 0-387-11602-8.
[53] Shih, Tien-Mo. *Numerical heat transfer*. Springer-Verlag, 1984. ISBN 3-540-13051-9.
[54] Mitchell, A.R. *The finite difference method in partial differential equations*. John Willey & Sons, 1985. ISBN 0 471 27641 3.
[55] Anderson, D. A. *Computational fluid mechanics and heat transfer*. Hemisphere publishing corporation, New York, 1984. ISBN 0-89116-471-5.
[56] Tveito, A. *Introduction to partial differential equations*. Springer-Verlag, 1998. ISBN 0-387-98327-9.
[57] Ganzha, V.G. *Numerical solutions for partial differential equations. Problems solving using Mathematica*. CRC Press, Inc., 1996. ISBN 0-8493-7379-4.
[58] Tyn, M.U. *Partial differential equations for scientist and engineers.* Elsevier Science Publishing Co., 1987, ISBN 0-444-01173-0.
[59] Stephenson, G. *Partial differential equations for scientists and engineers*. Longman, 1980. ISBN 0-582-44696-1.
[60] VVedensky, D. *Partial differential equations with Mathematica*. Adison-Wesley, 1993. ISBN 0-201-54409-1.
[61] Baehr, H. D. *Heat and Mass Transfer*. Springer, New York , 1998.
[62] Bejan, A. *Heat Transfer*. John Wiley, New York, 1993.
[63] Incropera, F. and DeWitt, D. *Heat and Mass Transfer*. John Wiley, 2nd Ed.,1985.
[64] Suryanarayana, N.V. *Engineering Heat Transfer*. West Pub. Co., Minneapolis/St Paul, 1995.
[65] Carslaw, H.S. and Jaeger, J.C. *Conduction of Heat in Solids*. Clarendon Press,Oxford, UK, 1959.

[66] Grigull, U. *Heat Conduction*. Springer-Verlag, New York; Hemisphere Pub Corp., Washington, D.C., 1984.
[67] Poulikakos, D. *Conduction Heat Transfer*. Prentice Hall, Englewood Cli_s, NJ, 1994.
[68] Kaviany, M. *Principles of Convective Heat Transfer*. Springer-Verlag, New York, 1994.
[69] Oosthuizen, P.H. and Naylor, D. *Introduction to Convective Heat Transfer Analysis*. McGraw-Hill, 1998.
[70] Modest, M.F. *Radiative Heat Transfer*. McGraw-Hill, New York, 1993.
[71] Myers, G.E. *Analytical Methods in Conduction Heat Transfer*. McGraw-Hill, New York, 1971.
[72] Adams, J.A., Rogers, D. F. *Computer-Aided Heat Transfer Analysis*. McGraw-Hill, New York, 1973.
[73] Wang, Z.J. *Spectral (Finite) Volume Method for Conservation Laws on Unstructured Grids*. Journal of Comp utational Physics, 178, 210-251, 2002.
[74] Ciegis, R. Diferencialiniu lygciu skaitiniai sprendimo metodai. Kaunas, 2003. ISBN 9986-05-588-1.
[75] *IEEE Standart Power Cable Ampacity Tables*, IEEE Std 835, 1994.
[76] *Calculation of the Continuous Current Rating of Cables (100% load factor)*. IEC Publication 287, 1982 and subsequent editions.
[77] *A Method for Calculating Reduction Factors for Groups of Cables in Free Air, Protected from Solar Radiation*. IEC Publication 1042, 1991.
[78] Buikis, A.,Ulanova, N. *Analytical-numerical method for temperature fields in multilayered system*. Advanced Computational Methods in Heat Transfer, VI, Sauthappton, Boston: WITp, 445-453, 2000.
[79] Abou khachfe, R., Jarny, Y. *Determination of heat sources and heat transfer coefficient for two-dimensional heat flow-numerical study*. Int. J. Heat Mass Transfer 44(7), 2001.
[80] Cai, R.X., Zhang, N. *Some algebraically explicit analytical solutions of unsteady nonlinear heat conduction*. Int. J. Heat Transfer. ASME 123(6), 2001.
[81] Chang, C.Y., Ma, C.C. *Transient thermal conduction analysis of a rectangular plate with multiple insulated cracks by the alternating method*. Int. J. Heat Mass Transfer 44(13), 2001.
[82] Chen, B.S., Gu, Y.X., Guan, Z.Q., Zhang, H.W. *Nonlinear transient heat conduction analysis with precise time integration method*. Numer. Heat Transfer Part B-Fundamentals 40 (13), 2001.
[83] Asllanaj, F. Jeandel, G., Roche, J.R. *Numerical solution of radiative transfer equation coupled with nonlinear heat conduction equation*. Int. J. Numer. Meth. Heat Fluid Flow 11 (5–6),2001.
[84] Krishnaprakas, C. K. *Combined Conduction and Radiation Heat Transfer in a Cylindrical Medium*. Journal of Thermophysics and Heat Transfer, Vol. 12, No. 4, 605-608, 1998.
[85] Talukdar, P., Mishra, S. C. *Transient conduction and radiation heat transfer with variable thermal conductivity.* Numerical Heat Transfer, Part A, 41: 851-867, 2002.

Acknolegment

This dissertation has been written during my activity as a research engineer in the Institute of Physics of Electrical Engineering and Information Technology Faculty of University of the Bundeswehr Munich.

I would like sincerely to thank Prof. Dr. H.-D. Ließ for accepting me to his research group and confiding this topic to me. His interest on the progress of my research work, supervision and provided support had been valuable help for me.

I wish to express my deep gratitude to Prof. Habil. Dr. R. Ciegis, who kindly agreed to supervise my Ph.D. dissertation in numerical heat transfer subject and gave me an intensive course on the mathematical modelling topic. I thank also Prof. R. Ciegis for his contribution as the second reviser of this work.

Prof. Habil. Dr. H. Dalichau I thank for the revision of this work as the third reviser. His remarks and suggestions on computer aided computational techniques were very valuable for me.

I would like to thank Prof. Dr. K. Landes for his contribution as the chairman of the examination committee and beyond it for interesting discussions about the research work.

I wish to acknowledge valuable discussions with the Prof. Dr. R. Rinkeviciene, Prof. Habil. Dr. A.J. Poska, and Prof. Habil. Dr. A. Smilgevicius from Vilnius Gediminas Technology University, Faculty of Electronics during preparation the dissertation manuscript.

I acknowledge valuable support of Dipl. –Ing. M. Glinka and Dipl.-Ing. M. Hiller from EIT 6 and Dr.-Ing. T. K. Wurst from LRT 10 for providing expensive laboratory equipment. Without this equipment would not had been possible to validate the research theory.

The co-workers and colleagues from my research team I deeply thank for the assistance with the programming of numerical algorithms and measurement software.

Last but not least, the technical staff from LRT 6 I thank for the help to set up the measurement equipment.

Finally, but most deeply, I thank my parents, without whose constant encouragement, support, assistance, and tolerance this dissertation would not have been possible.